WHEAT GERM AGGLUTININ-CONJUGATED POLY-DL-LACTIC-CO-GLYCOLIC ACID (PLGA) NANOPARTICLES FOR ENHANCED UPTAKE AND RETENTION OF PACLITAXEL BY COLON CANCER CELLS

WANG CHUNXIA

(B.S.(Pharm), Shan Dong University)

(M.S. (Pharm), Peking Union Medical College)

A THESIS SUBMITTED

FOR THE DEGREE OF DOCTOR OF PHILOSOPHY

DEPARTMENT OF PHARMACY

NATIONAL UNIVERSITY OF SINGAPORE

2009

Acknowledgements

TABLE OF CONTENTS

Content   Page

Summary

The ideal goal of cancer chemotherapy is to destroy cancer cells without harming healthy cells. Most current anticancer drugs cannot greatly differentiate between cancerous and normal cells. This leads to systemic toxicity and adverse effects. Targeted delivery of anticancer agents could offer a more efficient and less harmful solution to overcome this drawback. The purpose of this project was to confirm the hypothesis that conjugation of WGA to PLGA nanoparticles loaded with paclitaxel (WNP) could improve the delivery of paclitaxel to colonic cancer cells.

Glycosylation patterns of representative colon cancer cells (Caco-2 and HT-29 cells) and normal cells (colon fibroblasts, CCD-18Co cells) were first investigated. Our results confirmed the higher expression levels of WGA-binding glycoproteins (N-acetylglucosamine and sialic acid) in the Caco-2 and HT-29 cells, than in the CCD-18Co cells. Most of the WGA-recognizable glycoproteins in the Caco-2 and HT-29 cells had molecular weight > 75 kDa, whereas the CCD-18Co cells showed an apparent lack of expression of such large proteins. The ranking order of expression of WGA-recognizable glycoproteins in the three cell lines was HT-29 > Caco-2 > CCD-18Co cells.

In vitro cytotoxicity and cellular uptake studies were then carried out to evaluate the potential of WGA for targeted activity against the colon cell models. WGA exhibited

different degrees of cytotoxicity against the Caco-2, HT-29 and CCD-18Co cells, but showed anti-proliferative activity in all 3 cell lines at concentrations $\geq$ 50 µg/ml. Cellular uptake of fWGA ranked in the order of Caco-2 > HT-29 > CCD-18Co cells. The higher binding of fWGA to the malignant cells may be associated with the greater expression of WGA-recognizable glycoproteins in these cells relative to the colon fibroblast cells.

WGA was conjugated onto the surface of paclitaxel-loaded PLGA nanoparticles to prepare the WNP formulation. Cellular uptake and cytotoxicity of WNP were evaluated in the three colon cell lines. *In vitro* anti-proliferation studies suggested that the incorporation of WGA enhanced the cytotoxicity of the paclitaxel-loaded PLGA nanoparticles against the cancerous Caco-2 and HT-29 cells. Paclitaxel uptake from the WNP formulation at 2h incubation was the highest in the Caco-2 cells compared to the other two cell lines. Caco-2 and HT-29 cells showed preferential uptake of WNP compared to PNP, suggesting that WGA conjugation to the PLGA nanoparticles was advantageous in facilitating the nanoparticle uptake by the cultured colon cancer cells. The greater efficacy of WNP correlated well with the higher cellular uptake and sustained intracellular retention of paclitaxel associated with the formulation, which again might be attributed to the over-expression of N-acetyl-D-glucosamine-containing glycoprotein on the colon cell surface. About 30% of the endocytosed WNP was observed in the late endo-lysosomes, but fluorimetric measurements

indicated successful escape of the WNP from the endo-lysosome compartment into the cytosol with increasing incubation time.

To evaluate the effect of mucin glycoprotein on the cellular uptake of WNP, the uptake experiments were repeated using a mucin-secreting cell line, LS174T. The LS174 cells showed no significant differences in paclitaxel uptake from the WNP formulation on day 3 of culture compared to day 6 of culture, despite the significantly higher production of mucin by day 6. The presence of mucin may therefore not be a barrier for the cellular uptake of WGA-conjugated nanoparticles. FRAP results showed that fWNP was capable of diffusing in the mucin layer, although the diffusion rate was slowed down by the viscous mucin. This diffusion capability allowed the fWNP to remain mobile in the mucin layer and enabled the particles to be transported into the cells. Interaction between the mucin glycoprotein and WGA is postulated to serve as a bridge between WNP and the colon cancer cells under the mucin layer.

On the basis of these results, it may be concluded that WNP has the potential to be applied as a targeted delivery platform for paclitaxel in the treatment of colon cancer.

LIST OF TABLES

LIST OF FIGURES

LIST OF ABBREVIATIONS

ANOVA	analysis of variance
ATCC	American Type Culture Collection
cm	centimeter
°C	Celsius degree
Da	dalton
DMSO	dimethyl sulfoxide
EDAC	1-ethyl-3-(3-dimethylaminopropyl)carbodiimide hydrochloride
EDTA	ethylenediaminetetraacetic acid
FBS	fetal bovine serum
FITC	fluorescein isothiocyanate
fWGA	FITC-labeled wheat germ agglutinin
fWNP	fWGA-conjugated paclitaxel-loaded PLGA nanoparticles
FRAP	Fluorescence recovery after photobleaching
h	hour
s	second
HBSS	Hanks balanced salt solution
HEPES	N-2-hydroxyethylpiperazine-N′-2-ethanosulfonic acid
HPLC	high performance liquid chromatography
IC50	50% growth inhibition concentration
IPM	isopropyl myristate
MES	2-(N-morpholino)ethanesulfonic acid
MEM	minimal essential medium
mg	milligram
min	minute
mM	millimolar
MTT	3-(4,5-dimethylthiazol-2-yl)-2,5-diphenyltetrazolium bromide
MW	molecular weight
NEAA	non-essential amino acids
NHS	N-hydroxysuccinimide
nm	nanometer
μm	micrometer
ml	milliliter
μl	microliter
M	molar
μM	micromolar
nM	nanomolar
PBS	phosphate-buffered saline
P/CreEL	conventional paclitaxel formulation
PLGA	poly(D,L-lactic-co-glycolic acid)
pH	the negative logarithm of hydrogen-ion concentration
PI	propidium iodide
PNP	paclitaxel-loaded PLGA nanoparticles
PTA	phosphotungstic acid
PVA	polyvinyl alcohol
PVDF	polyvinylidene difluoride

RME   receptor-mediated endocytosis
SD   standard deviation
SDS   sodium dodecyl sulfate
SDS-PAGE   sodium dodecyl sulfate-polyacrylamide gel electrophoresis
SEM   scanning electron microscopy
TEM   transmission electron microscopy
WGA   wheat germ agglutinin
WNP   WGA-conjugated paclitaxel-loaded PLGA nanoparticles
UV   ultraviolet
V   volt

List of publications and conference presentations

1. Wheat Germ Agglutinin-Conjugated PLGA Nanoparticles for Enhanced intracellular delivery of paclitaxel to Colon cancer cells. Wang CX, Ho PC, LY Lim (submitted).

2. The effect of mucin of LS174T cells on the uptake of WGA-conjugated PLGA nanoparticles. Wang CX, Ho PC, LY Lim (in preparation).

3. The cytotoxicity and uptake of wheat germ agglutinin on colon cell lines, Wang CX, Ho PC, LY Lim, Abstract for American Association of Pharmaceutical Scientists Annual Meeting, 11 – 15 November 2007, San Diego, USA.

4. Loratadine transdermal patches. Liu Yuling, Wang Chunxia. Patent CN03134651.0 (China).

5. Nonlogarithmic titration method for the determination of dissociation constant of loratadine, Chinese Pharmaceutical jounal, Wang Chunxia, Liu Yuling. 2003, 38(11): 860-861.

6. The New Development of Transdermal Drug Delivery System, Acta Pharmaceutica Sinica, Wang Chunxia, Liu Yuling, 2002,37(12): 999-1002.

Chapter 1

Introduction

1.1 Chemotherapy for colon cancer

Successful systemic cancer chemotherapy, first developed in 1946, was highlighted in a review by Gilman and Philips (Gilman & Philips, 1946) which also marked the beginning of modern cancer chemotherapy (Pratt et al., 1994). Chemotherapy is often needed for colon cancer patients after surgical removal of the tumor in order to reduce the risk of recurrence. Various anticancer agents are used, depending on the stages of colon cancer and patient condition. While most are highly effective, anticancer agents are also potent agents which can cause serious side effects. Unfortunately, the systemic administration of most chemotherapeutic drugs is non-discriminative, causing both cancerous and healthy tissues to be concomitantly exposed to the drugs, resulting in high mortality and morbidity. This provides the impetus to develop drug delivery platforms capable of targeting the delivery of anticancer agents to cancerous colonic cells.

1.1.1 Colon cancer

Anatomically, the colon, also known as the large intestine or large bowel, is part of the intestine that extends from the cecum to the rectum. Colon cancer refers to cancer that is located in the colon or rectum, and it is sometimes called "colorectal cancer". In the United States, colon cancer is the third most commonly diagnosed cancer and the second leading cause of cancer-related deaths (American Cancer Society. Cancer

Facts & Figures, Atlanta, 2008). In Asia, colon cancer is also the third commonest cancer disease, but its incidences in many Asian countries are rapidly increasing (Sung, 2007). In Singapore, colon cancer has overtaken lung cancer as the commonest cancer and is the second commonest cause of cancer-related deaths (http://www.nccs.com.sg/pat/08_03.htm, Jan. 2008).

Cancer is caused by the uncontrolled growth and spread of abnormal cells. Colon cancer usually starts as a polyp, which is an overgrowth of normal cells. If the cells in a polyp are allowed to grow unchecked, they can become cancerous. Colon cancer is highly curable if diagnosed early. The earlier the polyps are discovered and surgically removed, the better will be the prognosis. Otherwise, the treatment and prognosis will depend on the disease progression at the point of diagnosis. Surgery is often the main treatment for early stage colon cancer and it can result in cure in approximately 50% of patients (Abraham et al., 2005). However, relapse following surgery is a major problem, and is often the cause of death. If surgery reveals that the cancer has spread to other organs or tissues, chemotherapy alone or combination with other modalities is usually prescribed (Oehler & Ciernik, 2006).

Cancer chemotherapy aims to shrink the tumor size, slow tumor growth and/or reduce the likelihood of metastasis developing. In most instances, the primary focus is on

killing rapidly dividing cells. Unfortunately, some normal cells also have a high rate of division e.g. cells in the bone marrow and hair follicles, and most chemotherapeutic delivery systems are unable to differentiate between rapidly dividing cancerous cells from other fast proliferating normal cells. Consequently, cancer chemotherapy is often associated with serious side effects. To circumvent this drawback, drug delivery targeted specifically to colon cancer cells is desired.

1.1.2 Anticancer agents

The first clinically effective anticancer drug developed was nitrogen mustard, an agent initially developed as a war gas. Alkylating drugs based on nitrogen mustard were subsequently synthesized and developed for cancer chemotherapy. These drugs, like nitrogen mustard, are DNA cross-linkers and they prevent DNA synthesis in cells. Many anticancer drugs with different mechanisms of action have since been developed (Cavalli et al., 2000), and they include alkylating and intercalating agents, as well as topoisomerase inhibitors, which cause direct DNA damage; antimetabolites that interfere with DNA synthesis by inhibiting key enzymes in purine or pyrimidine synthesis, or by misincorporation into the DNA molecule to cause strand breaks or premature chain termination; antibiotic cytotoxic agents that alkylate DNA or inhibit topoisomerase II or both; spindle poisons that bind to tubulin to inhibit tubulin polymerization or microtubule depolymerization.

At the mechanistic level, cellular microtubules-interacting agents are one of the most attractive and promising approaches for cancer chemotherapy. Microtubules are filamentous polymers that constitute one of the major components of the cytoskeleton. They are a superb target because of their important function in mitosis and cell division. Table 1.1 shows a list of microtubule-targeted drugs currently in clinical use or under clinical development.

Table 1.1 Microtubule-targeted drugs, their binding sites on tubulin, and their stages of clinical development (Jordan & Kamath, 2007)

Binding Domain	Drugs	Therapeutic uses	Stage of clinical development
Vinca Domain	Vinblastine (Velban)	Hodgkin's disease, testicular germ cell cancer	In clinical use, many combination trials in progress
	Vincristine (Oncovin)	Leukemia, lymphomas	In clinical use, many combination trials
	Vinorelbine (Navelbine)	Solid tumors, lymphomas, lung caner	In clinical use, many clinical trials, Phases I-III, single and combination
	Vinflunine	Bladder, non-small cell lung cancer, breast cancer	Phase III
	Cryptophycin 52	Platinum-resistant advanced ovarian caner	Phase II
	Halichondrius (E7389)		Phase II
	Dolastatins (TZT-1027, Tasidotin)	Vascular targeting agents	Phase I, II
	Hemiasterlins (HTI-286)		Phase I
	Maytansinoids (conjugated to humanized monoclonal antibody)	Colon, lung, pancreas	Phase II
Colchicine Domain	Colchicine	Non-neoplastic diseases (gout, familial Mediterranean fever), also actinic keratoses	Appears to have failed most cancer trials, presumably due to toxicity

	Combretastatins (AVE8062. CA-1-P, CA-4-P (combretastatin A4 phosphate), N-acetylcolchicinol-O-phosphate, NPI-2358, ZD6126)	Vascular –disrupting agents	Phase I, II
	2-Methoxyestradiol	Multiple myeloma, glioblastoma multiforme carcinoid, prostate, breast	Phase I, II
	Methoxybenzene-sulfonamide (ABT-751, E7010)	Solid tumors, vascular-disrupting agent	Phase I, II
	Diketopiperazine (NPI-2358)	Vascular-disrupting agent	Phase I
Taxane Site	Paclitaxel and analogs (Taxol, TL00139, XRP9881, XRP6258, BMS844476, BMS188797, TPI287)	Ovarian, breast, lung tumors, Kaposi's sarcoma, trials with numerous other tumors	In clinical use and in combination and single drug trials, Phase I-III
	Docetaxel (Taxotere)	Prostate, brain, breast, and lung tumors	Phase I-III
	Epothilone (Ixabepilone, epothilones B (patupilone), D, ZK-EPO, KOS-862, KOS-1584)	Taxol-resistant tumors	Phases I, II, III
	Discodermolide	Synergistic with taxanes	Phase I
Other Microtubule Binding Sites	Estramustine	Prostate, often in combination	Phases I, II, III, in combinations with taxanes, epothilones, and Vinca alkaloids
	Arsenic trioxide (trisenox)	Vascular-disruptive agent	
	Noscapine	Leukemia, lymphoma	Phase I

There are two distinct groups of microtubule-interacting agents; the first group inhibits the assembly of tubulin heterodimers into microtubule polymers while the other stabilizes microtubules under normally destabilizing conditions to prevent their disassembly. The latter, of which paclitaxel is a representative compound, will be the focus of this project. A variety of natural products have been discovered over the last decade to inhibit the proliferation of human cancer cells through a paclitaxel-like

mechanism. These compounds represent a whole new set of structurally varied lead

compounds for anticancer chemotherapy.

1.1.3 Paclitaxel

Paclitaxel, a diterpenoid derivative, was first discovered at the Research Triangle

Institute (RTI) in 1967 when Drs. Monroe E. Wall and Mansukh C. Wani isolated the

compound from the bark of the Pacific yew tree, *Taxus brevifolia*, and noted its

antitumor activity in a broad range of rodent tumors. By 1970, the two scientists had

determined the extremely complex structure of paclitaxel (Hennenfent & Govindan,

2006) (Figure 1.1).
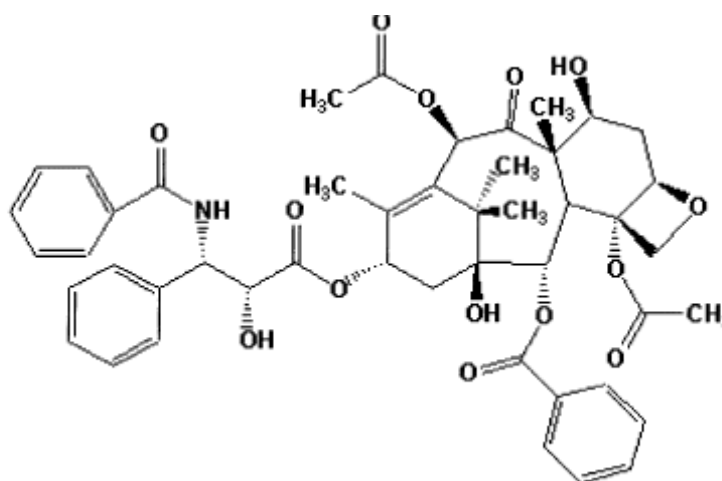
Figure 1.1 Molecular structure of paclitaxel (Singla et al., 2002)

Since then, paclitaxel has been found to be effective against a wide variety of tumors, including refractory ovarian cancer, breast cancer, lung cancer, colon cancer, head and neck carcinomas, and acute leukemia (McGuire & Rowinsky, 1995). It works by interfering with the normal function of microtubules in cells. Paclitaxel binds specifically to the β subunit of tubulin, the "building block" of microtubules (Horwitz, 1994), and the resultant complex does not have the ability to disassemble. This adversely affects cell function because the shortening and lengthening of microtubules (termed dynamic instability) is necessary for the transport of other cellular components. For example, during mitosis, microtubules position the chromosomes during their replication and subsequent separation into the two daughter-cell nuclei (Horwitz, 1994; Wang et al., 2005). Consequently, the stabilization of microtubules prevents cancer cells from restructuring their cytoskeleton in a flexible manner and hinders their aggressive division (Wang et al., 2005). Although normal cells can also be adversely affected, cancer cells are far more susceptible to paclitaxel treatment because of their much faster rate of cell division. Further research has indicated that paclitaxel also induces programmed cell death (apoptosis) in cancer cells by binding to a protein called Bcl-2 (B-cell leukemia 2), which is responsible for arresting apoptosis (Akay et al., 2004).

Despite its effectiveness, paclitaxel is not without disadvantages. One of the major clinical problems associated with paclitaxel is its extreme hydrophobicity, and thus very low solubility in water (~6-30 mg/ml). The clinical formulation, Taxol[®], contains paclitaxel (6 mg/ml) dissolved in a 50:50 v/v mixture of the surfactant, Cremophor EL[®] (polyoxyethylated castor oil), and dehydrated ethanol (Straubinger, 1995; Hennenfent & Govindan, 2006). Cremophor EL[®] has been found to contribute to serious side-effects, e.g. severe hypersensitivity reactions, and is incompatible with common PVC intravenous administration sets. To avoid the hypersensitivity reactions, patients have to be pretreated with corticosteroids (e.g. dexamethasone), diphenhydramine and H_2-receptor antagonist (e.g. cimetidine, ranitidine) before Taxol[®] administration (Singla et al., 2002). Precipitation of paclitaxel is also an issue when the formulation has to be diluted for clinical use (Pfeifer et al., 1993).

Though paclitaxel is a very potent anticancer agent against colon cancer cells, its efficacy is limited because of low solubility and poor specificity against cancer cells. In order to improve the bioavailability, resolve the intractable solubility and minimize the cytotoxicity and adverse side effects associated with paclitaxel therapy, a targeted drug delivery system needs to be developed. Many modified formulations and more water-soluble analogues of paclitaxel have been investigated (Ibrahim et al., 2002; Kim et al., 2004; Soepenberg et al., 2004). Among the methods proposed,

nanoparticles of biodegradable polymers are promising in resolving the twin issues of

the adjuvant problem and the controlled and targeted delivery of the drug (Serpe et al.,

2004; Weissenbock et al., 2004; Musumeci et al., 2006). A nanoparticle formulation

of paclitaxel bound to albumin (ABI-007) has been approved for the treatment of

metastatic breast cancer (Gradishar et al., 2005). Paclitaxel incorporated into polymer

nanoparticles has demonstrated a significant specificity of action mainly because of

changes in its tissue distribution and pharmacokinetics (Couvreur et al., 1980). These

changes, directed by the nanoparticle pharmacokinetics, have the potential to improve

the therapeutic efficacy of paclitaxel with concomitant reduction of its side effects and

toxicity. In this project, paclitaxel was used as a model drug to develop a nanoparticle

delivery system with WGA as a targeting moiety with the view to resolve current

clinical issues associated with paclitaxel therapy.

1.1.4 Targeted delivery of anticancer agents

Much effort has been expended to improve the selectivity of cancer chemotherapeutic

agents, and significant improvement in patient survival has been achieved in recent

years. Nevertheless, the developments of novel selective anticancer agents and new

ways of delivering both old and new agents are possibly the most important goals of

modern anticancer research.

Targeted cancer chemotherapy aims to direct adequate concentration of the chosen agent to tumor cells while affecting as few healthy cells as possible. In principle, this can be achieved by passive or active targeting. Passive targeting exploits the enhanced permeability and retention (EPR) characteristics of tumor vessels. Rapidly growing tumors develop extensive vasculatures to meet their requirement for nutrient supply and waste disposal, but the blood vessels are abnormally hyper-permeable, with defective architecture and impaired lymphatic drainage (Nie et al., 2007). Circulating macromolecular drugs or particulate delivery systems that have difficulty permeating normal blood vessels can extravasate through such tumor blood vessels, and they become entrapped due to the impaired lymphatic drainage in tumor tissues. Consequently, the EPR effect can be applied to facilitate the selective accumulation of an appropriately designed drug delivery system at a tumor site. To achieve efficient accumulation, the delivery system must also avoid systemic clearance by the reticuloendothelial system (RES), usually achieved by controlling the size and surface properties of the delivery systems (Gref et al., 1994). To avoid RES uptake, a hydrophilic surface and small particle size under 100 nm are the most often mentioned requirements (Ameller et al., 2003; Owens & Peppas, 2006). Active targeting, on the other hand, is often achieved by exploiting the differences in membrane biochemistry between cancer and normal cells. Active targeting of a drug to cancer cells may involve the conjugation of tissue- or cell-selective ligands

(Brannon-Peppas & Blanchette, 2004) that bind specifically with receptors on the surface of tumor cells, examples of which include lectin-carbohydrate and antibody-antigen interactions (Allen, 2002). Selectivity is ensured by choosing ligands that bind to antigens or receptors that are either uniquely expressed or over-expressed on the target cells compared to normal tissues. To increase the payload to be delivered to the tumor site, the drug may be concentrated in a carrier, e.g. nanoparticles, which is then conjugated with the targeting ligand (Fonseca et al., 2002; Garber, 2004).

Since drug administration routes and the mechanisms of drug delivery are different, specific bioconjugates have to be designed according to the delivery pathways and the characteristics of the tissues involved. The possibility of targeting drugs specifically to the colon has been shown to be feasible (Chourasia & Jain, 2003), and ligands such as lectins may have the potential to achieve this goal (Dalla Pellegrina et al., 2005). Wheat germ agglutinin (WGA) is an example of plant lectins that binds specifically to the N-acetyl-D-glucosamine sugar residues expressed by cancer cells and normal gastrointestinal epithelial cells. This specific characteristic may allow WGA to be applied as a ligand for targeting drug delivery to colon cells. Moreover, the binding of WGA to the gastrointestinal epithelial cells could prolong the retention time, result in high local concentration and improve the absorption profile of the drug. Selective

binding to cancer cells that expressed the WGA-binding glycoprotein would also facilitate the uptake of the WGA-conjugated delivery system into the cells.

The colonic mucosa, like other exposed epithelial surfaces, is covered by a mucus gel layer which protects the underlying epithelium against mechanical damage, biological agents and chemical irritants. Mucus is a complex mixture of large glycoproteins (mucins), water, electrolytes, sloughed epithelial cells, secretory immunoglobulin A (Ig A), lysozyme, lactoferrin and α_1-antitrypsin (Macfarlane et al., 2005). It forms a dynamic viscoelastic gel with high water content (95%) and specific physical properties, which allows the gel to flow. An important function of the mucus gel is to provide a medium for interaction between the lumen and the mucosal cells, and it has been referred to as an "unstirred aqueous layer" (Aksoy & Akinci, 2004). The macromolecular glycoprotein component (mucin) is responsible for the viscoelastic nature of mucus. In the intestinal mucus, the glycoproteins contain 77.5% of carbohydrates which comprise N-acetyl-galactosamine, N-acetyl-glucosamine, galactose, fucose and sialic acid at a dry weight molar ratio of 1.0:0.6:0.7:0.3:0.5 (Moghimi et al., 2001). The high viscosity of mucus can hinder drug diffusion and, consequently, drug absorption by underlying cells.

Most common malignant tumors of the large intestine are characterized by mucin production. The adenocarcinoma, a major colon tumor, forms moderate to well-differentiated glands that secrete variable amounts of mucin. The most aggressive tumor of the colon, the mucinous carcinoma, is associated with abundant mucin secretion (Aksoy & Akinci, 2004), which may impede normal drug delivery to the cancer cells. In this respect, mucoadhesive drug delivery systems that bind with mucin may prove advantageous, as they could improve contact between drug and intestinal cells, as well as prolong the residence time.

1.2 Polymeric nanoparticles

1.2.1 Nanoparticulate systems for drug delivery

Nanoparticles are engineered submicron-sized systems that range in size from a few nanometers to several hundred nanometers depending on their intended use (Haley & Frenkel, 2008). A variety of organic and inorganic materials, including polymers, lipids, ceramic and metals, have been used to construct nanoparticles (Yezhelyev et al., 2006). Most inorganic nanoparticles have a central core (usually metallic) and a protective organic surface coating. Organic nanoparticles include liposomes and other lipid-based carriers, polymeric nanoparticles, micelles and various ligand-targeted products. Structurally, nanoparticles have also been classified as dendrimers, micelles,

nanospheres, nanocapsules, liposomes, fullerenes and nanotubes. Based on their manufacturing methods and materials used, the size and shape of nanoparticles vary.

Therapeutic drugs may be incorporated into nanoparticles by surface attachment or encapsulation (Haley & Frenkel, 2008). Nanoparticulate drug delivery systems are highly versatile. Drug payloads range from small molecular weight drugs to macromolecules, from highly water-soluble agents to strongly hydrophobic drugs. The method of delivery may vary from the simple, localized delivery using a catheter-based approach (Song et al., 1998) to sophisticated targeted delivery whereby the conjugation of biospecific ligand onto the nanoparticle surface could direct drug delivery to the tissue of interest (Moghimi et al., 2001). In addition, the small particle size of nanoparticles yields a high surface area per unit weight ratio that can greatly facilitate drug dissolution and absorption in the gastrointestinal fluids. Nanoparticulate systems have been demonstrated to improve drug bioavailability (de Salamanca et al., 2006), facilitate drug solubilization (Merisko-Liversidge et al., 2003), sustain drug effect in target tissues (Moghimi et al., 2001) and improve the stability of therapeutic agents (Chavanpatil et al., 2006). Since the latter half of the 1980s, nanoparticles have been studied as carriers for drug delivery to challenge many diseases, including cancer, HIV, and diabetes (Yih & Al-Fandi, 2006). Much of the research has concentrated on improving the bioavailability of drugs with poor

absorption characteristics and providing controlled release of drugs. Table 1.2 gives examples of the many different types of nanoparticulate systems currently under various stages of clinical investigation (Wang et al., 2008).

Tabel 1.2 Examples of polymeric nanoparticles in clinical development

Compound	Name	Status	Indication
Albumin-paclitaxel	Abraxane or ABI-007	Market	Metastatic breast cancer
Paclitaxel-poliglumex	CT-2103; Xyotax	Phase III	Various cancers, particularly non-small-cell lung cancer; ovarian cancer
PEG-aspartic acid-doxorubicin micelle	NK911	Phase I	Pancreatic cancer
HPMA copolymer-doxorubicin	PK1; FCE28068	Phase II	Various cancers, particularly lung and breast cancer
HPMA copolymer-doxorubicin-galactosamine	PK2; FCE28069	Phase I/II	Particularly hepatocellular carcinoma
HPMA copolymer-paclitaxel	PNU166945	Phase I	Various cancers
HPMA copolymer-camptothecin	MAG-CPT	Phase I	Various cancers
HPMA copolymer-platinate	AP5280	Phase I/II	Various cancers
HPMA copolymer-DACH-Platinate	AP5346	Phase I/II	Various cancers
Dextran-doxorubicin	AD-70, DOX-OXD	Phase I	Various cancers
Modified dextran-camptothecin	DE-310	Phase I/II	Various cancers
PEG-camptothecin	Prothecan	Phase II	Various cancers

Abbreviations: PEG, polyethylene glycol; DACH, diaminocyclohexane; HPMA, N-(2-hydroxypropyl)methacrylamide.

Therapeutic agents of interest are incorporated into polymer nanoparticles either by physical entrapment within the polymeric matrix or by surface adsorption or conjugation. The size and surface properties of the nanoparticles determine their fate in the human body. Unless there is intended drug delivery to the RES, the size and surface of the nanoparticles must be designed to avoid RES clearance. Nanoparticles smaller than 100 nm in diameter have been found advantageous in this respect (Munshi et al., 1997). So is the coating of nanoparticles with the hydrophilic polymer, polyethylene glycol (PEG) (Laverman et al., 2001). Targeted drug delivery is realized by surface conjugation with a biospecific ligand, which may also favorably modify the intracellular disposition of the nanoparticles. Biocompatible, hydrophilic or hydrophobic polymer nanoparticles with surface-pendant amine, carboxyl or aldehyde groups have been fabricated for further bio-conjugation. A wide variety of ligands, such as folic acid (Das et al., 2008), antibody (Natarajan et al., 2008), and aptamers (Farokhzad et al., 2004) have been used for surface modification of polymeric nanoparticles to impart cancer cell targeting capability.

Polymers employed for nanoparticle fabrication have included synthetic polymers, such as Poly (D, L-lactic-co-glycolic acid) (PLGA), polyacrylates and polycaprolactones, and natural polymers (Wong et al., 2007). In particular, the application of polymer nanoparticles in oncology has grown greatly with the advent of

biodegradable polymers (Raghuvanshi et al., 2002; Kreuter et al., 2003). Biodegradable polymers are macromolecular materials capable of being degraded into simpler products through chemical or enzyme-catalyzed hydrolysis in the body. Biodegradable and biocompatible polymers as drug carriers are desirable to minimize toxicity and avoid the requirement to surgically remove the spent carriers. For these reasons, nanoparticles made of biodegradable materials are often fabricated to provide sustained drug release within the target site (Westedt et al., 2007; Yang et al., 2007). A good example of a biodegradable and biocompatible polymer is PLGA, an FDA-approved biodegradable and biocompatible polymer for biomedical applications.

1.2.2 PLGA nanoparticles

PLGA is a synthetic copolymer of lactic acid and glycolic acid and is one of the most widely used FDA-approved biodegradable polymers for controlled release drug delivery systems. The biodegradation of PLGA occurs through a hydrolytic chain cleavage mechanism. *In vivo*, PLGA undergoes chemical hydrolysis as well as enzymatic cleavage of its backbone ester linkages (Astete & Sabliov, 2006) to form the biologically compatible moieties, lactic acid and glycolic acid. The degradation products are subsequently eliminated from the body as carbon dioxide and water by the tricarboxylic acid cycle (Jalil & Nixon, 1990; Anderson & Shive, 1997). The

chemical structure of PLGA is illustrated in Figure 1.2, where "m" and "n" refer to

the relative amounts of lactide and glycolide units, respectively, in a specific PLGA

copolymer. The composition of PLGA can be varied by modifying the chain length

(molecular weight), as well as the ratio of lactic to glycolic acid monomers in the

polymer chain. This flexibility of composition is advantageous as it can be

manipulated to yield appropriate physical properties for a particular application. For

example, the *in vivo* degradation rate of PLGA can be tailored by controlling the ratio

of "m" and "n", with slower degradation rates observed for polymers with higher m/n

ratios (Lin et al., 2000).

PLGA: Poly(D,L-lactide-co-glycolide)

Breakdown by hydrolysis

Lactic acid   Glycolic acid
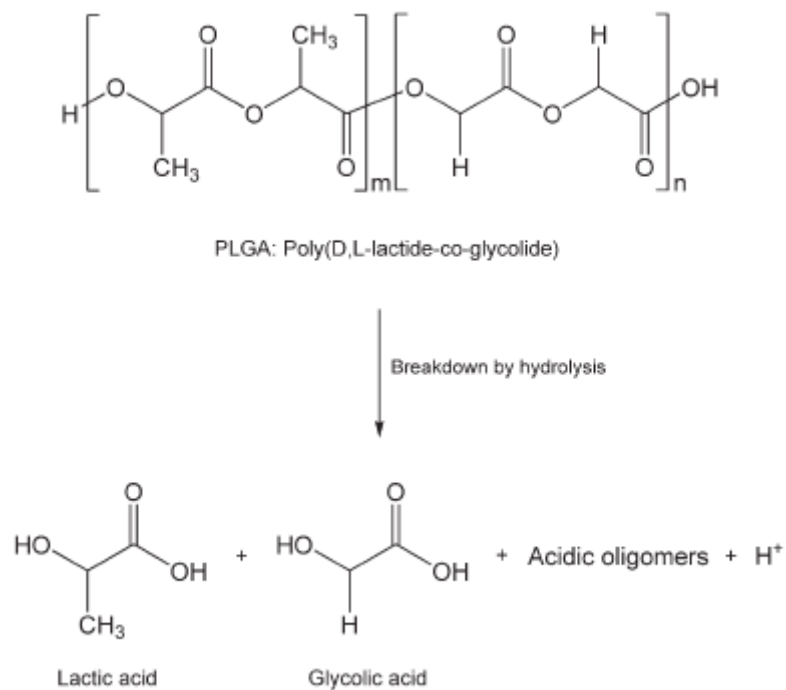
Figure 1.2 Chemical structure of PLGA and its degradation products (Taluja et al.,

2007)

PLGA has a long history of safe use as surgical sutures and implants, and it is applied in at least 12 different marketed products from 10 different companies worldwide (Avgoustakis, 2004). PLGA is used not only as a resorbable suture material and a scaffold for tissue engineering, but also in drug delivery (Ignatius & Claes, 1996; Day et al., 2005). PLGA delivery platforms have been developed for the sustained and targeted delivery of plasmid DNA (Abbas et al., 2008); recombinant HIV envelope (env) protein (Moore et al., 1995); hormones (Sun et al., 2008) and anticancer agents (Gryparis et al., 2007; McCarron et al., 2008). PLGA nanoparticles have been formulated as colloidal carrier systems to improve drug efficacy (Brigger et al., 2002; Sahoo et al., 2004; Fukumori & Ichikawa, 2006). Drug release from PLGA nanoparticles is controllable through the rate of drug diffusion in the polymer matrix and/or degradation of the polymer matrix (Hariharan et al., 2006).

1.2.2.1 Preparation

Preparation of nanoparticles is frequently based on the use of dispersed systems in which solid or liquid phases are dispersed in fluid media to constitute embryos of the final particles. Single and multiple emulsion systems have been used to encapsulate drugs into polymeric particles. Normally, an organic solvent is required to dissolve

the polymers in the emulsion step. To decrease droplet size and avoid droplet coalescence, surfactants are usually required.

Techniques for preparing PLGA nanoparticles may be divided into bottom-up and top-down approaches. The bottom-up techniques, which include emulsion or microemulsion polymerization, interfacial polymerization and precipitation polymerization, employ the monomers as a starting point, and nanoparticle fabrication occurs simultaneously with monomer polymerization into PLGA. Top-down techniques include the emulsion evaporation, emulsion diffusion, solvent displacement and salting out methods in which nanoparticles are prepared from preformed PLGA (Panyam & Labhasetwar, 2003; Astete & Sabliov, 2006). A good review on the characteristics of PLGA nanoparticles prepared by these different methods as a function of processing parameters (polymer concentration, co-polymer ratio, polymer molecular mass, surfactant concentration, solvent used, phase volume ratio) has been published by Astete and Sabliov (Astete & Sabliov, 2006).

Of the techniques reported, emulsion evaporation and emulsion diffusion are the two most frequently employed. In the emulsion diffusion method, the PLGA polymer is dissolved in an organic phase which is partially miscible in water, and the organic phase is emulsified with an aqueous surfactant solution under stirring or sonication.

Diffusion of the organic solvent and the counter diffusion of water into the emulsion droplets induce polymer nanoparticle formation (Quintanar-Guerrero et al., 1998). The emulsion evaporation method is similarly based on emulsification principles, except that the organic solvent for dissolving the polymer/drug is highly volatile, and is evaporated off following emulsification. Examples of appropriate solvents include ethyl acetate, chloroform and methylene chloride. Like the emulsion diffusion method, the aqueous phase also contains a dissolved surfactant to impart stability, and emulsification is carried out under high-shear stress to reduce the size of the emulsion droplet. Important parameters in emulsion evaporation method that may affect nanoparticle size are: PLGA co-polymer ratio, polymer concentration, solvent characteristics, surfactant/polymer molecular mass, viscosity, phase volume ratios, stirring rate, and temperature. Our group has shown that paclitaxel can be incorporated at a high loading efficiency into PLGA nanoparticles using a modified emulsion solvent evaporation method (Mo & Lim, 2005).

1.2.2.2 Applications

Biodegradable nanoparticles formulated from PLGA have been widely investigated for sustained and targeted delivery of therapeutic agents, including plasmid DNA, proteins, and low molecular weight compounds (Panyam & Labhasetwar, 2003; Jiang et al., 2005; Sahoo & Labhasetwar, 2005). Encapsulation in PLGA nanoparticles

could protect susceptible protein therapeutic agents from physical denaturation and chemical degradation, thereby lengthening their half-life. The administration route for the proteins can also be changed from injection, which is invasive and associated with poor patient compliance, to a more acceptable non-invasive route.

PLGA nanoparticles are also extensively applied for the delivery of anticancer agents due to their capacity to enhance drug efficacy by regulating the drug release rate, improving drug stability and prolonging drug circulation time *in vivo*. Incorporation of anticancer agents in nanoparticles has been shown to result in a more favorable circulation half life, area under the concentration-time curve (AUC) and peak plasma concentration (Wang et al., 2004; Kim et al., 2005; Mathot et al., 2006; Lecaroz et al., 2007). An example is the paclitaxel-loaded PLGA nanoparticles (Vicari et al., 2008), which not only reduced the dose and frequency of administration of paclitaxel, but also provided improved targeting of the drug to cancer cells. Other anticancer agents investigated with PLGA nanoparticles included doxorubicin, camptothecin and 5-fluorouracil (Betancourt et al., 2007; Li et al., 2008; McCarron et al., 2008). Nevertheless, PLGA nanoparticles are not without shortcomings, one of which is their non-site specific targeting capability. Another is the rapid removal of the naked PLGA nanoparticles from the bloodstream by the RES system. Complete clearance

takes only a matter of minutes, with most of the nanoparticle dose concentrating in the liver and spleen (Panagi et al., 2001).

Several approaches to improve the selectivity of the delivery system have been investigated (Allen, 2002; Nobs et al., 2004; Alexiou et al., 2006), the most common of which is the application of nanoparticles conjugated with targeting ligands. Ligand conjugation allows the specific delivery of the drug load to cancer cells, which not only increases therapeutic efficacy, but also reduces side effects associated with non-discriminatory drug deposition. In one study, monoclonal antibody (mAb)-modified PLGA nanoparticles (Kocbek et al., 2007) were shown more likely to be bound to the targeted invasive epithelial breast tumor cells than non-coated nanoparticles. PLGA nanoparticles functionalized with the A10 RNA aptamer (Cheng et al., 2007) also resulted in enhanced nanoparticle delivery to the prostate tumor in the xenograft mouse model compared to equivalent non-conjugated nanoparticles. In yet another study, PLGA nanoparticles conjugated with poly (L-lysine)-poly(ethylene glycol)-folate were observed to improve cellular uptake of the nanoparticles into the folate receptor over-expressing KB cells by folate receptor-mediated endocytosis (Kim et al., 2005).

A few PLGA-based drug delivery formulations have been in use in the clinic. Lupron Depot^{TM}, an injectable suspension formulation of leuprolide acetate-loaded PLGA microspheres, is the first peptide formulation for the treatment of advanced prostate cancer. Peptide release occurs over a period of 1, 3 or 4 months, and is governed mainly by the PLGA degradation rate (Okada et al., 1994; Taluja et al., 2007). Nutropin Depot^{TM} is another PLGA microsphere formulation, and it has been approved by the FDA in late 1999 for the treatment of pediatric growth hormone deficiency (Johnson et al., 1996). Consisting of micronized particles of recombinant human growth hormone (rhGH) embedded in a PLGA matrix, this formulation requires only one or two doses a month compared to the conventional therapy that requires multiple doses per week. There are as yet no PLGA nanoparticle-based drug delivery formulations in the market.

1.2.3 Cellular uptake of nanoparticles

Some anticancer drugs can only exhibit their effects when there is adequate cellular uptake either because their receptors are located in the cytosol or their site of action is an intracellular organelle. Paclitaxel is one such example. To achieve cytosolic delivery, the drug-carrier systems are required to overcome several barriers, which include traverse across cell membrane, endosomal uptake and degradation, metabolism and efflux transport. To this end, nanoparticles have certain distinct

advantages, and paclitaxel-loaded PLGA nanoparticles have been developed recently by a few research groups (Mu & Feng, 2003; Wang et al., 2003). Due to their small size, nanoparticles can penetrate deep into tissues through fine capillaries, cross the fenestration present in the epithelial lining (e.g., liver), and are generally taken up efficiently by the cells, which allows for efficient drug accumulation at the target sites in the body (Vinogradov et al., 2002). Figure 1.3 depicts a typical intracellular trafficking pathway for nanoparticles and other colloidal drug-carrier systems.
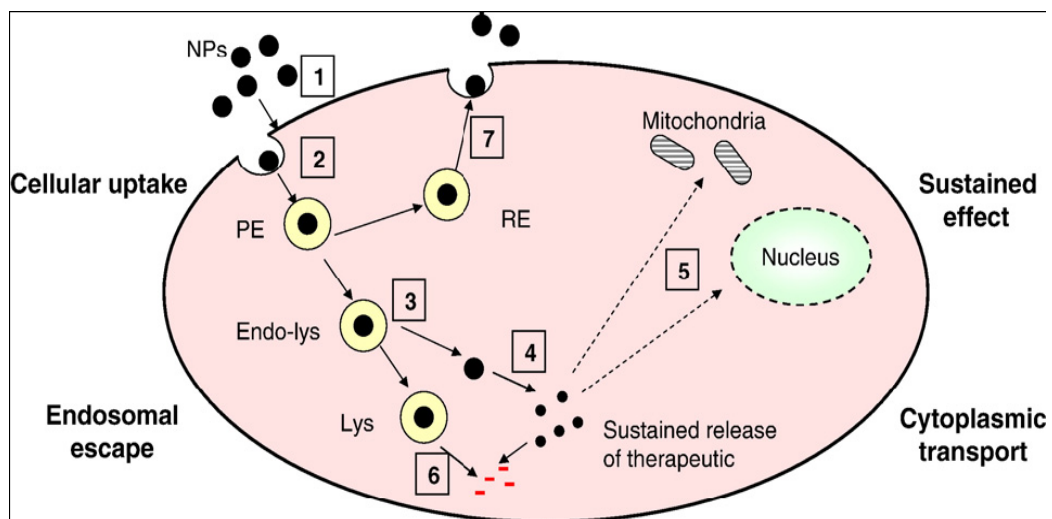
Figure 1.3 Schematic drawing of steps involved in cytosolic delivery of therapeutics using polymeric nanoparticles (NPs). (1) Cellular association of NPs, (2) Internalization of NPs into the cells by endocytosis, (3) Endosomal escape of NPs, (4) Release of therapeutic in cytoplasm, (5) Cytosolic transport of therapeutic agent, (6) Degradation of drug either in lysosomes or in cytoplasm, (7) Exocytosis of NPs. (Vasir & Labhasetwar, 2007)

Generally, two mechanisms are available for the uptake of nanoparticles by absorptive epithelia; these are paracellular transport and endocytosis. However, the paracellular route is limited by the small surface area of the intercellular spaces and the tight junctions between the epithelial cells (Nellans, 1991). Most of the nanoparticle formulations are designed to associate with cell membrane and be internalized into cells by means of endocytic mechanisms. Endocytosis of nanoparticles depend on the physicochemical properties of the particles and the physiological state of the *in vivo* environment (Florence, 2004). Nanoparticles not functionalized with a ligand are internalized by cells through adsorptive endocytosis, which is initiated by non-specific physical adsorption of the nanoparticles to the cell surface through electrostatic forces, hydrogen bonding or hydrophobic interactions (Segretain et al., 1992). Following endocytosis, the intracellular vesicles would fuse with organelles referred to as endosomal compartments. Various types of membrane vesicles have been observed to play active roles in endocytosis. Among the various uptake routes, receptor-mediated endocytosis (RME) has attracted most attention for the design of targeted drug delivery systems as it actively transfers the delivery system into the intracellular milieu only when triggered by specific ligand-receptor interaction at the cell membrane. Another reason why RME is attractive is that, while nanoparticles generally have relatively higher intracellular uptake rates compared to microparticles (Desai et al., 1996; Desai et al., 1997), the non-specific cellular uptake of

nanoparticles is often not of a high enough capacity to enable cytosolic accumulation of therapeutic level of an anticancer drug. This has been an important rate-limiting step for the cellular uptake of cationic liposomes in the transfection of Chinese hamster ovary (CHO) cells (Hui et al., 1996), and for gene transfer by chitosan nanoparticles (Chan et al., 2001).

1.3 Wheat germ agglutinin for drug targeting

1.3.1 Wheat germ agglutinin

Lectins are carbohydrate-binding proteins originating from plants, microorganisms or animals. They are multivalent molecules with two or more sugar-binding sites that can cause agglutination of plant and animal cells, and precipitation of polysaccharides, glycoproteins, peptidoglycans and glycolipids. Lectins can recognize and bind with specific sugar residues in cell membranes (Rodrigues et al., 2003). The specificity, multivalent feature and relatively low immunogenicity of lectins underpin their appeal as ligands for developing site-specific nanoparticulate systems for anticancer drug delivery.

Wheat germ agglutinin (WGA) is a lectin purified from the germinating seeds of common wheat (Triticum vulgare). It is a 36-kDa protein consisting of two identical subunits, each of which comprises of an assembly of four homologous domains (Figure 1.4).
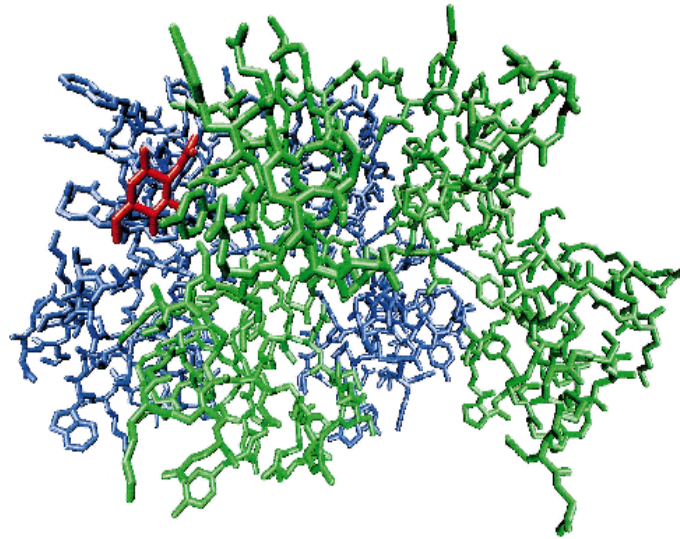
Figure 1.4 Structure of N-acetylglucosamine–wheat germ agglutinin complex: red,

N-acetylglucosamine; blue / green, wheat germ agglutinin (Lehr, 2000)

WGA consists of a group of closely related isolectins with an isoelectric point at about pH 8.5-9 (Monsigny et al., 1980; Sugawara et al., 2008). The receptor sugar for WGA is N-acetyl-D-glucosamine and *N*-acetyl-D-neuraminic acid residues (Kennedy et al., 1995). WGA can bind to oligosaccharides containing terminal N-acetyl-D-glucosamine or chitobiose, structures which are common to many serum and membrane glycoproteins (Kennedy et al., 1995). Native WGA can also interact with some glycoproteins via the sialic acid residues (Monsigny et al., 1979; Monsigny et al., 1980). WGA shows preferential binding to the dimers and trimers of sugar (Pan et al., 2005). The agglutination between WGA and its receptors occurs very rapidly, as disclosed in one study in which all the binding sites available for WGA on the Caco-2 cell membrane were occupied within 10 min of incubation (Wirth et al., 2002).

WGA does not only bind to cell surface and human enterocytes, but the WGA-receptor interaction triggers internalization by the cells by receptor-mediated endocytosis (Mo & Lim, 2004). The endocytic process involves the epidermal growth factor receptor, which is present at considerable density on enterocytes (Serpe et al., 2004) (Figure 1.5).
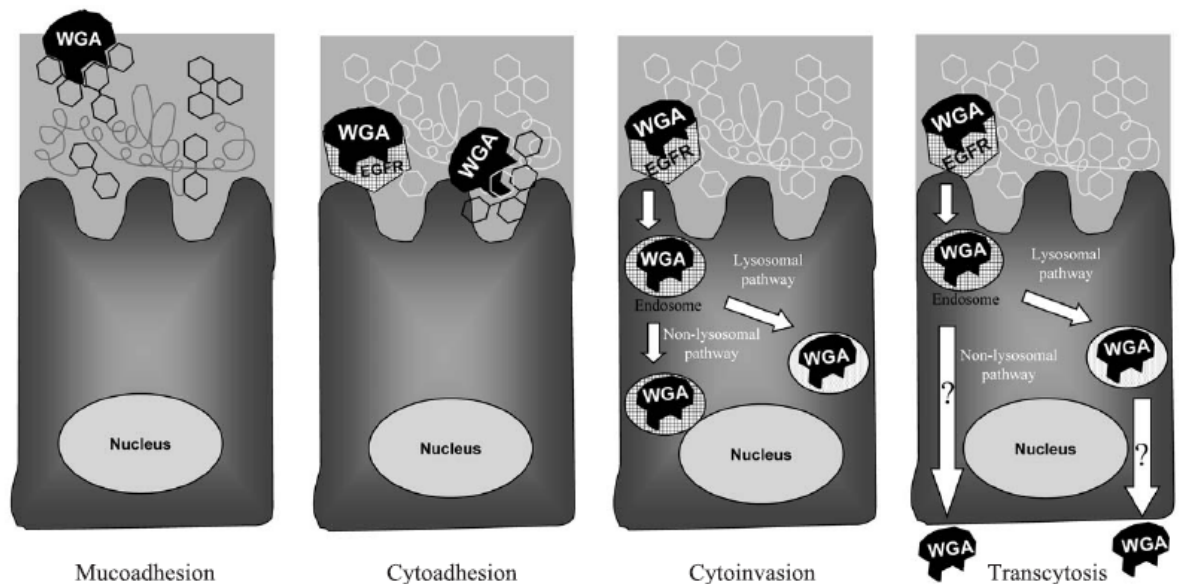
Figure 1.5 Possible pathways for lectin-mediated drug delivery to enterocyte as exemplified by WGA (Gabor et al., 2004)

WGA has the potential to be a good ligand for the targeted delivery of anticancer drugs to the colon. Lectin affinity chromatography has shown that WGA can bind to colon tissue (Serpe et al., 2004). Compared with plant lectins of different carbohydrate specificity, e.g. peanut agglutinin (PNA) and Ulex europaeus isoagglutinin I (UEA-I), WGA has the highest binding rate to intestinal cell lines of

human origin, human colonocytes and prostate cancer cells (Gabor et al., 1998). Sugar receptors for WGA, the *N*-acetyl-D-glucosamine and *N*-acetyl-D-neuraminic acid residues, are expressed in the glycocalyx of gastrointestinal cells (Matsuo et al., 1997; Khanvilkar et al., 2001), and WGA is rapidly internalized into the cytoplasm of human enterocyte-like Caco-2 cells (Gabor et al., 1998). WGA also has relatively good resistance to acid pH and enzymatic degradation, and WGA-binding sites are ubiquitous along the gastrointestinal tract (Gabor et al., 1997). Moreover, data from several studies have demonstrated that WGA-conjugated drugs have improved intracellular availability in the colon cells due to a combination of features such as cytoadhesion, cytoinvasion and partial lysosomal accumulation (Wirth et al., 1998; Gabor et al., 2002).

Colon cancer is often accompanied by alterations in the production of glycoproteins on the cell surface (Singhal & Hakomori, 1990). In a study of human colonic mucin, Boland et al. confirmed the different expression of carbohydrate residues in 21 colon cancer specimens relative to normal tissues (Boland et al., 1982). Another study relating lectin-binding patterns in normal and neoplastic colonic mucosa showed different patterns for WGA staining in the carcinoma specimens compared with normal mucosa (Campo et al., 1988). The aberrant glycosylation patterns expressed during malignancy or colitis underscore the attraction of using a lectin-based delivery

platform for colon-specific drug delivery. In addition, saturation analysis using the fluorescently labeled WGA indicated that the WGA-binding capacity of Caco-2 cells was about 13 fold higher than that of normal human colonocytes (Gabor et al., 1997). The evidence to date suggests that WGA-mediated drug delivery is a promising strategy to overcome the mucosal barrier and possibly the enzymatic barrier for colonic drug delivery (Dalla Pellegrina et al., 2005).

1.3.2 Applications

WGA recognizes both sialic acid and N-acetyl-D-glucosamine, and has been shown to transcytose across the small intestinal epithelia into the systemic circulation (Giannasca et al., 1994). Specific binding followed by internalization of WGA in intestinal and alveolar epithelial cells have been demonstrated by many researchers (Ishiguro et al., 1992; Lehr, 2000; Yi et al., 2001). Mucosal immunogenicity studies with tomato lectin, WGA, *Phaseolus vulgaris* (PHA) and *Ulex europaeus* I (UEA-1), showed that WGA is one of the least immunogenic among the lectins studied (Lavelle et al., 2000). Cytoadhesion of WGA was followed by immediate endocytosis, with 30% (monolayer) to 60% (single cell) of the bound WGA internalized within 20 min.

WGA-conjugated colloidal particles have been investigated for their capacity to enhance drug targeting and drug uptake by cancer cells. In one study,

WGA-conjugated chitosan-Ca-alginate microparticles (MPs) were designed to deliver 5-FU to colon region (Dodov et al., 2009). The results suggested that WGA-conjugated MPs maintained the same sugar specificity as the WGA and prolonged residence time in colon. In another study, WGA was covalently attached to liposomes through avidin-biotin interaction, giving rise to particles of around 120 nm in diameter (Abu-Dahab et al., 2001). The amount of cell-associated WGA-liposomes after 30-min incubation with A549 cells was more than 10-fold that of the unmodified liposomes. More recently, WGA was covalently conjugated to PLGA microspheres by a carbodiimide/N-hydroxysuccinimide method, and the interaction of these particles with Caco-2 cell monolayers was investigated using BSA- or glycine-conjugated PLGA microspheres as control (Ertl et al., 2000). WGA-PLGA nanoparticles were also studied to deliver the model drug, mometasone furoate (MF), to A549 cells. The cellular uptake of nanoparticles, intracellular drug levels, and anti-proliferative activity were assessed (Surti et al., 2008). Surti et al. (Surti et al., 2007) also demonstrated an improved and sustained antiproliferative activity obtained with the WGA-conjugated nanoparticles in vitro. The same group showed that the WGA-conjugated budesonide nanoparticles exhibited better bioavailability when administered into the lungs of rats compared to unconjugated nanoparticles (Surti & Misra, 2008). WGA-grafted PLGA nanospheres and micospheres have also been reported to show enhanced binding and uptake by Caco-2 monolayers (Ertl et al.,

2000; Weissenboeck et al., 2004). WGA conjugated with doxorubicin has also been explored as an acid-labile chemotherapeutic prodrug for targeting against colon carcinoma cells (Wirth et al., 1998). Almost all of these studies demonstrated the phenomenon of greater cellular uptake of drug and drug delivery systems following WGA conjugation. However, the effect of such conjugation on drug retention within the colon cancer cells has not been investigated. Moreover, not many of the studies have used normal cells as controls when assessing the effects of the the drug delivery platforms in colon cell culture.

Our laboratory had demonstrated that WGA-receptor mediated endocytosis potentiated the anticancer activity of paclitaxel against A549 and H1299 cell lines compared with the conventional formulation, which was attributed to efficient intracellular drug accumulation via WGA-receptor-mediated endocytosis (Mo & Lim, 2004; Mo & Lim, 2005). *In vivo* study showed that an intratumoral injection of WNP at a paclitaxel dose of 10 mg/kg was effective at arresting the growth of A549 tumor nodules in the SCID mouse model (Mo & Lim, 2005). To sum up, WGA remains its cytoadhesion and cytoinvasion properties after conjugation onto PLGA nanoparticles. WGA-PLGA system had superior *in vitro* and *in vivo* anti-proliferation activity against A549 cells compared with non-conjugated PLGA nanoparticles. On the basis

of these results, it may be concluded that WGA-PLGA nanoparticles has significant potential application as a targeted delivery system of anti-cancer agents.

1.4 Barriers for intracellular drug delivery

There are diverse biological barriers interposed between the site of administration and the target cell that drugs which act intracellularly must be able to overcome. Effective intracellular drug delivery involves the successful traversing of these biological barriers, which may involve the modulation of the permeability of relevant biological barriers, or the enhancement of the concentration and residence time of the delivery systems at the biological barriers. Indiscriminate deposition of the drug at other sites must be avoided to limit adverse effects and ensure biocompatibility. If the target cells are not readily accessible, adequate systemic absorption of the drug is required to ensure therapeutic drug concentrations are reached in the circulation. The absorbed drug will then need to be directed to the target cells, where an appropriate residence time is required for cellular uptake, preferably in a controlled manner. In the next sections, the biological barriers to intracellular drug delivery in the colon will be discussed followed by methods employed to enhance the intracellular bioavailability.

1.4.1 Biological barriers

There are numerous barriers that can hinder effective drug delivery in the gastrointestinal tract. The interplay between digestive fluids and peristalsis can dilute and accelerate the transit of drugs and their delivery systems, leading to poor absorption. The harsh environment in the gastrointestinal tract can cause drug degradation by chemical or enzymatic hydrolyses; and drug access to the absorptive cells can be limited by the overlying viscous mucus layer (Shah & Rocca, 2004). However, as a site for drug delivery, the colon offers distinct advantages on account of a near neutral pH, a much longer transit time, and relatively low proteolytic enzyme activity. Systemic bioavailability is also less of a concern for localized drug delivery to the colon.

Nevertheless, there are still several challenges to the effective delivery of therapeutic agents to the colon. This includes the need to maintain the structural integrity of the drug and delivery system during transit to the colon by building in resistance to enzymatic and chemical degradation along the GIT. There is also considerable resistance to the penetration of the mucosal interface, in particular the mucus layer, which is about 25-115 μm thick in the human colon (Matsuo et al., 1997; Strugala et al., 2003). The gel-like consistency of the mucus layer is a diffusive barrier, although it can also be successfully exploited for drug delivery through the development of mucoadhesive formulations. The fixation of a drug delivery system close to the

absorption site has been shown to improve the bioavailability of the therapeutic agent.

At the cellular level, the first barrier encountered by the delivery system is the plasma

membrane. Even for drugs that managed to enter the cells, the existence of multidrug

resistance (MDR) efflux pumps in many cancer cells can keep the intracellular drug

levels below the cell-killing threshold by actively extruding the drugs from the cells.

Drugs taken up by the cells via endocytosis may have to initiate endo-lysosomal

escape to avoid degradation. Within the cytosolic milieu, there are microtubules,

intermediate dilaments and microfilaments that are organized into a dense network to

form the cytoskeleton (Lechardeur & Lukacs, 2006). These filaments may impede the

diffusion of the drug or drug delivery system, and will have to be overcome if the

drug were to reach its target site within the cell.

1.4.2 Strategies to enhance intracellular accumulation

Although there are diverse mechanisms by which macromolecules and small particles

can traverse the epithelial layer (Conner & Schmid, 2003), most nanoparticle-based

drug delivery platforms are designed to gain cellular entry by RME. Thus, they are

formulated to have an appropriate ligand conjugated on their surface that will aid in

cellular recognition, binding and internalization. A wide variety of ligands has been

explored for the targeting of anticancer agents (Ross et al., 1994; Chu et al., 2006;

Mamot et al., 2006). Alternatively, the nanoparticles may be conjugated with lectin

molecules capable of enhancing interaction with the mucus layer. The latter promotes nanoparticle transport across the intestinal mucosa by bringing the nanoparticles in closer proximity to the surface of epithelial cells (Irache et al., 1994; Clark et al., 2000). To initiate endosomal escape, the drug may be conjugated to the nanoparticles by acid-labile linkages that will hydrolyze in the low pH environment of the endosomes (Hoffman et al., 2001; Jones et al., 2003). In this respect, PLGA nanoparticles may have an advantage, as they have been reported to successfully cross the endosomal barrier to deliver the drug payload into the cytoplasm (Panyam et al., 2002). Encapsulation within nanoparticles could also be a mechanism to protect anticancer drugs from membrane efflux pumps associated with multidrug resistance, and exocytosis (Panyam & Labhasetwar, 2003; Park et al., 2006; Ma et al., 2009). Reversing MDR phenotypes by colloidal drug carriers or P-gp inhibition by lipids or nonionic surfactants used in the formulations were suggested as a possible mechanism for the enhanced toxicity in cancer cells (Wong et al., 2006). Nanoparticles localized in the cytoplasmic compartment may be slow in diffusing across the cell membrane for exocytosis because of the gel-like viscous characteristics of the cytoplasmic fluid (Panyam & Labhasetwar, 2003).

1.5 Statement of purpose

WGA can serve as a specific ligand to actively interact with colon cell membrane through RME. PLGA nanoparticles may also play an important role to improve the bioavailability of paclitaxel by resolving its intractable solubility profile and providing a large surface area for the drug to interact with the biological milieu at the absorption site. Moreover, the interaction between WGA and cell membrane or mucus can enhance the residence time of the nanoparticles at the absorption site, while the presence of intracellular glycocalyx offered further opportunity to retain the nanoparticles within the cytosol.

Our objective was to exploit the cytoadhesive and cytoinvasive properties of WGA to develop a colon cancer targeted PLGA nanoparticulate system for paclitaxel. PLGA have been widely applied as a carrier in drug delivery systems because of its biocompatible and biodegradable properties. The nanoparticle formulation was preferred because the small size of the nanoparticles might afford evasion from RES capture *in vivo*, while encapsulation of paclitaxel within the nanoparticles allowed enhanced drug payload delivery to the target cells. Previous work in our laboratory has shown that the surface of PLGA nanoparticles could be readily activated for WGA conjugation, and the resultant nanoparticles were effective at delivering paclitaxel into lung cancer cells *in vitro* and *in vivo* (Mo & Lim, 2005; Mo & Lim,

2005). This provided the proof of concept of WGA as a targeting ligand to enhance the efficiency of delivery of paclitaxel to cancer cells. Colon cancer is targeted in this project because it has been the leading cause of tumor death worldwide, and chemotherapy for colon cancer is often associated with serious side effects. Moreover, colon cancer with mucin production is often difficult to treat (Nakamori et al., 1994; Matsuda et al., 2000).

Mucin is widely expressed in the intestine and in colon cancers. The major component of mucin is glycoproteins, which include many WGA-recognizable glycoproteins. Nanoparticles can be made to interact with the mucin, a phenomenon known as mucoadhesion, by conjugation with WGA. It is generally accepted that mucoadhesive polymers will increase drug concentration in the vicinity of the intestinal epithelial cells by its close proximity with the intestinal mucosa, and this in turn will enhance drug absorption. However, mucin is also an impediment layer to drug delivery as it slows down drug diffusion considerably.

The hypothesis for this project was that the conjugation of WGA to PLGA nanoparticles loaded with paclitaxel (WNP) could improve the delivery of paclitaxel to colonic cancer cells. Paclitaxel has broad antineoplastic activity, including against colorectal cancer cells. Its clinical application is however, limited by its poor

solubility in aqueous media and its non-specific activity against both cancerous and normal cells. Incorporating the drug in a hydrophobic polymer carrier may alleviate the solubility issue. PLGA was proposed as the polymer of choice for this purpose because of its proven history of use in biomedical applications. Nonetheless, cellular uptake of PLGA nanoparticles has been shown to be of low capacity (Chen & Langer, 1998) and specificity (Kim et al., 2005). Therefore, WGA was proposed as a targeting moiety to bind the PLGA nanoparticles to the cancerous colon tissue, and to facilitate the uptake of the nanoparticles by the colonic cells via RME. A combination of these mechanisms should allow a higher intracellular accumulation of paclitaxel by the cancerous cells, thereby realizing the potential of the drug without the attendant side effects.

To prove this hypothesis, studies were conducted with the following specific objectives:

1. To screen selected cancer cell models for WGA-binding affinity

2. To assess the cytotoxicity of WGA against the chosen colon cancer cell models

3. To determine the uptake capacity, cellular paclitaxel accumulation and cytotoxicity profile of the WNP on selected colon cancer cell models and compare the data with those obtained with the clinical paclitaxel formulation.

4. To evaluate the effect of mucin on the intracellular delivery of the WNP by

   repeating the studies in an established mucin-secreting cell model (LS174T).

5. To evaluate the intracellular trafficking of WNP in the colon cancer cell model

Chapter 2

Screening for wheat germ agglutinin-binding glycoprotein in colon

cell models

2.1 Introduction

Lectins, including WGA, have become important tools in glycoconjugate research because they can be used reliably to detect, isolate and purify specific glycoconjugates. Research on the applications of glycoconjugates has been driven by a recent explosion of interest in glycobiology, i.e. the biological activities of glycoconjugates (Large and Warren 1997), in particular glycoproteins (proteins containing covalently bound carbohydrate) that may have therapeutic potential (Conradt 1991). Glycosylation is a key step in a number of cellular processes, and glycoproteins are ubiquitous constituents of all living cells (Amoresano et al. 2000). Carbohydrate-mediated recognition plays a very important role in fertilization, immune defence, viral replication, parasitic infection, cell–matrix interaction, cell–cell adhesion and enzymatic activity (Komath et al. 2006). Many cancer cells, including colon cancer cells, overexpress some kind of glycoproteins, and the structural changes in the expression of these molecules contribute to functional differences between cancer and normal cells. Cell surface glycosylation changes during oncogenesis is further thought to be correlated with malignancy potential (Tang et al. 2005).

Lectins, including WGA and some other adhesion molecules, can not only recognize specific receptor-like structures of the cell membrane, but may subsequently trigger

active transport of the lectin-receptor complex by vesicular transport processes into the cell (Lehr 2000). Several previous studies have confirmed the binding of lectin or lectin-conjugated drug delivery systems to glycoconjugates on cell surface, followed by the facilitated uptake of the systems by the cells (Hussain et al. 1997; Qaddoumi and Lee 2004; Ono et al. 2006). On this basis, lectins have been used as targeting molecules to localize particular glycoconjugates, such as glycoproteins or glycolipids, onto cell surface or intracellular receptors. For example, lectins labeled with fluorophore or gold particles are important probes for detecting cell surface components and intracellular receptors in immunological and biochemical assay procedures (Kimura et al. 1979; Roth 1983). More recently, lectin-conjugated trifunctional nanobiosensors have been shown to bind to the surface glycoproteins of A549 cells, suggesting their potential application in mapping glycoconjugates on cell surfaces (Xie et al. 2008).

In order to use WGA as a tumor-targeting ligand, there is a need to establish the expression profile of its receptor glycoproteins in target cells. WGA has a well defined and narrow receptor specificity, its receptors comprising of oligosaccharides containing terminal N-acetyl-D-glucosamine or sialic acid (Kennedy et al. 1995). These structures are common to many serum and membrane glycoproteins (Kennedy et al. 1995), making it pertinent to determine whether a WGA-based targeting drug

delivery platform is capable of discriminating diseased cells from normal cells. The experiments in this section were set out to evaluate whether model colon cancer cells over expressed the specific oligosaccharides that would bind the proposed WGA-conjugated anticancer drug delivery platform.

Intensified research in glycobiology has led to the development of many new techniques for analyzing biological carbohydrate molecules. Some of these techniques include 2-Dimensional Nuclear Magnetic Resonance (2-D NMR) and Fast Atom Bombardment Mass Spectroscopy (FAB-MS). These methods are indispensable for a complete structural analysis of pure glycol molecules, but may not be readily accessible because they require expensive equipment and skilled operators. There are situations where a less refined analysis that can be performed in a short period of time with small amounts of material is sufficient. Other than the above sophisticated methods, surface membrane glycoproteins can also be investigated using histochemical techniques, while high-resolution electrophoresis is widely used for analyzing complex protein mixtures. A combination of these techniques with the sensitive biotin-based labeling and biotin-avidin-peroxidase detection system allows the rapid analysis of small quantities, ng to about 1 μg, of glycoproteins immobilized on membranes. Lectin blot analysis is an example of a glycoprotein analytical method that combines histochemical techniques with electrophoresis.

For this study, a preliminary comparative electrophoretic study was undertaken using lectin blot analysis to investigate the surface and intracellular glycoproteins expressed in model colon cells. The 3 colon cell lines evaluated were the Caco-2, HT-29 and CCD-18Co cells. Caco-2 cells originate from an old male colon cancer patient. They have been the standard *in vitro* model of intestinal function because they display the characteristics of enterocytic differentiation, including the brush border of villus tip and tight junctions (Hidalgo et al. 1989). However, Caco-2 cells are also known to display a mixed morphology and functionality depending on the passage number of the culture (Hidalgo et al. 1989; Jumarie and Malo 1991). HT-29 cells originated from a human intestinal adenocarcinoma. They are poorly differentiated but contain a small proportion of mucin-secreting cell types which can be selected under certain culture conditions, such as in the presence of methotrexate (Lesuffleur et al. 1991; East et al. 1992). CCD-18Co cells are normal colon fibroblast cells which exhibit most of the known characteristics of intestinal sub-epithelial myofibroblasts (Valentich et al. 1997).

2.2 Materials

Caco-2 cells (passage 55-65) were obtained from the Riken Cell Bank (Tsukuba, Ibaraki, Japan); HT-29 (passage 140) and CCD-18Co cells (passage 7) were obtained from the American Type Culture Collection (ATCC; Rockville, MD, USA); tissue

flasks and 96-well plates were from NUNC (Roskilde, Denmark); streptomycin, penicillin, Hank's balanced salt solution (HBSS), *N*-[2-hydroxyethyl] piperazine-*N*´-[2-ethanesulfonic acid] (HEPES), dimethyl sulfoxide (DMSO) and wheat germ agglutinin (WGA) were all from the Sigma Chemical Company (St. Louis, MO, USA); minimal essential medium (MEM), fetal bovine serum (FBS) and non-essential amino acids (NEAA) were from Gibco BRL Life Technology (Grand Island, NY, USA); biotinylated-wheat germ agglutinin and Vectastain Elite ABC kit were from Vector Laboratory (Burlingame, CA, USA); protease inhibitor was from Roche Diagnosis (Basel, Switzerland); polyvinylidene fluoride (PVDF) membrane was from Bio-Rad Laboratories Inc (Hercules, CA, USA); Supersignal west pico and west femto chemiluminiscence reagent were from Pierce biotechnology Inc (Rockford, IL, USA). All the solvents used in the experiments were HPLC grade.

2.3 Methods

2.3.1 Basic theory of lectin blot analysis

Western blot, which electronically transfers proteins from a gel to a membrane, is a popular method for detecting cellular proteins. By combining the resolving power of electrophoresis with the specificity of immunological detection, it can detect a protein in a mixture of any number of proteins, and provide information on protein size and identity (Rosenberg, 1996). Often, the electrophoretic blots are combined with

avidin-biotin methods to provide a more complete interpretation of the glycocalyx structural data. Proteins from cells are separated by conventional SDS-PAGE, then transferred and immobilized onto suitable membranes for lectin binding. Visualization of the bound lectin is provided via biotinylated lectin-avidin binding, in which the lectin is tagged with biotin, thus allowing it to bind with a preformed avidin. Avidin has such an extraordinarily high affinity for biotin (dissociation constant of about 10^{-15}, a million times higher than antibody–antigen affinity) (Green 1975) that the binding of avidin to biotin is essentially irreversible. By covalently linking avidin or biotin with ligands, such as fluorochromes, enzymes or EM markers, the biotin-avidin system can be utilized to study a wide variety of biological structures and processes. This system has proven to be particularly useful in the detection and localization of antigens, glycoconjugates and nucleic acids by employing biotinylated antibodies, lectins and nucleic acid probes, respectively (Milton. 1998). When applied in Western blotting for the analysis of glycoproteins by lectins, it is known as a lectin blot.

Gordon and Pena (Gordon and Pena 1982) have discussed the advantages of using biotinylated lectins for detecting glycoproteins on membranes. Their method involved the preparation of an avidin-biotinyl-peroxidase (ABC) complex which served as the protein probe. In this study, we made use of a biotin-conjugated WGA and the commercially available ABC complex. The use of avidin-biotinylated WGA has some

advantages over the use of ^{125}I-labelled lectins in that it is faster, it gives better resolution and it precludes the use of radioactive isotopes (Gordon and Pena 1982). Furthermore, the biotinylated WGA is stable on storage over several months and it binds to the ABC via specific biotin/avidin interactions, and not to the glycocomponents of either avidin or peroxidase (Rohringer and Holden 1985).
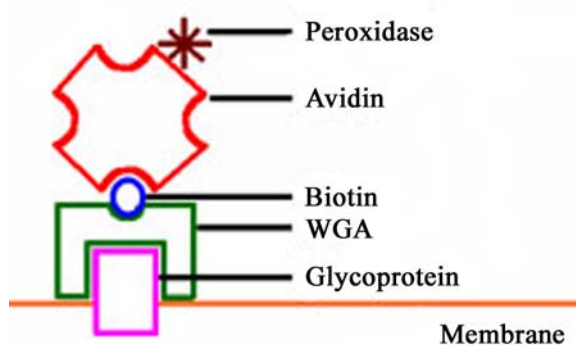
Figure 2.1 A diagram depicting the principles of a lectin blot. Biotinylated WGA attaches to the membrane glycoprotein of a cell, the biotin label in the WGA is amplified with avidin, and the resultant complex is quantified by chemiluminescence measurement.

2.3.2 Cell culture

Caco-2 cells at passages 55-65 were cultured in MEM supplemented with 10% of FBS, 1% of NEAA, 100 U/ml of penicillin and 100 µg/ml of streptomycin. HT-29 and CCD-18Co cells were cultured in McCoy's 5A and Eagle's MEM, respectively. Cell cultures were incubated at 37°C in a humidified atmosphere of 5% CO_2 and 95%

air (NuAire US autoflow, NuAire Inc., MN, USA), with medium exchange on alternate days.

2.3.3 Whole cell protein and cell membrane protein extraction

For total cell protein extraction, cells were cultured on 25 cm^2 flasks for 3 days. Confluent cells were washed thrice with ice-cold PBS and then scraped off into PBS with a cell scraper. Cell suspension was transferred into 1.5 ml-eppendorf tubes and centrifuged at 3,000 g for 2 min at 4 ˚C (MIKRO 22R, Andreas Hettich GmbH & Co KG, Tuttlingen, Germany). The supernatant was discarded and the cell pellet was resuspended in lysis buffer (PBS containing 1% of Triton X-100 and protease inhibitor according to the instructions by the supplier). After 30 min incubation on ice with occasional vortex, the cell lysate was centrifuged at 10,000 g at 4 ˚C for 20 min, and aliquots of the supernatant were stored at -80˚C till further use.

Cell membrane protein was extracted using the Mem-PER eukaryotic membrane protein extraction reagent kit (Pierce Biotechnology, Rockford, IL, USA) according to the manufacturer's instructions. Traditional methods for isolation of membrane protein are tedious, time consuming, and require gradient separation and expensive ultracentrifugation equipment (Kashino 2003; Kang et al. 2008; Wang et al. 2008). By comparison, the Mem-PER eukaryotic membrane protein extraction reagent kit,

which enriches integral membrane proteins from cultured mammalian cells using a mild detergent-based protocol [Figure 2.2], provides a faster and easier method to isolate membrane proteins. In addition, the isolated membrane (hydrophobic) protein fraction can be used directly for SDS-PAGE analysis.
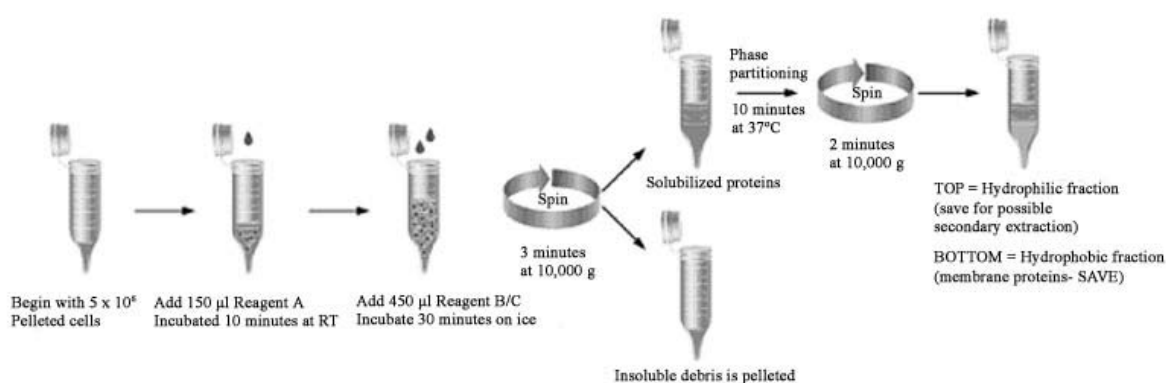
Figure 2.2 Mem-PER reagent protocol [Pierce Biotechnology, Rockford, USA]

The Mem-PER eukaryotic membrane protein extraction method required the cells to be lysed with a detergent, and a second detergent was added to solubilize the membrane proteins. After a quick centrifugation, the cocktail was incubated at 37 °C to separate the hydrophobic membrane proteins from the hydrophilic proteins through phase partitioning. The hydrophilic proteins were assumed to be the intracellular proteins excluding the cell membrane protein. The membrane proteins were stored at -80°C until analysis.

2.3.4 Protein quantification

Protein was quantified using the Micro BCA protein assay according to the manufacturer's instructions. It combined the reduction of Cu^{2+} to Cu^{1+} by protein in an alkaline medium with the highly sensitive and selective colorimetric detection of the cuprous cation (Cu^{1+}) by bicinchoninic acid. The principle underlying the assay is illustrated as follow:

1. protein (peptide bonds) + Cu^{2+} $\longrightarrow$ tetradentate-Cu^{1+} complex

2. Cu^{1+}complex + bicinchoninic acid (BCA) $\longrightarrow$ BCA-Cu^{1+} complex
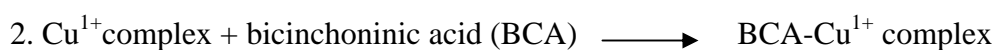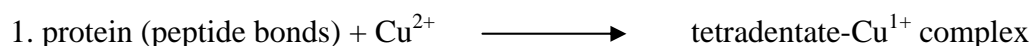
A working solution was prepared by mixing 2.5 parts of solution A (sodium carbonate, sodium bicarbonate and sodium tartarate in 0.2 N NaOH), 2.4 parts of solution B (4% BCA in water) and 0.1 part of solution C (4% cupric sulfate pentahydrate in water). The calibration curve was obtained by incubating 100 µl of the working solution with 100µl of standard BSA solution (concentration ranging from 0.5 to 20 µg/ml) at 37°C for 2h, followed by cooling at room temperature for 10 min, and measuring the absorbance of the samples at 562 nm (UV-1601 spectrophotometer, Shimadzu Corp. Kyoto, Japan). A linear calibration curve was obtained by plotting the sample absorbance as a function of the protein concentration.

2.3.5 Lectin blot analysis

A 7.5% polyacrylamide resolving gel and a 4% stacking gel were used according to the procedure of Laemmli (Laemmli 1970). Protein samples equivalent to 5 µg of protein were size-fractionated by electrophoresis on a 7.5% SDS-PAGE (Mini-PROTEAN 3 System, Bio-Rad Laboratories, Hercules, CA, USA) at 150 V for 1.5 h, and transferred to PVDF membranes, which were blocked by overnight incubation in a buffer (TBST) containing 1% of Tween 20, 200 mM of NaCl and 50 mM of Tris. The membranes were probed with biotinylated WGA for 1 h. After washing thrice with TBST, 10 min each time, the membranes were incubated for 1 h at room temperature with the avidin-biotin- peroxidase solution from the Vectastain reagent kit. The glycoprotein was detected using the west pico chemiluminescence system. Bands were visualized in a CCD imaging machine (Fluorchem® HD2, Alpha Innotech, San Leandro, CA, USA).

2.4 Results and Discussion

2.4.1 Protein quantification

Cell membrane proteins (hydrophobic part) and intracellular proteins (hydrophilic part) were quantified using the Micro BCA assay. Cellular protein concentrations in the samples were found to be around 0.8-1.5 mg/ml. This concentration was deemed adequate for the loading of small volume of protein samples for lectin blot analysis.

2.4.2 Lectin blot analysis

Lectin blot analyses of Caco-2, HT-29 and CCD-18Co cells cultured in 25 cm^2 flasks showed significant protein bands, confirming the sensitivity of the analysis in detecting N-acetyl-D-glucosamine-containing glycoproteins in the cell membrane and the intracellular compartment of these cells (Figure 2.3). The objective of this section is to obtain a full range of the glycosylation pattern of various colon cancer cells and normal cells. However, due to the unavailability of different types of colon cancer cells and normal cells, Caco-2, HT-29 and CCD-18Co cells were selected to represent colon cell models in our study. Amongst the 3 cell lines, the HT-29 cells showed the greatest abundance of WGA-recognizable glycoproteins both in the membrane protein sample (Figure 2.3 a) and the intracellular protein sample (Figure 2.3 b). Most of the WGA-recognizable glycoproteins in Caco-2 and HT-29 cells had molecular weight > 75 kDa, whereas the CCD-18Co cells showed an apparent lack of such large proteins. The ranking order of expression of WGA-recognizable glycoproteins in the three cell lines was HT-29 > Caco-2 > CCD-18Co.

(a)   (b)
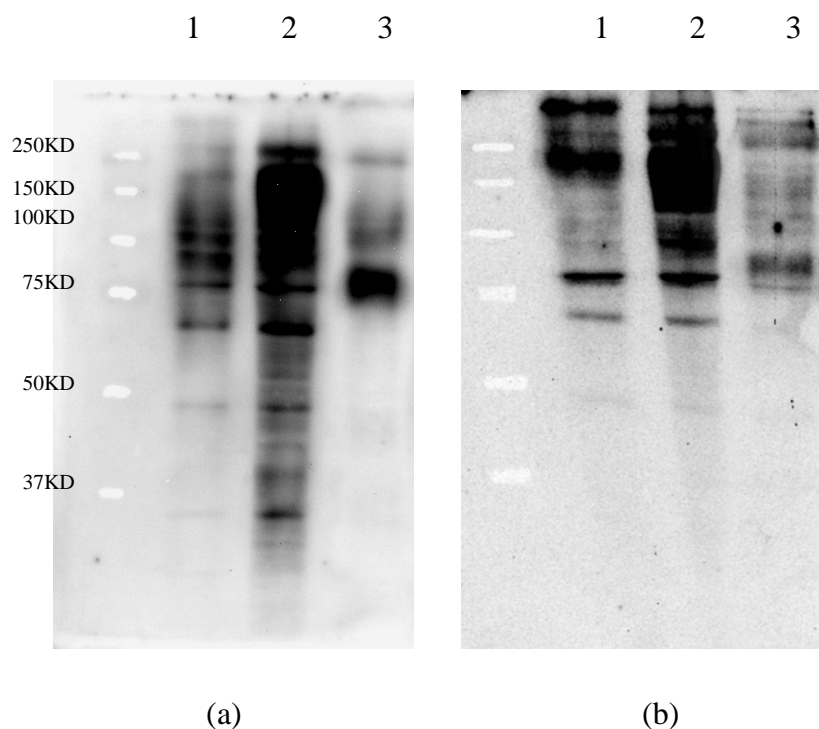
Figure 2.3 Lectin blot analysis of (a) cell membrane proteins and (b) intracellular proteins in Caco-2 (Lane 1), HT-29 (Lane 2) and CCD-18Co (Lane 3) cells.

These results confirmed the higher expression levels of WGA-binding glycoproteins in the human colon cancer cell lines, Caco-2 and HT-29, than in the human colon fibroblasts, CCD-18Co, which served as surrogate normal colon cells in this study. The existence of N-acetyl-D-glucosamine proteins in both the cell membrane and intracellular compartments of these cells would provide promising therapeutic targets for WGA-based drug delivery systems. On this basis, we hypothesized that WGA-conjugated nanoparticles could be developed to efficiently deliver anticancer drug payloads to colon cancer cells via glycoprotein-WGA mediated endocytosis. We

proposed that the targeting nanoparticles would not only be internalized, but would reside within the cancer cells to allow for an adequate release of anticancer drug to kill the cells.

2.5 Conclusion

Lectin blot analyses confirmed the differential expression levels of N-acetyl-D-glucosamine-containing glycoproteins in the cell membrane and intracellular compartments of Caco-2, HT-29 and CCD-18Co cells. The ranking order of expression of these glycoproteins in the cells was HT-29 > Caco-2 > CCD-18Co, suggesting that normal colon cells may express lower WGA-recognizable glycoproteins than cancerous colon cells.

Chapter 3

Uptake and cytotoxicity of wheat germ agglutinin in colon cell models

3.1 Introduction

The potential utility of cytoadhesive and cytoinvasive wheat germ agglutinin (WGA) as a 'shoehorn' (Gabor et al., 2002) to improve intracellular uptake of anticancer drugs has attracted increasing attention. Aub and his collaborators (Aub et al., 1963) first reported that a lipase preparation of wheat germ preferentially interacted with tumor specific sites that contained the N-acetyl glucosamine (GlcNAc) moiety. Subsequently, WGA was isolated and found to agglutinate leukemia cells (Burger & Goldberg, 1967; Kitao et al., 1978). Interest in this cell-agglutinating and sugar-specific protein grew when it was found to be a very useful tool for the investigation of carbohydrates on cell surfaces, and the separation and characterization of glycoproteins (Sharon & Lis, 2004). WGA has many biological properties, including its function as recognition molecules in cell-molecule and cell-cell interactions, and insight into its action has paved the way for a large number of investigations on the use of lectins as tumor diagnostic tools. It is believed that all malignant cells share a common property of high lectin-agglutinability that is closely correlated with the loss of contact inhibition and tumorigenicity (Rapin & Burger, 1974).

Lectin-mediated drug delivery relies on the specific interaction between the glycocalyx covering the surface of most epithelial cells and the carbohydrate binding

site of the lectin ligand. WGA is a dimeric protein characterized by high disulfide and glycine contents (Miller & Bowles, 1982; Wright, 1987). It is a lectin with four apparently equivalent binding sites that bind specifically to N-acetyl-D-glucosamine and N-acetyl-D-neuraminic acid residues on the plasma membrane (Nizheradze, 2000). WGA has been shown to bind to intestinal cell lines of human origin, e.g. human colonocytes, and prostate cancer cells (Zhang et al., 2006). In addition, WGA has been observed to rapidly internalize into the cytoplasm of human enterocyte-like Caco-2 cells (Dalla Pellegrina et al., 2005). Unlike many proteins, WGA is relatively stable to low pH and is able to resist proteolytic attack (Gabor et al., 1997).

The interesting biochemical characteristics aside, WGA is attractive as a targeting ligand because it is a protein component of the human diet, being present in wheat germ and flour (Dalla Pellegrina et al., 2005, Matucci et al., 2004). Wheat flour contains about 300 mg of WGA per kg (Gabor et al., 2004). In cereals, WGA concentrations range from 13 to 53 mg/kg (Watzl et al., 2001). While clinical toxicity of WGA has not been confirmed conclusively due to a lack of relevant *in vivo* studies (Gabor et al., 2004), the amount of peroral WGA required for optimizing drug delivery (nanomolar concentration) is expected to be safe, given that wheat germ forms part of the regular diet of man. To date, most toxicity studies of WGA have only been recorded in animal or *in vitro*, with toxicity observed only at very high

peroral doses of 7g WGA / kilogram body weight in rats, and even then, only when the WGA dose was administered daily over 10 days (Dalla Pellegrina et al., 2005). Such doses are significantly higher than the typical dose ingested in a regular human diet since the estimated quantity of dietary lectins is in the range 0-200 mg/person per d (Watzl et al., 2001). Therefore, within a huge range of concentrations, WGA is believed to be non-toxic (Dalla Pellegrina et al., 2005). However, it is worth noting that WGA administered to *in vitro* cell models within the same range of concentrations has been shown to be cytotoxic for the human colon cancer cells (Pusztai et al., 1993).

WGA has been shown to bind to intestinal cell lines of human origin, with human colonocytes exhibiting the highest binding to WGA when compared to other plant lectins (Gabor et al., 1997). Our objective was to exploit the cytoadhesive and cytoinvasive properties of WGA to develop a colon cancer targeted PLGA nanoparticulate system for paclitaxel. To this end, the cytotoxicity and uptake of pure WGA to colon cancer cells and normal cells had to be investigated. However, there is a scarcity of study comparing the affinities and cytotoxicity of WGA to normal versus cancerous colon cell lines. Therefore, the objectives of the study in this section were to determine the differential uptake and cytotoxicity of WGA in a variety of human colon cell models derived from normal and cancerous tissues. Caco-2, HT-29 and

CCD-18Co cells were selected for the experiments. The Caco-2 and HT-29 cell monolayers are established *in vitro* surrogates of the human intestinal epithelium. Caco-2 cells spontaneously differentiate into monolayers of polarized enterocyte-like cells, connected by tight junctions, that express features characteristic of mature small intestinal cells, but they lack mucus-secreting goblet cells (Howell et al., 1992). HT-29, an undifferentiated human colon cell line originating from a human colon adenocarcinoma, can be modulated *in vitro* under specific culture conditions to control its degree of differentiation and polarization (Le Bivic et al., 1988). They form mucus-producing goblet cells under the cultivation medium in the presence of methotrexate (Lesuffleur et al., 1993). The third cell line used in the project was CCD-18Co cells. These are colonic fibroblasts, and they served as representative of normal colon cells.

3.2 Materials

Wheat germ agglutinin (WGA), FITC-labeled wheat germ agglutinin (fWGA, FITC content 2.5 mol/mol lectin), FITC-labeled bovine serum albumin (fBSA, FITC content 10 mol/mol albumin), glycine, propidium iodide (PI), DNA-free RNase, SSC buffer solution isopropyl myristate (IPM), sodium hydroxide (NaOH), sodium dodecyl sulfate (SDS), N-(2-hydroxyethyl) piperazine-N'-(2-ethanesulfonic acid) (HEPES), Hank's balanced salt solution (HBSS), non-essential amino acid,

trypsin/EDTA (10×), penicillin G, streptomycin sulfate, sodium bicarbonate, 3-(4,5-dimethylthiazolyl-2)-2,5-diphenyl tetrazolium bromide (MTT), Eagle MEM, dimethyl sulfoxide (DMSO) and trypan blue were products of the Sigma Chemical Co. (St. Louis, Missouri, USA). The Micro BCA protein assay kit was purchased from the Pierce Co. (Rockford, USA). MEM and McCoy 5A were from Invitrogen (Grand Island, NY, USA). Caco-2 cells (human, male colon cancer cell line, passage number 40) were purchased from the cell bank of the Riken Bioresource Center (Koyadai, Tsukuba, Ibaraki, Japan). HT-29 cells (human, female colon cancer cell line, passage number 140) and CCD-18Co cells (human colon fibroblast, passage number 7) were purchased from the American Type Culture Collection (Virginia, USA). All chemicals were of analytical grade.

3.3 Methods

3.3.1 Cell culture

Caco-2 cells at passages 50-60 were cultured in MEM supplemented with 10% of FBS, 1% of NEAA, 100 U/ml of penicillin and 100 μg/ml of streptomycin. HT-29 cells were cultured in McCoy's 5A medium supplemented with 100 U/ml of penicillin, 100 μg/ml of streptomycin and 10% (v/v) of FBS. CCD-18Co cells were cultured in Eagle's MEM supplemented with 100 U/ml of penicillin, 100 μg/ml of streptomycin and 10% (v/v) of FBS. Cell cultures were incubated at 37°C in a humidified

atmosphere of 5% CO_2 and 95% air (NuAire US autoflow, NuAire Inc., MN, USA), with medium exchange on alternate days. Cells were sub-cultured every 3 days after trypsinization with trypsin/EDTA solution (0.05 %w/v trypsin; 0.53mM EDTA).

3.3.2 Cytotoxicity of WGA

In vitro cytotoxicity profile of the WGA was evaluated using the MTT assay. The MTT [3-(4,5-dimethylthiazol-2-yl)-2,5-diphenyltetrazolium bromide] assay, first described by Mosmann in 1983, is based on the ability of a mitochondrial dehydrogenase enzyme from viable cells to cleave the tetrazolium rings of the pale yellow MTT to form dark blue formazan crystals (Figure 3.1). Being largely impermeable to cell membranes, these crystals would accumulate within healthy cells. Solubilization of the cells by the addition of a detergent results in the concomitant liberation and solubilization of the formazan crystals, which are quantified by a simple colorimetric assay (Scudiero et al., 1988). The number of surviving cells is directly proportional to the level of the formazan product created.
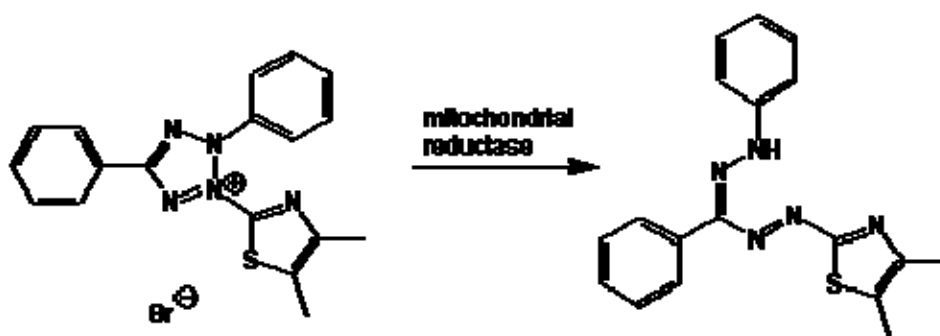
Figure 3.1 Biotransformation of MTT to formazan in cells

To assess the cytotoxicity of WGA against the Caco-2, HT-29 and CCD-18Co cells, the cells were separately seeded onto 96-well plates at a density of 8,000-10,000 cells/well. When the cells had reached confluence, they were washed with 2×200 µl of PBS before incubation with 200 µl of WGA solution (10 to 200 µg/ml in respective culture medium) for 4 to 72h in the incubator. Cells treated with 0.1% (w/v) of aqueous SDS and cells exposed to the culture medium were used as positive and negative controls, respectively. After the specified incubation periods, the WGA and control solutions were aspirated and the cells were washed thrice with 200 µl of PBS followed by incubation with 200 µl of MTT solution (1 mg/ml in PBS) for 3h at 37°C. The cells were lysed with 200 µl of DMSO to extract the intracellular purple product, and the absorbance of the resultant solutions was measured at 590 nm using a plate reader (Spectra Fluor, Tecan Group Ltd, Switzerland).

3.3.3 Protein quantification

Cell lysate protein was quantified using the Micro BCA assay according to the manufacturer's instructions. The principle underlying the Micro BCA protein assay is illustrated as follows:

1. Protein (peptide bonds) $+ Cu^{2+} \longrightarrow$ tetradentate-Cu^{1+} complex

2. Cu^{1+}complex $+$ Bicinchoninic Acid (BCA) $\longrightarrow$ BCA-Cu^{1+} complex

This method utilizes bicinchoninic acid (BCA) as the detection reagent for Cu^{1+}, which is formed when Cu^{2+} is reduced by protein in an alkaline environment. A purple-colored reaction product is produced by the chelation of two molecules of BCA with one cuprous ion (Cu^{1+}). This water-soluble complex exhibits a strong absorbance at 562 nm.

3.3.4 Uptake of FITC-WGA (fWGA)

Caco-2, HT-29 and CCD-18Co cells were separately seeded onto 96-well plates at a density of about 1.0×10^5 cells/ well. Confluent cells on Day 3 were washed twice with 200 μl of HBSS/HEPES (HBSS buffered with 10 mM of HEPES to pH 7.4), pre-incubated with 200 μl of pre-warmed HBSS/HEPES for 1h at 37°C, and incubated for 0.5 to 5h at 37°C with 200 μl of 20 μg/ml fWGA solution in HBSS/HEPES. Uptake was terminated by washing the cell monolayer twice with 200μl of HBSS/HEPES. The washed cells were solubilized with 200 μl of 5% SDS in 0.1M NaOH. Cell-associated fWGA was quantified by measuring the fluorescence of the cell lysate in the plate reader (excitation wavelength 485 nm, emission wavelength 535 nm) and expressed as the uptake amount of WGA (μg) associated with unit weight (mg) of cellular protein.

3.3.5 Visualization of fWGA cellular uptake

Laser scanning confocal microscopy (LSCM, also referred to as CSLM, Confocal Scanning Laser Microscopy) is an established tool for obtaining high-resolution images and 3-D reconstructions of a variety of biological specimens (Matsumoto, 1993). CLSM allows for a sharp observation of thin optical sections in thick, intact specimens. Compared to conventional fluorescence microscopy, confocal microscopy has several advantages. The major advantage is its ability to overcome out-of-focus reflection. Conventional fluorescence photomicrographs have poor contrast and often appear blurred due to fluorescent light scattered around the image, especially fluorescence originating from planes other than the plane of focus. Most of the unfocused light is excluded in confocal microscopy, which also enables the observation of selected thin layers from a thick specimen. As a result, confocal images have significantly improved resolution and contrast (Cullander, 1998; Robinson, 2001).

Fluorescence microscopy is frequently applied to observe the endocytosis of polymer nanoparticles in absorptive cells. However, it is often not easy to discriminate between the particles internalized and those externally attached to the cellular membrane by observation under the conventional fluorescence microscope. In 1983, Sahlin and his colleagues (Sahlin et al., 1983) found that trypan blue (TB,

concentration 0.2 mg/ml) at pH 4 could be the most effective of a series of dyes acting as a quenching agent for the extracellular fluorescence. The intracellular fluorescence was unaffected by TB because the dye was excluded by viable cells. Another study showed the internalization of fluorescent polystyrene microparticles by PMN cells was successfully differentiated from extracellular particles using the same technique (Thiele et al., 2001). In order to differentiate between the membrane-binding and internalized fWGA, the TB quenching technique was also used in our study.

Caco-2, HT-29 and CCD-18Co cells were cultured on Lab-Tek chambered cover glasses (Nalgene, Nunc International, Naperville, IL, USA) at a seeding density of 1.0 $\times$ 10^4 cells/cm^2 and incubated at 37°C in 95% air/5% CO_2 environment. On the 3rd day post seeding, cell monolayers were rinsed twice with pre-warmed HBSS/HEPES and pre-incubated for 30 min at 37°C with 0.2 ml of HBSS/HEPES before they were incubated for 1 h at 37 °C with fWGA solution (20 μg/ml in HBSS/HEPES). Uptake was terminated by removing the test or control solution. The cells were washed thrice with cold PBS before the extracellular fluorescence was quenched by incubating the cells with 0.2 ml of TB solution (0.2 mg/ml in MES, pH 4) for 3 min. The cells were then fixed for 10 min in 0.5 ml of acetone/methanol (1:1) at 4 °C. Cell nuclei were stained with propidium iodide (2 μg/ml in 2 × SSC containing 25 μg/ml RNase A) for 10 min at room temperature followed by repeated washings in PBS. The cells were

observed under a confocal laser scanning microscope (Zeiss, Heidelberg, Germany) at

40 × magnifications.

3.3.6 Statistical analysis

Data were analyzed by one-way ANOVA with the Tukey′s test applied for paired

comparisons of mean values (SPSS 10.0, SPSS Inc, Chicago, IL). A p value ≤ 0.05

was considered statistically significant**.**

3.4 Results

3.4.1 *In vitro* cytotoxicity profile of WGA against colon cell lines

Figure 3.2 shows the *in vitro* cytotoxicity profiles of WGA against the Caco-2, HT-29

and CCD-18Co cells. Based on our lab's experience, the WGA were considered to be

cytotoxic when they reduced the mean cell viability by 20% or more compared to the

culture medium control. It was observed that the cell viability for all 3 cell lines

decreased with increasing WGA loading concentration and exposure time. The

Caco-2 cells were resistant to ≤ 10 μg/ml of WGA, even at up to 72h of exposure.

When the WGA concentration was increased 5 fold to 50 μg/ml, however, the cell

viability fell below 80% after 24h exposure. By comparison, the HT-29 and

CCD-18Co cells were resistant to WGA at up to 200 μg/ml as long as the exposure

time did not exceed 4h. Prolongation of the co-incubation time to 24h caused these cells to be vulnerable even at a lower WGA concentration of 50 μg/ml.

(A)
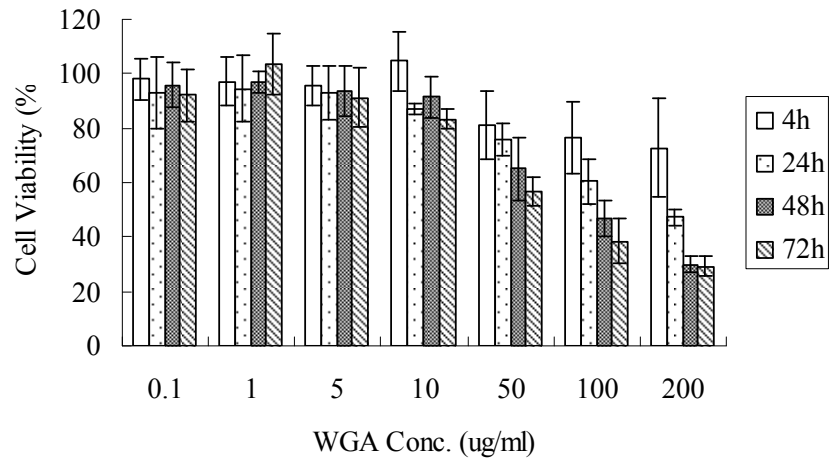
(B)
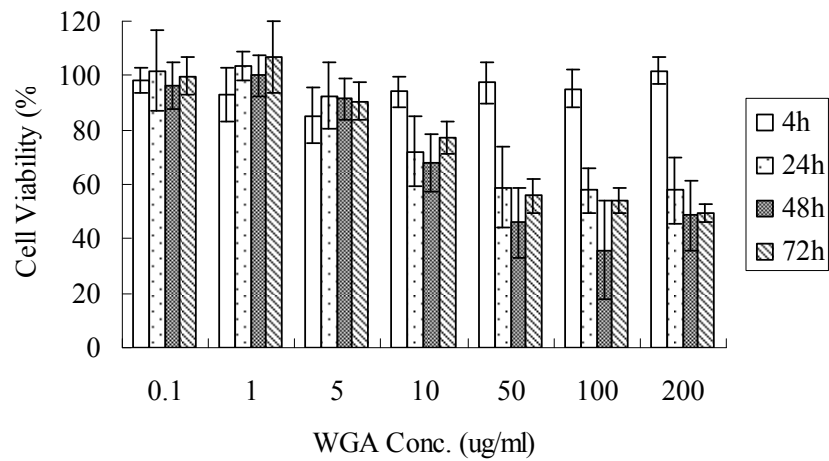
(C)
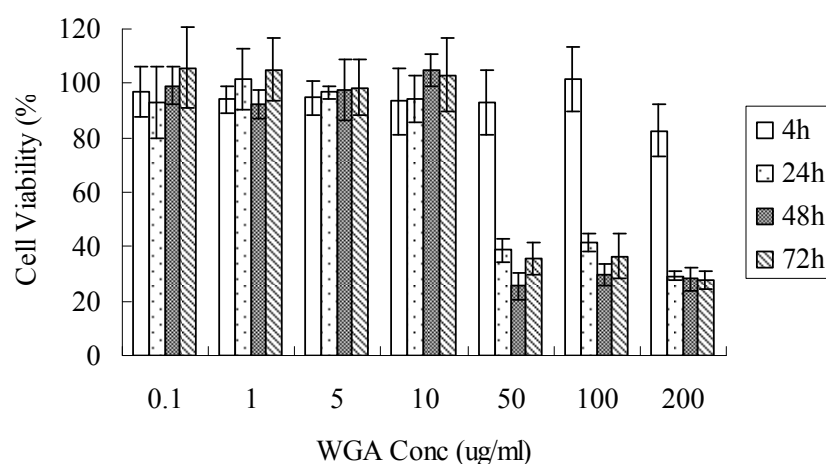
Figure 3.2 *In vitro* cytotoxicity profiles of WGA against (A) Caco-2; (B) HT-29 and (C) CCD-18Co cells. WGA was applied at loading concentrations of 0.1, 1, 5, 10, 50, 100 and 200 μg/ml for periods ranging from 4 to 72h. Cell viability determined by the MTT assay was expressed as a percent of that obtained for cells exposed to culture medium. SDS served as positive control. Data represent mean ± SD, n=6.

3.4.2 Uptake of WGA by colon cell lines

Uptake of fWGA was studied in the cell lines, Caco-2, HT-29 and CCD-18Co with initial fWGA loading concentrations of 5, 10, 20 and 50 μg/ml. The Caco-2 and HT-29 cells were representative of colon cancer cells while the CCD-18 Co cells served as control normal colon cells. Figure 3.3 shows the results of the uptake studies, the fWGA uptake data was expressed as the uptake amount of WGA (μg) associated with unit weight (mg) of cellular protein.

At all loading concentrations employed, the three colon cell types showed increased fWGA uptake with increasing incubation time from 0.5 to 5h. WGA didn't show cytotoxic activity against these cell lines at the test loading concentrations. The fWGA uptake profile typically showed a rapid initial uptake rate followed by a slower rate of uptake after 30 min. The rank order of fWGA uptake was Caco-2 > HT-29 > CCD-18Co cells. Although the Caco-2 cells showed a consistent 1.5 fold higher uptake of fWGA compared to HT-29 cells at all time points examined, the HT-29 cells also exhibited a substantial capacity for WGA binding, the cellular WGA uptake reaching about 50% of the initial fWGA load administered to the cells at the loading concentration of 10μg/ml at 2h.

(A)
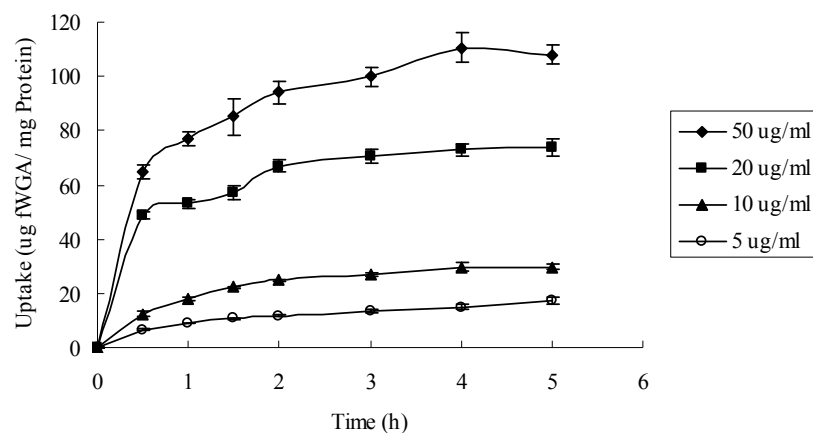
(B)
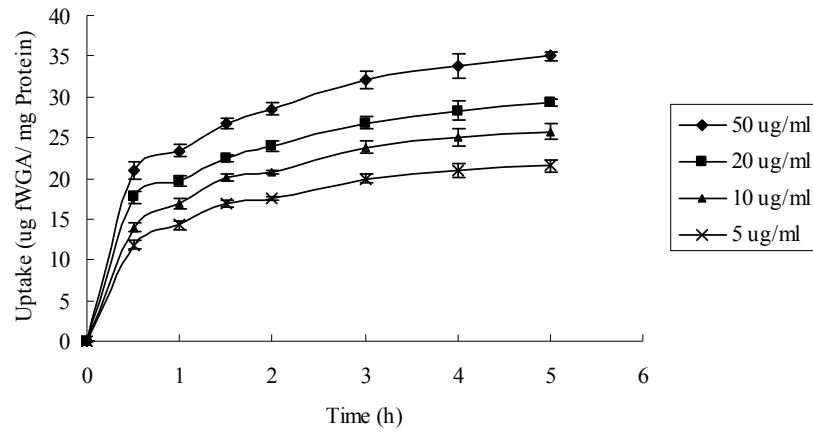
(C)
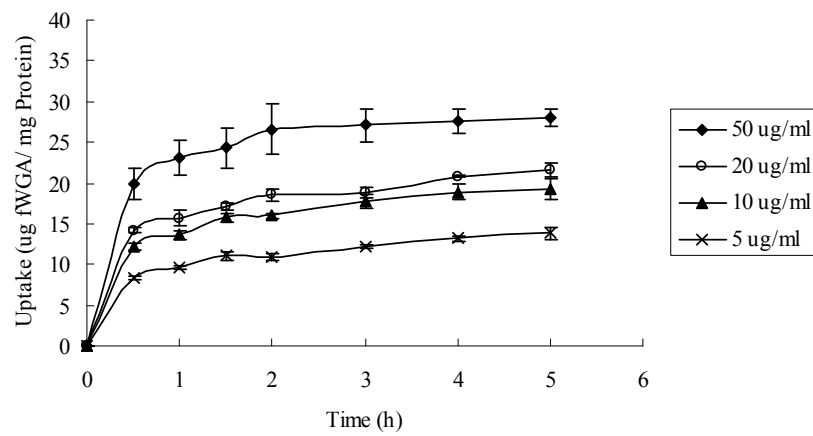
Figure 3.3 Uptake of fWGA by (A) Caco-2, (B) HT-29 and (C) CCD-18Co cells as a

function of incubation time (Data represent mean $\pm$ SD, n=4)

(A)
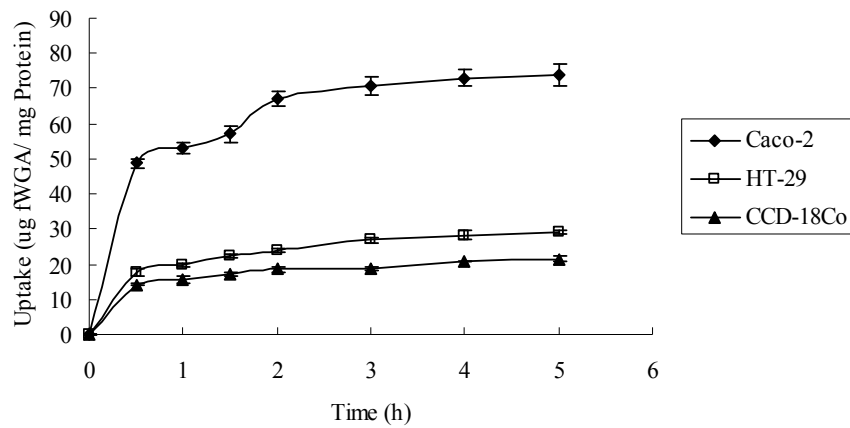
(B)
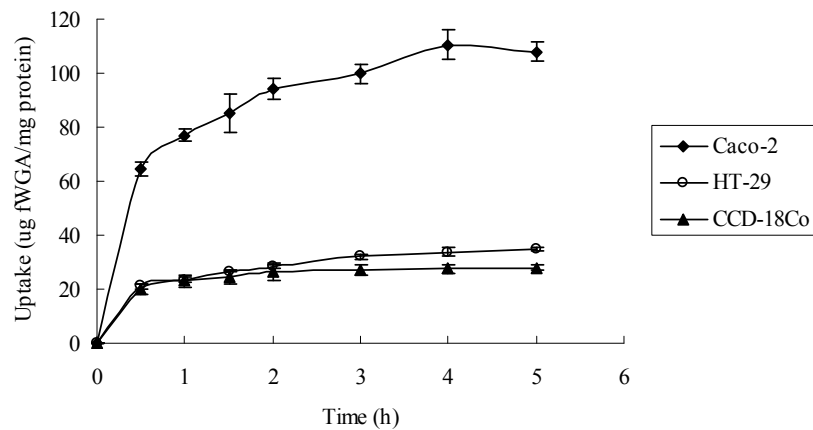
Figure 3.4 Uptake of fWGA by the Caco-2, HT-29 and CCD-18Co cells when

exposed to fWGA loading concentration of (A) 20 µg/ml and (B) 50 µg/ml (Data

represent mean ± SD, n=4)

Figure 3.4 is a comparison of the fWGA uptake profiles for the three colon cell lines

at fWGA loading concentrations of 20 and 50µg/ml. At both concentrations, fWGA

uptake by the cell lines was time and concentration-dependent. While all 3 cell lines showed rapid initial uptake followed by saturation after about 2h, the effect of fWGA loading concentration on the cellular uptake was not the same for the 3 cell types. WGA uptake by the Caco-2 cells at the loading concentration of 20 μg/ml was about 2.5 and 3.0 times higher than those of the HT-29 and CCD-18Co cells, respectively, whereas at the 50 μg/ml loading concentration, Caco-2 cells showed 3 fold higher WGA binding than the HT-29 cells, whose WGA uptake capacity at this loading concentration was comparable to that of the CCD-18Co cells.

3.4.3 Laser scanning confocal photomicrographs

Confocal imaging of the cells after uptake experiments supported the quantitative data generated from the uptake studies. Figures 3.5 showed the confocal images following 1h uptake of fWGA by the colon cells, which was captured by the combined PI and FITC channels. The intensity of the fluorescence (green) was scattered in the cytosol, with some fluorescence present in the vicinity of the nuclei (red), indicating that the fWGA had been internalized by the cells. Subsequent treatment of the cell monolayers with trypan blue, which quenched extracellular fluorescence, did not affect the fluorescence intensity observed under the confocal microscope. This indicated that the imaged fluorescence was located inside the cells. Moreover, the

images were acquired by the sectioning function of CLSM, providing further evidence

indicating the internalization of the fluorescently labeled WGA.

Before trypan blue treatment   After trypan blue treatment

(a)
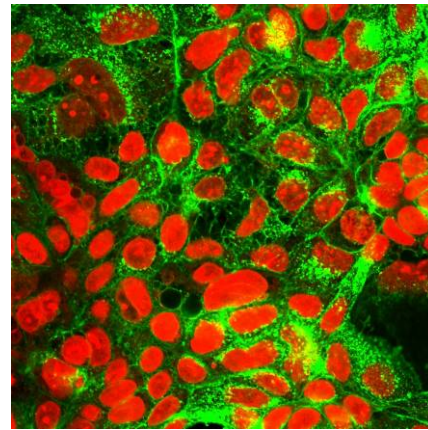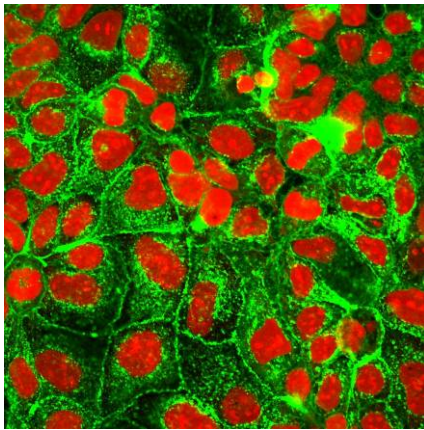
(b)
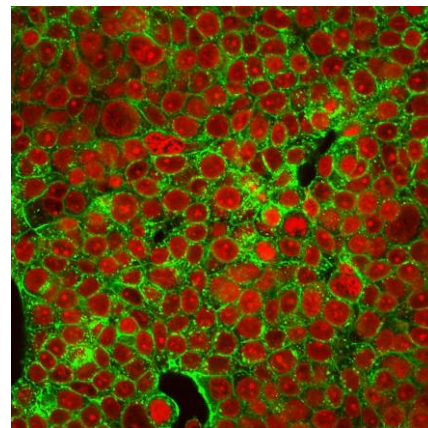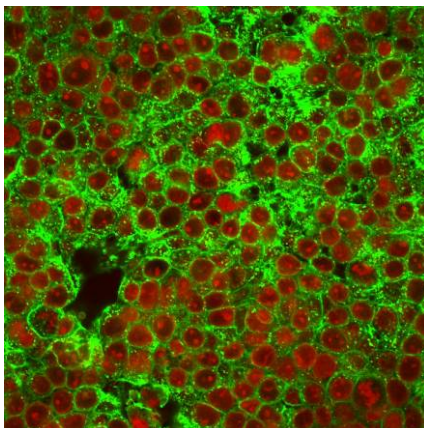
(c)
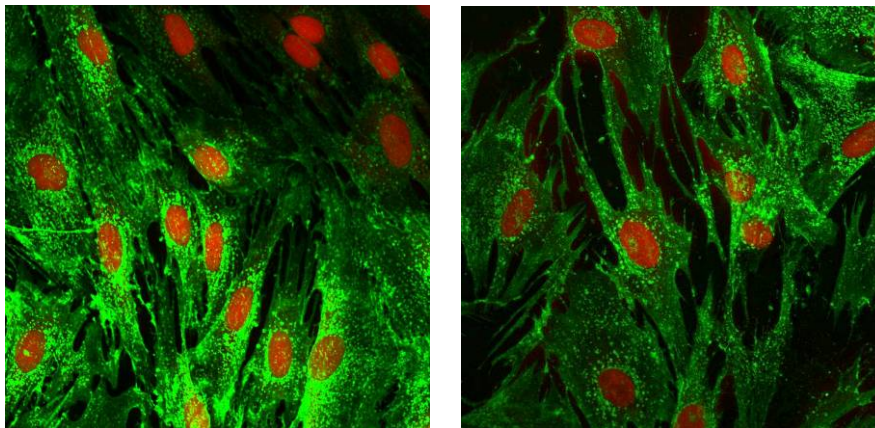
Figure 3.5 Confocal images of (a) Caco-2, (b) HT-29 and (c) CCD-18Co cells incubated for 1 h with 20 µg/ml of FITC-WGA. The images were acquired before and after the cells were treated with 0.2 mg/ml of trypan blue post-uptake, which quenched extracellular fluorescence.

3.5 Discussion

For WGA to be applied as a cytoadhesive and cytoinvasive ligand, its binding characteristics with target cells has to be evaluated and this can be investigated using the fluorescein-labeled derivative. In order to evaluate the selective potential of WGA for colon cancer cells, fWGA uptake by the cancerous Caco-2 and HT-29 cells were compared in this study to that of CCD-18Co cells, a colon fibroblast chosen to represent normal colon cells.

Taken together, the fWGA cellular uptake data supports the hypothesis that WGA-binding residues, likely to be N-acetylglucosamine and sialic acid residues or

their derivatives (Nizheradze, 2000), were expressed in the glycocalyx of the three cell lines, particularly the Caco-2 and HT-29 cell lines. Cellular uptake of fWGA in all cases was a concentration- and time-dependent saturable process, the uptake efficiency ranking in the order of Caco-2 > HT-29 > CCD-18Co cells. Given the insignificant difference in imaged fluorescence following trypan blue treatment of exposed cells monolayers, it may be concluded that the measured fluorescence of lyzed cells was contributed predominantly by internalized fWGA. Thus, the uptake data could be attributable to endocytosed fWGA rather than fWGA adsorbed on the cell membrane surface.

Garbor et al. (Gabor et al., 2004) have reported that the intracellular trafficking of free fWGA was mediated by clathrin, because the observed decrease in cell-associated fluorescence intensity with time at 37°C was indicative of fluorescence quenching in an acidic environment, such as lysosomes. Moreover, the decrease in fluorescence intensity could be fully compensated by the addition of monensin, an agent that reduced the acidity of an intracellular compartment. Published data (Villegas & Broadwell, 1993; Mo & Lim, 2004) have suggested that the cellular internalization of WGA was mediated by receptor-mediated endocytosis (RME) and adsorptive endocytosis (AE), both of which are energy-dependent, saturable processes. RME is initiated by ligand binding to specific receptor proteins embedded within the plasma

membrane, while ligands are adsorbed onto the cell membrane by non-specific interactions in AE (Lehr, 1994). Kramer and his colleagues (Kramer & Canellakis, 1979) have reported that the binding of WGA to the surface polypeptides of HeLa cells induced an extensive endocytosis of both bound and unbound surface polypeptides. Raub et al. (Raub et al., 1986) demonstrated that the endocytosis of WGA by Chinese hamster ovarian (CHO) cells occurred via invaginated regions of both coated and uncoated membranes, with a large fraction of the receptors returning to the cell surface at a mean $t_{1/2}$ of 17 min. Thus, there may be more than one mechanism for the uptake of WGA depending on the cell type and the glycoprotein expression pattern in the diseased state. In the case of Caco-2 cells, the binding of WGA has been attributed to the presence of specific carbohydrate binding sites on the cell surface (Gabor et al., 2002), and the internalized WGA has been observed to accumulate into lysosomal compartments within 1h (Gabor et al., 2002).

The uptake of WGA by the Caco-2, HT-29 and CCD-18Co cells has been ascribed to the simultaneous presence of two phenomena, a linear non-specific uptake and a non-linear specific saturable uptake (Brandhonneur et al., 2009). If the specific (non-linear) process predominates over the non-specific process, the saturation is more apparent, which was the case in our study. This is in agreement with the findings of Brandhonneur et al., who reported a higher specific uptake relative to the

non-specific uptake for WGA-grafted PLGA microspheres by alveolar macrophages (Brandhonneur et al., 2009). In addition, the authors noted that the cellular was dependent on the particle-to-cell ratio. Though the adhesion of WGA to the colon cancer cells was found to be specific, the affinity of the lectins to the glycocalyx of the cells was quite different. The amount of carbohydrate necessary for 50% inhibition of WGA-binding to Caco-2 cells was 2 times more than that of HT-29 cells (Gabor et al., 1998). Our glycosylation pattern study using SDS-PAGE analyses (section 2.4.2) has detected the presence of multiple WGA-reactive glycoproteins in the mw bands between 37 and 250 kDa in Caco-2 and HT-29 cells. However, the fWGA uptake data are not completely consistent with the cell membrane glycocalyx pattern for the Caco-2 and HT-29 cells. Though HT-29 cells express more WGA-reactive glycoproteins than Caco-2 cells, the uptake of fWGA by HT-29 cells is lower than that of Caco-2 cells. This inconsistence might be due to the different analytical method, glycocalyx availability on cell membrane surface, affinity of WGA to the cell surface glycoprotein, or the single cell size.

The cellular uptake of fWGA by three cell lines ranked in the order of Caco-2 > HT-29 > CCD-18Co. The higher binding of WGA to the malignant cells relative to colon fibroblast cells may be associated with the expression of N-acetylglucosamine and Sialic acid of the cells. The selectivity of WGA for agglutination with the colon

cancer cells relative to the normal fibroblast CCD-18Co cells enable WGA a good candidate for formulating a WGA-mediated targeting chemotherapeutic drug delivery system for the treatment of colon cancer.

Cytotoxicity of WGA showed a concentration and time-dependence against the 3 cell lines studied. WGA was cytotoxic to the three colon cell lines Caco-2, HT-29 and CCD-18Co cells at concentrations ≥ 50 µg/ml, particularly upon prolonged exposure. Several mechanisms might have accounted for the cytotoxicity of WGA. Lectin-dependent macrophage-mediated cell lysis was suggested to be one such mechanism (Wang et al., 2000), with the sugar-binding moiety of the lectin molecule being partly responsible for anti-cytoproliferative activity. A study by Kim et al. showed lectin cytotoxicity to be mediated by soluble lectins that bind to a specific receptor that internalized and triggered programmed cell death (apoptosis) (Kim et al., 1993). Though cytotoxicity of WGA can be advantageous when WGA is directed to malignant cells, it could be a source of concern, particularly when the colon fibroblasts appeared to be even more susceptible to its deleterious effects. Among the three cell lines, the CCD-18Co cells appeared to be the most vulnerable to the cytotoxic effects of WGA at higher concentration (≥ 50 µg/ml) and longer incubation time. However, this study uses only one fibroblast cell line. The *in vivo* study showed no toxic effect to rats (Dalla Pellegrina et al., 2005). In volunteers consuming wheat

germ with equivalent of 200 mg active agglutinin, no side effects were reported (Watzl et al., 2001). WGA at concentrations $\geq$ 50 μg/ml exhibited cytotoxicity to varing degrees against cancer and normal cells after long exposure. On the basis of these data, the WGA-conjugated PLGA nanoparticles (NPs) should be formulated to deliver less than 50 μg/ml of WGA to the cells so as to minimize cytotoxicity, in particular to the normal tissues.

While it is possible to control the cellular contact time when the formulation is applied to *in vitro* cell cultures, the cellular contact time will be more difficult to control or predict under *in vivo* conditions. The time taken for food to travel through the digestive tract, also known as bowel transit time, can range between 14 to 24h and it varies greatly from person to person (Fireman et al., 2005). Thus, it is possible for the NPs administered perorally to be retained in the colon for 20h, or even longer in view of the bioadhesive property of WGA. Some studies have shown that the binding capacity of WGA to cell membranes was affected by food and mucus (Gabor et al., 2004). This remains debatable because WGA binding to Caco-2 cells was not shown to be affected by co-administered wheat flour, starch from potatoes or wheat germ, saccharose, glucose, basic and neutral amino acids (Rodrigues et al., 2003).

3.6 Conclusion

In summary, WGA can mediate cytoadhesion and cytoinvasion of conjugated drug delivery carrier to surmount the membrane barrier by temperature-dependent active transport mechanisms (Lehr, 2000; Wirth et al., 2002; Weissenbock et al., 2004). The conjugation with WGA facilitates cellular uptake, whereas the enzymic barrier might be overcome by colloidal formulations or enzyme inhibitors (Gabor et al., 2002). Thus, WGA-mediated drug delivery may be a promising strategy to improve the availability of poorly permeable drugs. Especially wheat germ agglutinin might enhance the uptake of conjugated drugs due to its cytoadhesive and cytoinvasive characteristics.

Cellular uptake efficiency of fWGA by the four colon cells ranked in the order of Caco-2 > HT-29 > CCD-18Co. WGA showed selectivity for agglutination with the malignant colon cancer cells relative to the normal CCD-18Co cells. Therefore, WGA may be a suitable ligand for formulating a lectin-mediated targeting chemotherapeutic drug delivery system for the treatment of colon cancer. Its cytoadhesive and cytoinvasive characteristics provide a promising pathway for improving the binding and cellular uptake of anticancer drugs in cancer tissues. WGA at higher concentration (≥ 50 μg/ml) exhibited varying degrees of cytotoxicity against both the malignant and normal lung cells after prolonged exposure. However, WGA showed no cytotoxicity if

the cells were co-incubated with the WGA at low concentration of 10 μg/ml for up to

72h. On this basis, the WGA-conjugated drug delivery system should be formulated to

give tissue exposure to 50 μg/ml or less of WGA so as to minimize cytotoxicity to

neighboring normal tissues.

Chapter 4

Evaluation of anticancer activity of wheat germ agglutinin-conjugated

paclitaxel-loaded PLGA nanoparticles

4.1 Introduction

The ideal goal of cancer chemotherapy is to destroy cancer cells without harming healthy cells. Most anticancer drugs fall short of this ideal. In the case of colon cancer, the intravenous delivery of anticancer agents often cause severe side-effects (Kuebler et al., 2007). To overcome this drawback, significant efforts have been made to develop appropriate targeting systems for colon-specific drug delivery (Patel et al., 2007; Casadei et al., 2008; Yang, 2008). Among the systems developed, nanotechnology-based platforms appear promising in improving therapeutic outcome by focusing drug delivery to the target site, and minimizing drug accumulation at nonspecific sites (van Vlerken et al., 2007).

Of the nanoparticulate systems reported in the literature, PLGA nanoparticles are versatile because they offer a biocompatible vehicle that also present opportunities for drug targeting at the cellular level (Mohamed & van der Walle, 2008). PLGA nanoparticles can provide sustained drug release and a surface amendable to chemical conjugation for targeting purposes, and they bypass the efflux activity of membrane transporters (Panyam & Labhasetwar, 2003; Sahoo & Labhasetwar, 2003; Keegan et al., 2006; Chen et al., 2008). Previous experiments in our laboratory have shown that the conjugation of WGA to PLGA nanoparticles loaded with paclitaxel (WNP nanoparticles) could improve the intracellular delivery of paclitaxel to small lung

cancer cells relative to lung fibroblasts (Mo & Lim, 2005; Mo & Lim, 2005). The purpose of the experiments in this section was to explore the possibility of extending the application of WNP to colon cancer chemotherapy.

Paclitaxel is one of the most effective anticancer agents and has a wide spectrum of activity against solid tumors, including colorectal cancer (Suffness & Wall, 1995). Its clinical application is, however, limited by an intractable insolubility in aqueous media and a non-specific activity against both cancerous and normal cells. The clinical formulation is Taxol®, which uses a 1:1 v/v mixture of Cremophor EL® and ethanol as vehicle (Singla et al., 2002). Several studies have shown Cremophor EL to be a problematic vehicle (Trissel et al., 1994; Trissel, 1996). The incorporation of paclitaxel into PLGA nanoparticles was promising in resolving the aqueous solubility of the drug. However, cellular uptake of PLGA nanoparticles is of low capacity (Chen & Langer, 1998) and specificity (Kim & Nie, 2005). To improve the efficiency of PLGA nanoparticles as a carrier for intracellular paclitaxel delivery, we functionalized the nanoparticle surface with WGA in order to promote their internalization and sustained retention by the target cells (Mo & Lim, 2005; Mo & Lim, 2005).

WGA is present at approximately 300 mg/kg in wheat flour (Pusztai et al., 1993). It is

a 36- kDa protein consisting of two identical subunits, with each subunit comprising

an assembly of four homologous domains (Lehr, 2000). WGA can specifically

recognize and bind rapidly with N-acetylglucosamine and sialic acid residues on cell

membrane, which leads to cellular internalization through receptor-mediated

endocytosis (Caldero et al., 1989). Histochemical studies have shown WGA to have

the highest binding rate to human colonic carcinomas, as well as normal human

colonocytes, compared with other plant lectins, e.g. peanut agglutinin (Campo et al.,

1988; Caldero et al., 1989; Heinrich et al., 2005). Experiments reported in Chapter 3

have further confirmed that fWGA was taken up by colon cells in the rank order of

Caco-2 > HT-29 > CCD-18Co, suggesting that WGA showed agglutination selectivity

for malignant colon cells relative to the normal colon cells. However, it is not known

whether WGA upon conjugation to PLGA nanoparticles would retain the capability to

participate in receptor-mediated endocytosis in the colon cells, which would be

critical in providing a conduit for the intracellular accumulation of paclitaxel.

The experiments in this chapter aimed to evaluate the differential uptake and efficacy

of WNP in appropriate colon cell models. The nanoparticles were prepared according

to the method developed in our laboratory (Mo & Lim, 2005). Cellular uptake of

WNP by the colon cancer cell lines, Caco-2 and HT-29, and colon fibroblast cell line,

CCD-18Co, was quantified by a fluorometric method through the use of fWGA to prepare the nanoparticles. The uptake data were correlated with cytotoxicity data of the formulation versus control formulations against the cell lines. In addition, we attempt to provide an understanding of the mechanism(s) of action of the formulations by monitoring paclitaxel-mediated apoptosis using flow cytometry, cell nuclei staining and microscopic examination.

WGA-conjugated, paclitaxel-loaded PLGA nanoparticles are designated as WNP, while the corresponding fWGA-conjugated nanoparticles are designated as fWNP. Control formulations consisted of (a) paclitaxel-loaded PLGA nanoparticles without WGA conjugation (PNP), (b) equivalent Taxol® formulation of paclitaxel dissolved in a 1:1 solvent mxture of Cremophor EL and ethanol at 6 mg/ml (P/CreEL), and (c) drug-free nanoparticles conjugated with WGA (WN), fWGA (fWN) and fBSA (fBN).

4.2 Materials

Resomer® RG 502H (lactide:glycolide = 50:50, acid number of 10.7 mg KOH/g) was a kind gift from Boehringer Ingelheim, Germany. FITC-labeled bovine serum albumin (fBSA, FITC content 10mol/mol albumin), 1-ethyl-3-(3-dimethylaminopropyl)carbodiimide hydrochloride (EDAC), 2-(N-morpholino)ethanesulfonic acid (MES), N-hydroxysuccinimide (NHS), glucose,

phosphotungstic acid (PTA), polyvinyl alcohol (PVA, mw 30,000 – 70,000), glycine and isopropyl myristate (IPM) were products of the Sigma Chemical Co.(St. Louis, Missouri, USA). Hoechst 33342 (trihydrochloride trihydrate) was purchased from Molecular Probes, UK. Paclitaxel (microcrystalline powder, >99.5% purity) was purchased from the 21CEC Company (Oaklands, UK) while MEM and McCoy 5A were from Invitrogen (Grand island, NY, USA). DNA-free RNase was from the Sigma Chemical Company; cell culture dish (100 mm) was from BD Biosciences (Falcon, NJ, USA). All other materials are the same as those listed in section 3.2.

4.3 Methods

4.3.1 Preparation of WGA-conjugated, paclitaxel-loaded PLGA nanoparticles

PLGA nanoparticles with and without the incorporation of paclitaxel were manufactured according to the method developed in our laboratory (Mo & Lim, 2005). This method was based on a modified emulsion solvent evaporation method (MESE) established for the preparation of PLGA nanoparticles (Murakami et al., 1999; Mo & Lim, 2005). Nanoparticles were prepared at ambient temperatures. PLGA (100 mg), IPM (30 mg) and, if required, paclitaxel (10 mg), were dissolved in 5 ml of methylene chloride. The organic phase was emulsified in 50 ml of aqueous surfactant solution (0.5 % (w/v) of PVA) by probe sonication (Sonics VC-130, Sonics and Materials Inc., CT, USA, 25 watts output, 2 min, pulse 2 s) on an ice bath, and further magnetically

agitated at 1,000 rpm (Thermolyne, Iowa, USA) for 5h to completely remove the

organic solvent (Scheme 1).

PLGA (100mg), IPM (30mg), Paclitaxel (10mg) dissolved in 5ml methylene
chloride

↓ probe sonication, 2 min

0.5%PVA solution on an ice bath

↓

Resultant NP dispersion was stirred at 1000 rpm for 5h to remove the organic

solvent

↓

NPs were washed with 4 x 50 ml of distilled water

↓

Dispersion was concentrated to 10 ml by crossflow filtration using MES buffer, pH

5.8
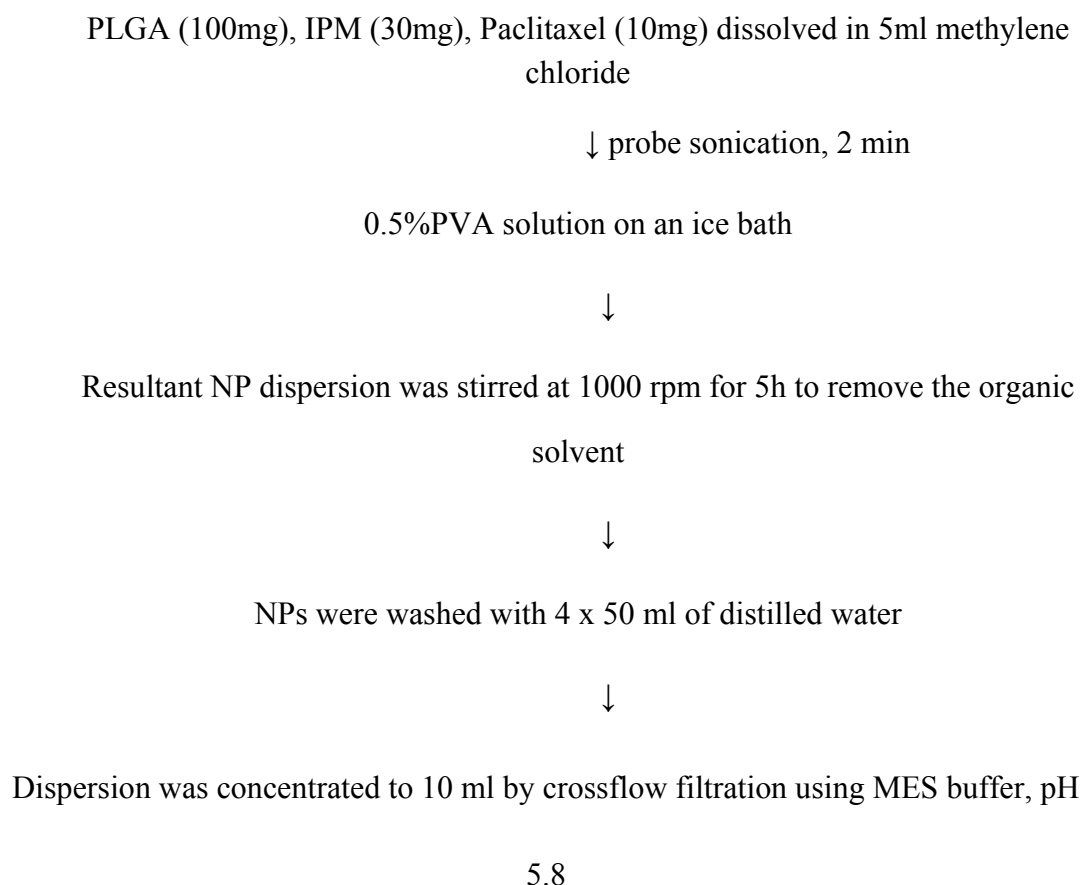
Scheme 1: Schematic diagram on the preparation of PLGA nanoparticles (NP) loaded

with paclitaxel.

WGA was conjugated to the surface of the PLGA nanoparticles by a two-step EDAC

method. This method involves the activation of the free carboxyl groups on the

particle surface in an EDAC/NHS aqueous mixture, followed by conjugation of the

activated groups with the amino groups in the lectin molecules. A schematic representation of the synthetic pathway is provided in Figure 4.1.
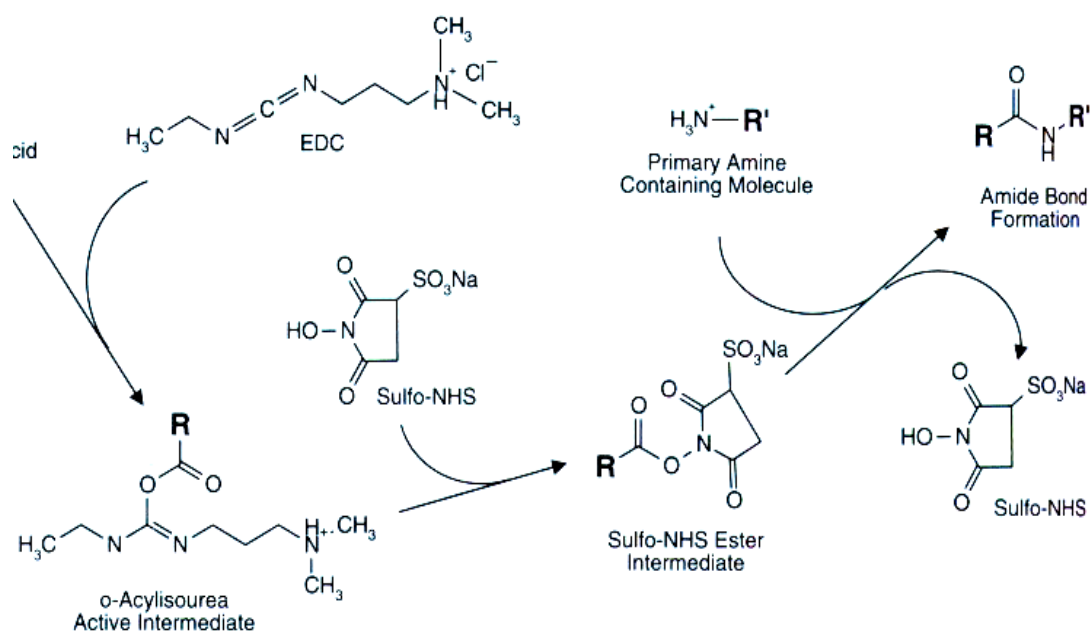
Figure 4.1 Activation of PLGA surface carboxyl groups by 1-ethyl-3-(3-dimethylaminopropyl) carbodiimide hydrochloride (EDAC) for subsequent surface conjugation with WGA

To conjugate the surface of the PLGA nanoparticles with WGA, hardened nanoparticles were washed with 4 × 50 ml of distilled water followed by 50 ml of MES buffer (0.11M, pH 5.8) in a crossflow cassette (Vivascience, Hanover, Germany; molecular cutoff 100,000). The dispersion was concentrated to 10 ml in the cassette and then mixed with 1 ml of 0.1M EDAC/0.7M NHS at 100 rpm for 1h at room temperature. Excess reaction medium was removed by crossflow filtration and the nanoparticles were washed with 3 × 50 ml of PBS. The nanoparticle dispersion was

added dropwise into a centrifuge tube containing 2 ml of WGA (1 mg/ml in PBS) under vortexing. The reaction was allowed to proceed overnight and unreacted WGA was separated from the nanoparticles by crossflow filtration with 3 × 50 ml of PBS. Excess coupling sites were blocked by incubating the nanoparticle dispersion (10 ml) with 1 ml of glycine solution (200 mg/ml in PBS) for 0.5h at ambient conditions. The preparation procedure is summarized in Scheme 2. Preparation of corresponding fWGA- and fBSA-conjugated PLGA nanoparticles followed similar procedures except that equivalent concentrations of fWGA and fBSA were used in place of WGA.

10 ml PLGA nanoparticle suspension

↓ under stirring speed of 100 rpm

Incubated with 1 ml of 0.1 M EDAC/0.07M NHS for 1h

↓

Excess reagents removed by washing with 3×10ml PBS using crossflow filtration and dispersion was concentrated to 10 ml

↓

Incubated overnight with 2 ml of WGA (1 mg/ml in PBS)

↓

Unbound WGA removed by crossflow filtration with 3×50 ml of PBS

↓
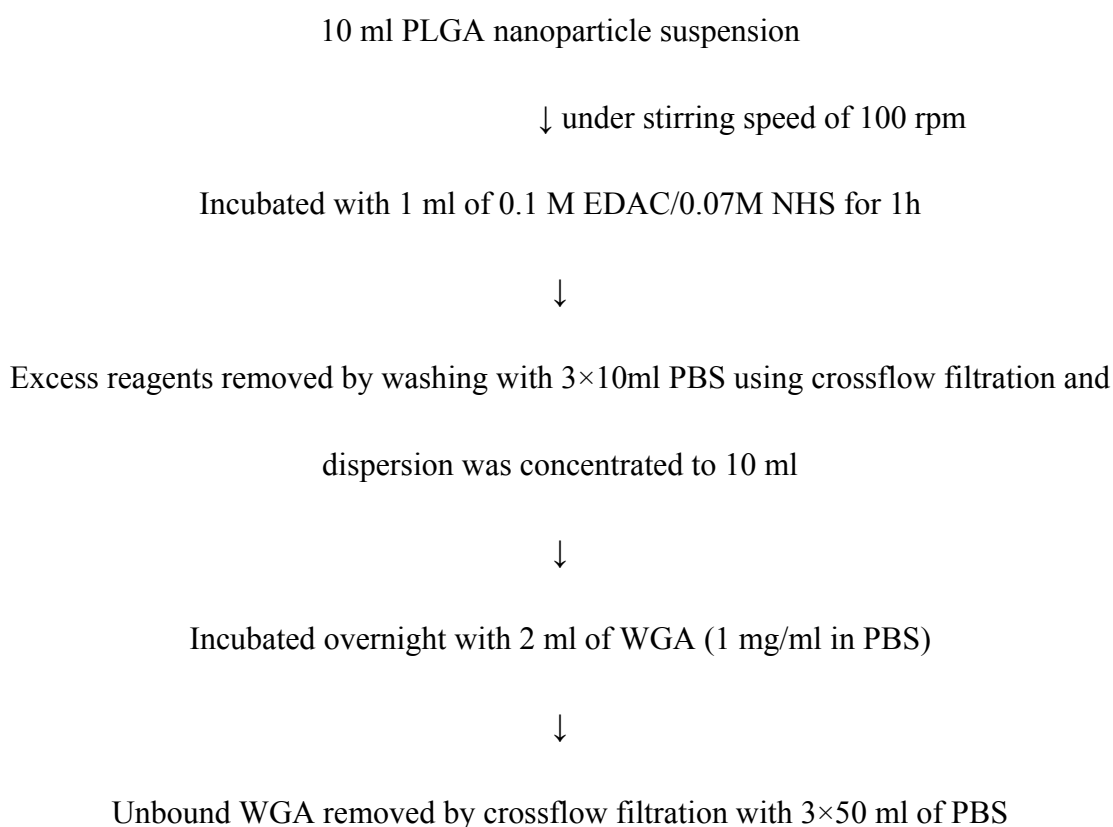
Incubated for 0.5 h with 1 ml of glycine solution (200 mg/ml in PBS)

↓

Excess glycine removed by cross-flow filtration with 3 × 20 ml of HBSS

↓

Nanoparticle dispersion concentrated to 10 ml and used immediately for analysis.

Scheme 2: Schematic diagram for the conjugation of WGA onto preformed PLGA NP.

4.3.2 Characterization of nanoparticles

4.3.2.1 Particle size, zeta potential and morphology

Particle size of PLGA nanoparticles was determined with a particle size analyzer based on the Photon Correlation Spectroscopy (PCS) principle (Zetasizer 3000HSA, Malvern Instruments Ltd., Worcestershire, England). The nanoparticle samples were diluted 1:10 (v/v) with deionized water before they were measured for mean size. The zeta potential of the PLGA nanoparticle dispersions was determined using the same particle size analyzer (Zetasizer 3000HSA). Nanoparticle dispersions were also diluted 1:10 v/v with distilled water before they were measured for zeta potential at an applied electric field of 150 V. The morphology of the nanoparticles was observed under a transmission electron microscope (TEM, Jeol Electron Microscope,

JEM-100CXII, Japan) and scanning electron microscopy (SEM, Hitachi S-4200, Japan). For TEM analysis, freshly prepared nanoparticle dispersion were placed on a copper grid with Formvar® films and stained with 1% w/v phosphotungstic acid (PTA) solution at room temperature for 1 min. Excess staining solution was removed with a blotting paper and the nanoparticles were air-dried before they were viewed under the TEM. For the SEM study, a drop of nanoparticle suspension was placed on a copper grid, air-dried, then mounted onto aluminium sample studs using double-sided carbon tapes and Au sputtered at 50 mA for 60 s. The nanoparticles were then viewed under a Hitachi S4200 Field Emission Scanning Electron Microscope at 5 kV.

4.3.2.2 WGA loading efficiency

To quantify the conjugated WGA, a co-solvent system that could dissolve both the particle and the protein was used. Lyophilized nanoparticles (FD3 Freezer drier, Dynavac engineering Pte Ltd., Wendouree, Australia) were accurately weighed out (5 mg) and the pellet was dissolved in 0.5 ml of DMSO. After about 1h incubation with the occasional manual agitation, 2.5 ml of a 0.05 N NaOH solution containing 0.5% w/v SDS was mixed gently. After about 3h, the sample was analysed for protein content using the Micro BCA protein assay. Protein-free blank PLGA nanoparticles subjected to the same processing procedures were used as control.

4.3.2.3 Determination of paclitaxel loading efficiency

To determine the paclitaxel loading efficiency, 3 mg of lyophilized nanoparticles were accurately weighed out and dissolved in 20 ml of a mixture of acetonitrile/water 50:50 (v/v) aided by bath sonication. 20 µl of the solution was analyzed by HPLC method. The HPLC method was developed and validated for the quantitation of paclitaxel. Chromatographic separation was achieved on an Agilent 1100 system (Agilent Technologies, Palo Alto, CA) equipped with a C_{18} column (200× 4.6 mm, 5 µm) (Waters, Milford, MA) preceded by a guard column (Waters). Flow rate of 1 ml/min was applied, with UV detection at 229 nm. The mobile phase consisted of 1:1 v/v acetonitrile and water. A linear standard curve was obtained over the concentration range of 0.1 to 10 µg/ml ($R^2 > 0.99$). Drug loading efficiency was calculated as the weight of paclitaxel relative to the weight of nanoparticles recovered following the lyophilization of the nanoparticles.

$$\text{Loading efficiency} = \frac{\text{Weight of paclitaxel recovered in the nanoparticles}}{\text{Weight of nanoparticles}}$$

4.3.2.4 *In vitro* drug release

The *in vitro* paclitaxel release profile of WNP was determined by measuring the residual paclitaxel in the particles after incubation with the release medium (PBS, pH 7.4) for specified time periods. Freshly prepared nanoparticle dispersion (0.3 ml) was

incubated with 30 ml of PBS at 37 ± 0.5 °C in centrifuge tube and shaken horizontally at 100 rpm (Shaker bath, Lab Line Instruments Inc., Illinois, USA). At predetermined time intervals, three tubes were taken out and centrifuged at 24,000 rpm, 4°C for 20 min. The pellet was freeze-dried overnight and re-dissolved in 20 ml of mobile phase. Paclitaxel content was determined by HPLC (method described in section 4.3.2.3). The amount of drug released into the medium was calculated by calculating the difference between the residual drug in the pellet and the initial drug load in the nanoparticles.

4.3.3 *In vitro* cytotoxicity of blank WGA-conjugated PLGA nanoparticles (WN)

In vitro cytotoxicity profile of WN against Caco-2, HT-29 and CCD-18Co cells was evaluated using the MTT assay. The cells were separately seeded onto 96-well plates at a density of 10,000 cells/well. Nanoparticle dispersions were prepared according to the procedures in section 4.3.1. The dispersions were diluted with culture medium to 0.1 to 5 mg/ml before administration to the cells at 200 μl/well. Upon reaching confluency, the cells were washed with 2×200 μl of PBS before incubation with 200 μl of nanoparticle dispersion for 24 or 72 h. Cells treated with 0.1% (w/v) of aqueous SDS and 1% aqueous dextran served as positive and negative controls, respectively. At the end of the specified incubation periods, the samples were aspirated and the cells were washed thrice with 200 μl of PBS followed by incubation with 200 μl of

MTT solution (1 mg/ml in PBS) for 4h at 37°C. The cells were lysed with 200 µl of

DMSO to extract the intracellular purple formazan, which was quantified by

measuring the absorbance of the resultant solution at 590 nm using a plate reader

(Spectra Fluor, Tecan Group Ltd, Switzerland).

4.3.4 Uptake of blank fWGA (fWN) and fBSA- (fBN) conjugated PLGA

nanoparticles

To quantify the uptake of fWN and fBN by the three cell lines, the respective cells

were seeded onto 24-well plates at a density of 1.0×10^5 cells/well. Confluent cells

were washed and pre-incubated with 200 µl of HBSS/HEPES for 1h at 37°C, then

incubated for 0.5 to 3 h at 37°C with 0.4 ml of the respective nanoparticle dispersion

(0.625, 1.25, 2.5, 3.33 or 5.0 mg/ml in HBSS/HEPES). Uptake was terminated by

washing the cell monolayers twice with HBSS/HEPES and solubilizing the cells with

0.4 ml of 5% SDS in 0.1M NaOH. Cell-associated fWN and fBN were quantified by

analyzing the fluorescence intensity of the cell lysates in the plate reader.

The plate reader was calibrated in the following manner. Cultured cells from the

respective cell lines were harvested from the 24-well plates and lyzed in 0.1 M NaOH

/ 5% SDS to a final concentration of 5×10^5 cells/ml. Freshly prepared fWN and fBN

dispersions were diluted in the cell lysate to give final concentrations ranging from

0.625 to 5.0 mg/ml, and the fluorescence intensity of the standard solutions were measured in the plate reader.

4.3.5 Antiproliferation activity of paclitaxel

The *in vitro* anticancer efficacy of a chemotherapeutic drug can be determined by its ability to inhibit the growth of tumor cells, also known as antiproliferation activity (Chang et al., 2003; Kanzawa et al., 2003). The MTT assay was used to investigate the anti-cytoproliferative activity of paclitaxel against the Caco-2, HT-29 and CCD-18Co cells. Cells were cultured on 96-well plates at a seeding density of 8×10^3 to 10×10^3 cells/well in 200 μl of cell culture medium. Cells were cultured for 24 h in 5% CO_2/95% air at 37°C to allow for attachment before they were washed with $3 \times$ 200 μl of sterile PBS followed by incubation with the paclitaxel solutions (10 to 1000 nM). The paclitaxel solutions were prepared by serially diluting a paclitaxel stock solution (1 μM in sterile DMSO) with cell culture medium. Medium containing 0.1% SDS was used as positive control and medium supplemented with 0.5% DMSO and 1% dextran was used as negative control. The cells were incubated for a further 4, 24, 48 and 72 h at 37°C before the paclitaxel was removed and the cells incubated with 100 μl of MTT solution (1 mg/ml in HBSS-HEPES, pH 7.4) for 4 h at 37°C. Intracellular formazan crystals were extracted into 100 μl of DMSO, and quantified by measuring the absorbance of the cell lysate at 590 nm (Spectra Fluor plate reader,

Tecan, Austria) with DMSO as blank (n=6). Cell viability was calculated as a percent based on the absorbance measured relative to the absorbance obtained from cells exposed only to the culture medium containing 0.5% DMSO.

Parallel experiments were conducted with paclitaxel-loaded formulations against the Caco-2, HT-29, and CCD-18Co cells. The cells were plated at 5,000-8,000 cells per well, cultured for 24 h to allow for attachment and exposed to WNP, PNP and P/CreEL diluted to specified paclitaxel doses with supplemented culture medium. Treatment with serum-supplemented medium was used as a negative control (0% cell death), and treatment with 0.1% SDS was used as a positive control (100 % cell death).

4.3.6 Cellular accumulation and efflux of paclitaxel

Caco-2, HT-29 and CCD-18co cells were seeded onto 12-mm dishes at a density of 2×10^4 cells/cm^2 and used after 3 days of culture in 10 ml of respective culture medium when they had reached confluency. Cellular uptake experiments were initiated by the addition of fresh culture medium containing WNP, PNP or P/CreEL to give final concentration equivalent paclitaxel concentration of 40 μg/ml. After 2h incubation at 37 ˚C, cells were immediately washed thrice with ice-cold PBS, harvested with a rubber scraper, centrifuged at 10,000g for 10 min, and the cell pellets

were lysed in 300 µl of methanol under sonication. Paclitaxel content in the supernatant was quantified under the chromatographic conditions described in section 4.3.2.3. The extraction recovery of paclitaxel was determined by comparing peak areas of extracts to those obtained on direct injection onto the column of the same amount of paclitaxel in methanol. More than 85% of the paclitaxel was extracted into the supernatant from cell lysis samples spiked with a known amount of paclitaxel by HPLC method. Relative standard deviations (RSD) for day-to-day and within-day precision for this assay were less than 10%. The HPLC peaks were recorded and integrated using the Agilent data analysis software.

To estimate the rate of efflux of cellular paclitaxel, subconfluent cells in 12-mm petri dishes were incubated with 6 ml of WNP, PNP and P/CreEL in culture medium for 2 h as described above. After the tested sample was aspirated and the cells were washed with PBS three times, the cells were further incubated with fresh culture medium devoid of drug for another 2 h at 37 ˚C. The paclitaxel content of the harvested cells was lyzed and the paclitaxel in the cell lysate was determined by HPLC method as described above and the data expressed as paclitaxel content (µg) per unit weight (mg) of total cell protein.

4.3.7 Visualization of cell-associated nanoparticles

It is often not easy to discriminate between particles internalized by cells and those externally attached to the cellular membrane by observation under the conventional fluorescence microscope. It is particularly complicated when the particles are bioadhesive and cannot be readily removed by simply washing the cells after the uptake experiments. The confocal microscope overcomes these shortcomings by 'optical sectioning', which allows the selective observation of specified thin layers of a specimen (Laurent et al., 1994). A series of confocal sections can then be combined to give a three-dimensional image of the specimen. In this study, the internalization of WNP by the colon cells was visualized under a confocal microscope.

Uptake experiments of fWNP were performed on cell monolayers cultured in Lab-Tek® eight-well chambers (Nalge Nunc Inc., Denmark, seeding density of 1.0×10^5 cells/cm^2). Cells were incubated with 200 µl of culture medium over 72 h before they were exposed to 100 µl of fWNP (1 mg/ml in HBSS/HEPES) for 1 h. Uptake was terminated by aspiring the nanoparticle dispersion followed by thrice washing with PBS. To differentiate between extracellular and internalized nanoparticles, the cells were incubated post-uptake with 200 µl of trypan blue (TB) solution (0.2 mg/ml in MES, pH 4) for 3 min so that any fluorescence attributed to extracellular WNP might be quenched. Cell monolayer was then fixed with 200 µl of methanol/acetone

(1:1 v/v) at 4°C for 5 min. Excess staining solution was removed by washing with 3 ×

0.4 ml of cold PBS and the cells were preserved with mounting medium for analysis

(Zeiss, Heidelberg, Germany, λ_{ex} 488nm, λ_{em} 530nm).

To measure the fluorescence of cell lysate before and after TB treatment, Uptake

experiments of fWNP were performed as described in confocal study. Uptake was

terminated by aspiration of the test or control samples and the cells were lyzed with

0.2 ml of 0.1N NaOH/5% SDS for 30 min and the cell-associated fluorescence was

measured at λ_{ex} 485nm and λ_{em} 535 nm.

4.3.8 Cell morphological and nucleus fragmentation examination

Caco-2 cells were seeded on 6-well plates at a density of 10,000 cells/well and treated

with WNP, PNP and P/CreEL formulations adjusted with culture medium to have the

same paclitaxel concentration of 40 μg/ml on the 3rd day post-seeding. Cells treated

with culture medium served as control. At predetermined time intervals (4 h and 24 h),

the cells were washed with cold PBS thrice and cell morphology was examined under

a total internal reflection microscope at 10 × (Nikon, Nikon Instruments Inc.,

Kanagawa, Japan).

Caco-2 cells were seeded on 6-well plates at a density of 10,000 cells/well and similarly treated with test samples as described in cell morphology study. Following the decanting of test sample, the cells were washed with cold PBS three times and fixed in 0.4 ml of a methanol: acetone (1:1 v/v) solvent mixture at 4 °C for 10 min. The cells were then washed with cold PBS, air-dried and stained with Hoechst 33342 for 10 min. Excess Hoechst 33342 was removed by washing with cold PBS and nucleus images of the cells were acquired under Nikon microscope.

4.3.9 Cell cycle analysis by flow cytometry

A cell cycle is composed of four phases: G_1, the phase in which the cell prepares for DNA replication; S phase, in which the DNA is replicated; G_2 phase, in which the cell pauses as it prepares to divide; and M, the mitotic (dividing) phase. The DNA content of a cell can provide information about the cell cycle and, by extension, the effect of stimuli on the cell cycle (Sherwood & Schimke, 1995; Terho & Lassila, 2006). Propidium iodide can intercalate with DNA so as to allow for the detection and quantification of the DNA content when the cells are individually passed through a beam emitted from the light source of a flow cytometer (Studzinski, 1995). The use of flow cytometry to quantify nuclear DNA stained with propidium iodide (PI) is one of the most widely used methods to measure the proportion of cells in different stages of the cell cycle. The effectiveness of this method lies in the linear correlation between

the amount of nuclear DNA and the fluorescence of PI stained nuclei (Terho & Lassila, 2006). In addition, there is no need to synchronize the cells to a specific phase since cells can be sorted based on the DNA content (Studzinski, 1995). As paclitaxel is known to induce G2/M arrest of the cell cycle by impairing the function of the mitotic spindle and other microtubule–containing structures (Wang et al., 2000), flow cytometry was used in this study to evaluate the effects of WNP, PNP and P/CreEL on the cell cycle distribution of the Caco-2 cells.

Caco-2 cells were seeded onto 75 cm^2 culture flasks at 3×10^6 cells/flask with 15 ml of culture medium. At 24 h post seeding, the cells were incubated with 10 ml of WNP, PNP and P/CreEL formulation (adjusted with HBSS/HEPES to paclitaxel concentration of 40 μg/ml) at 37 °C for 5 to 24h. Cells treated with culture medium served as control. At the end of the specified incubation period, the test medium was collected into a centrifuge tube, and the cells were harvested by trypsinization and pooled with respective medium. The cells were then washed twice with 5 ml of PBS, fixed by dropwise addition of 4.5 ml of 70% ethanol with vortex mixing to avoid aggregation, and stored at -20°C overnight. Ethanol was removed by centrifugation (MIKRO 22R, Andreas Hettich GmbH & Co KG, Tuttlingen, Germany) at 1400 g, and the cells were washed twice with 5 ml of PBS before staining (0.1% of Triton X-100, 20 μg/ml of PI and 200 μg/ml of RNase in PBS, 1 ml) for 30 min at room

temperature. The cell cycle distribution of 10,000 cells in each sample was analyzed

by flow cytometry (Dako Cytomation Cyan ADP/LX, Fort Collins, CO, USA), and

the data analyzed using the Summit v4.3 software (Dako Colorado, Inc., USA).

4.3.10 Cellular trafficking of WNP

One of the key potential advantages of WNP is its capability to traverse biological

barriers, which will assist in the intracellular delivery of therapeutic molecules.

Insight into the intracellular translocation of WNP is therefore important in providing

a measure of its effectiveness as an anticancer drug delivery system. In this study, we

aimed to monitor the time-dependent transport of fWNP in the cytoplasm of Caco-2

cells. To this end, Lysotracker Red DND-99 was used to stain the late endosome and

lysosome, while Hoechst 33342 was used to stain the cell nuclei.

The uptake experiments were performed on cell monolayers cultured in Lab-Tek®

eight-well chambers. 100 µl of fWNP (1 mg/ml in HBSS/HEPES) were added into

the chamber and the cells were incubated for further specified time periods from 0.5

to 3 h. 0.5h before the end of the incubation period, Lysotracker Red DND-99 was

applied to the incubation medium at a final concentration of 1 µM to stain the acidic

organelles (e.g., endosomes and lysosomes). Uptake was terminated by removing the

medium from the chamber. Hoechst 33342 was then applied to each chamber at a

final concentration of 20 µM and the cells incubated for a further 10 min to allow for nucleus staining. The cells were washed thrice with ice-cold HBSS/HEPES and fixed with 100 µl of methanol/acetone (1:1 v/v) at 4°C for 5 min. Cell images from the bottom of the chamber to the cell monolayer surface were recorded using the confocal microscope (Z-series images), then reconstructed to provide the intracellular trafficking pathway of fWNP. Control experiments were performed by exposing the cells to 100 µl of WGA (2 mg/ml in HBSS/HEPES) for 1h before the uptake study.

4.3.11 Statistical analysis

Data are presented as mean ± standard deviation. Differences between mean values were analyzed for significance by one-way ANOVA using the SPSS 10.0 software. P values ≤ 0.05 were considered to be significantly different.

4.4 Results

4.4.1 Characterization of WGA-conjugated paclitaxel-loaded PLGA nanoparticles

4.4.1.1 Particle size, zeta potential and morphology

As shown previously by our laboratory, and confirmed in this study, the MESE was a simple and reproducible method for the preparation of WGA-conjugated paclitaxel-loaded PLGA nanoparticles. Following WGA conjugation, the mean particle size of the PLGA nanoparticles increased by about 50 nm to 322 $\pm$ 5 nm (n

= 3), while the binding of positively charged WGA to the carboxylic groups of PLGA resulted in a lowering of the zeta potential of the nanoparticles to -3.3 $\pm$ 0.2 mV (n = 3) (Table 4.1). These results were consistent with those obtained in previous experiments conducted by our laboratory (Mo & Lim, 2005). The nanoparticles had a narrow size distribution, indicating a relatively homogeneous population, and appeared relatively spherical in shape when viewed under the TEM and SEM (Figure 4.2).The electron micrographs showed no evidence of particle aggregation.

	Size (nm)	Zeta potential (mV)
Before WGA conjugation	223 $\pm$ 2	-14.9 $\pm$ 1.8
After WGA conjugation	322 $\pm$ 5	-3.3 $\pm$ 0.2

Table 4.1 Size and zeta potential of PLGA nanoparticles before and after conjugation with WGA (Data represent mean $\pm$ SD, n=3)

<center>(A)   (B)</center>
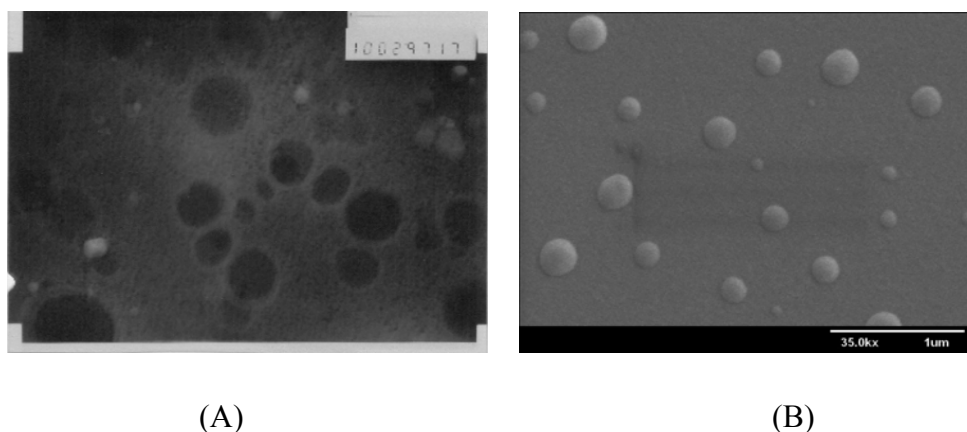
Figure 4.2 (A) TEM (magnification 100,000x) and (B) SEM (magnification of 35,000x) micrographs of WNP

4.4.1.2 WGA loading efficiency

Calibration of the Micro BCA protein assay with WGA standard solutions yielded the following linear equation: absorbance = $0.0388.$Conc (μg/ml) + 0.1483 (R^2 = 0.9992). The WGA conjugation efficiency for the nanoparticles was found to be 18.1 $\pm$ 2.5 μg WGA/mg nanoparticles (n =3), and was within narrow limits between batches. The collective data suggest that the WN nanoparticles were reproducible on a batch to batch basis.

4.4.1.3 Determination of paclitaxel loading efficiency

Linear calibration equation of peak area as a function of concentration for paclitaxel solutions assayed by HPLC was: Area = 35577 C (μg/ml) + 46960 R^2 = 0.9997. The presence of all excipients such as PLGA, PVA and IPM had no influence on the

retention time and peak area of paclitaxel. The paclitaxel loading efficiency was found to be 53.6 ± 1.8 μg paclitaxel / mg nanoparticles.

4.4.1.4 *In vitro* drug release

The *in vitro* release profile of paclitaxel from WNP was showed in Figure 4.3. There was a burst-release in the first 6h followed by a slow release rate over 120h.
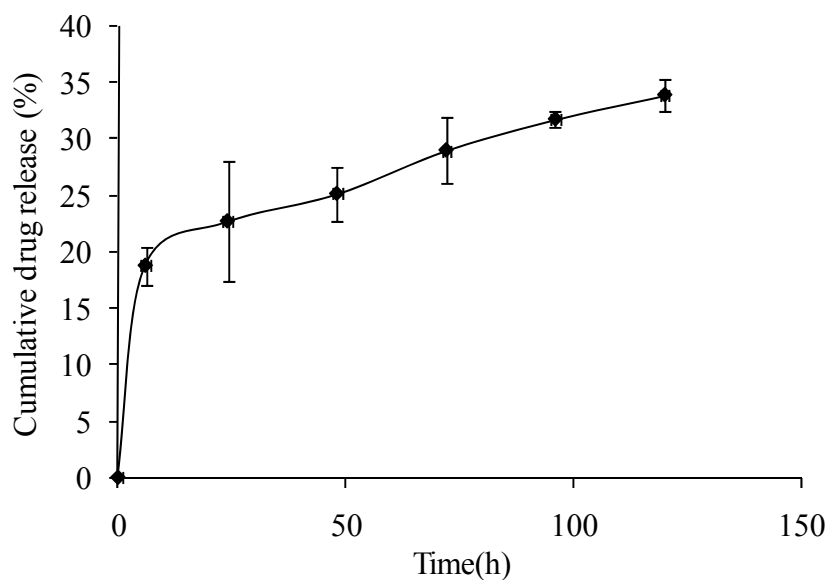
Figure 4.3 *In vitro* release profiles of paclitaxel from WNP into PBS, pH 7.4, 37°C (Mean $\pm$ SD, n=3)

4.4.2 *In vitro* cytotoxicity profile of blank WGA-conjugated PLGA nanoparticles

In vitro cytotoxicity experiments of WN were conducted with culture medium as control medium, and 0.1% SDS and 1% dextran as positive and negative controls,

respectively (Figure 4.4). Based on the dextran data, the nanoparticles were considered to be cytotoxic when they reduced the mean cell viability by 20% or more compared to the cell culture medium control. On this basis, the viability of Caco-2 and HT-29 cells were considered to be unaffected by 24h of incubation with up to 5 mg/ml of nanoparticle. At the the incubation time of 72h, the viability of these two cell types was adversely affected by the nanoparticles at 5 mg/ml. The CCD-18Co cells were more sensitive to the WN, exhibiting lower cell viabilities when exposed to 5 mg/ml of nanoparticles at 24h, and to 2.5 mg/ml of nanoparticles at 72h. Subsequent experiments were performed using equivalent WGA-conjugated PLGA nanoparticle concentrations that did not reduce the viability of the cells to below 80%.

(a)
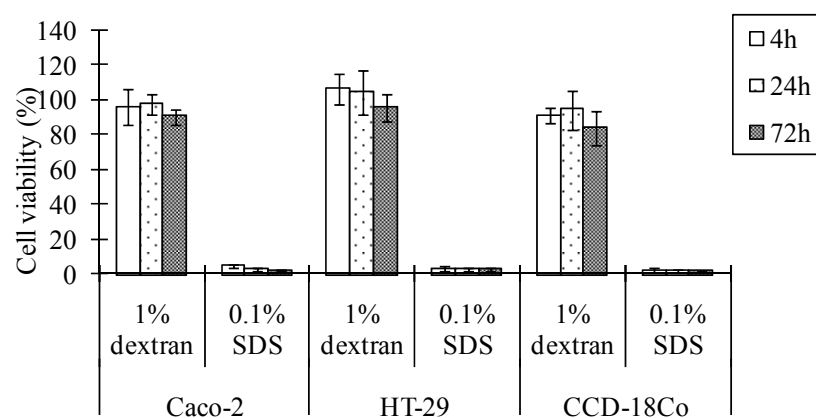
(b)
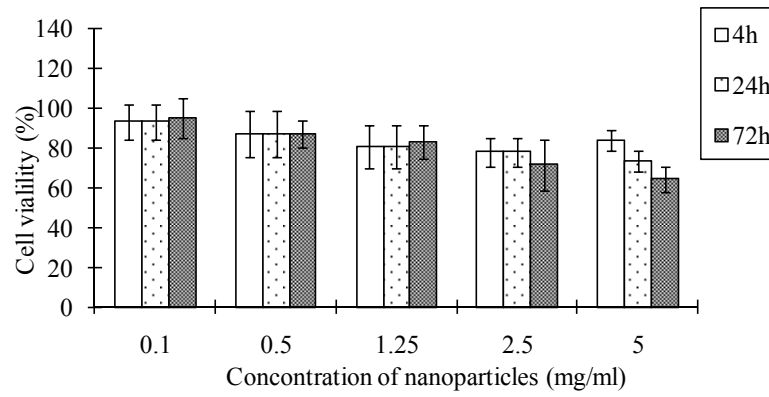
(c)
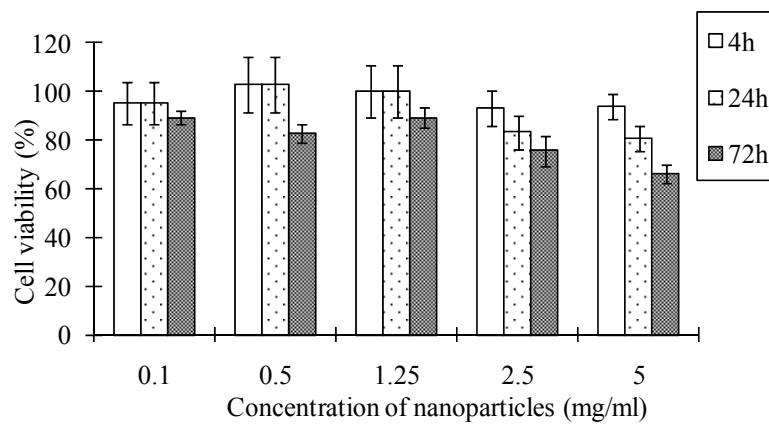
(d)
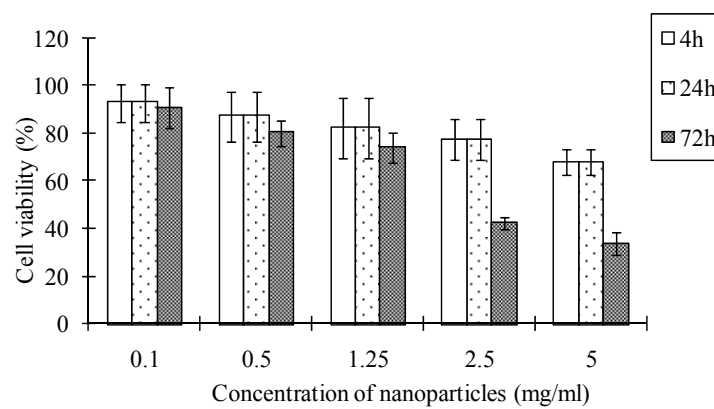
Figure 4.4 In vitro cytotoxicity profile of blank WGA-conjugated PLGA

nanoparticles against colon cells (a) positive and negative control; (b) Caco-2 cells; (c)

HT-29 cells; (d) CCD-18Co cells (Mean ± SC, n = 6)

4.4.3 Uptake of blank fWGA-conjugated PLGA nanoparticles

To determine whether the conjugation of WGA to the PLGA nanoparticles would

compromise its capacity to bind to receptors expressed in cell membranes, uptake

studies of fWN were conducted in the colon cancer cell lines (Caco-2 and HT-29) and

normal colon cells (CCD-18Co), fBSA-conjugated PLGA nanoparticles (fBN) served

as control. The uptake study was conducted over incubation time periods ranging

from 0.5 to 3h, using nanoparticle loading concentrations ranging from 0.625 to 5

mg/ml.

As shown in Figures 4.5 and 4.6, the 3 cell lines showed successful uptake of fWN,

indicating that the conjugated WGA retained its capacity to recognize and bind to

receptors expressed in the cell membranes. Uptake of the nanoparticles by all 3 cell

lines was concentration- and time-dependent, the cellular uptake increasing with

nanoparticle loading concentration and exposure time. At the nanoparticle loading

concentration of 1.25 mg/ml, the uptake by the Caco-2 cells was increased by 2-fold,

from 0.57 to 1.29 mg NP/mg protein, by prolonging the incubation time from 0.5 to

3h. Uptake of fWN by Caco-2, HT-29 and CCD-18Co cells at 0.5h were 0.57, 0.50 and 0.26 mg NP/mg protein, respectively. At the fixed incubation time of 2h, an 8-fold increase in nanoparticle loading concentration resulted in 9.1, 5.2 and 4.8 folds increase in the cellular uptake of the nanoparticles by the Caco-2, HT-29 and CCD-18Co cells, respectively. At all time points and loading concentrations studied, the ranking order of uptake for the WGA-PLGA nanoparticles was Caco-2 > HT-29 > CCD-18Co, suggesting a selectivity of the delivery system for colon cancer cells over normal cells. This would be advantageous when the system is used to deliver an anticancer agent to the colon tissues. Corresponding cellular uptake of fBN by the 3 cell types is shown in figure 4.7. Compared with fWN, the cellular uptake of fBN was of lower capacity in all 3 cell types. Uptake of fWN by the Caco-2 cells was about 12 fold higher than uptake of fBN at the nanoparticle concentration of 1.25 mg/ml at 3 h co-incubation.
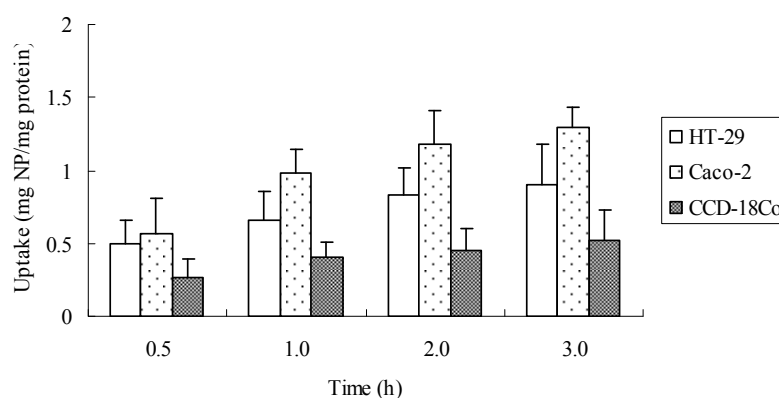
Figure 4.5 Uptake of fWN by Caco-2, HT-29 and CCD-18Co cells as a function of incubation time at loading concentration of 1.25 mg/ml (Mean ± SD, n = 3)
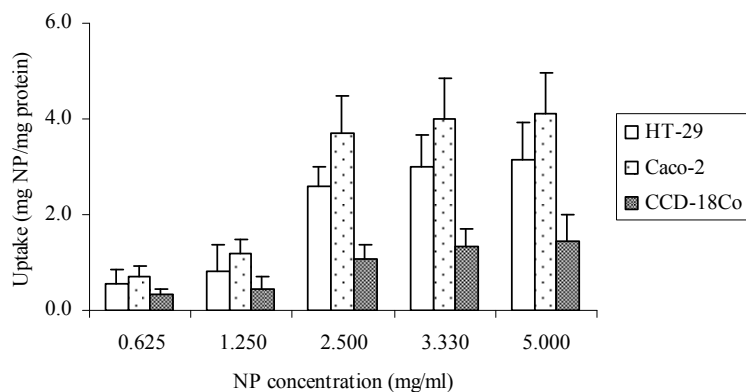
Figure 4.6 Uptake of fWN as a function of loading concentration by Caco-2, HT-29 and CCD-18Co cells over an incubation period of 2h (Mean ± SD, n = 3)
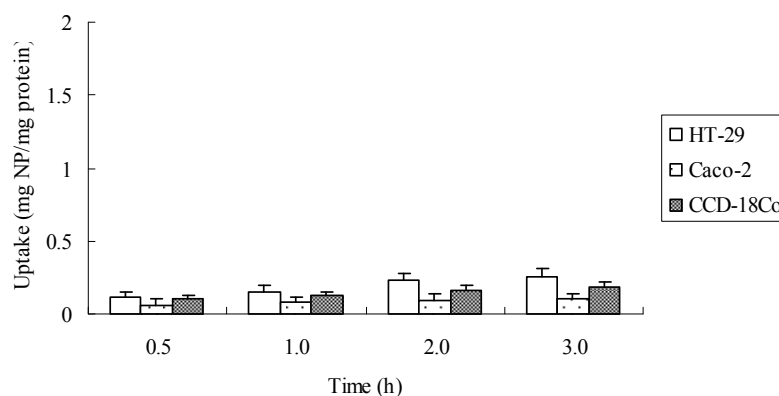
Figure 4.7 Uptake of fBN as a function of incubation time at loading concentration of 1.25 mg/ml (Mean ± SD, n = 3)

4.4.4 Antiproliferation activity of paclitaxel

Viability of all the three colon cell lines after exposure to paclitaxel was found to decrease with increasing exposure time and concentration (Figure 4.8), with the

HT-29 cells being the most sensitive to the anticancer drug. These results indicate that

the commercial paclitaxel was efficacious.

(a)
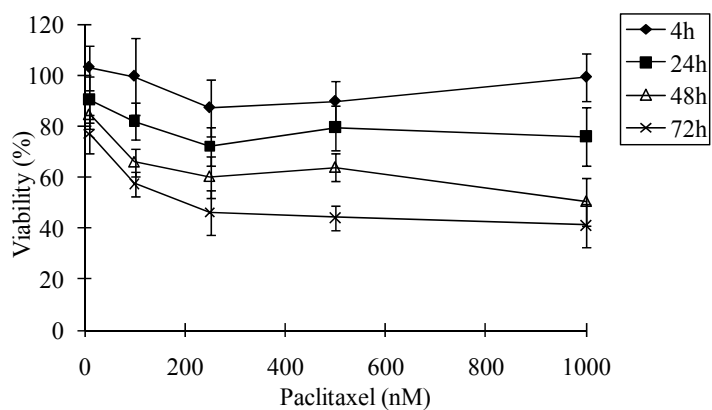
(b)
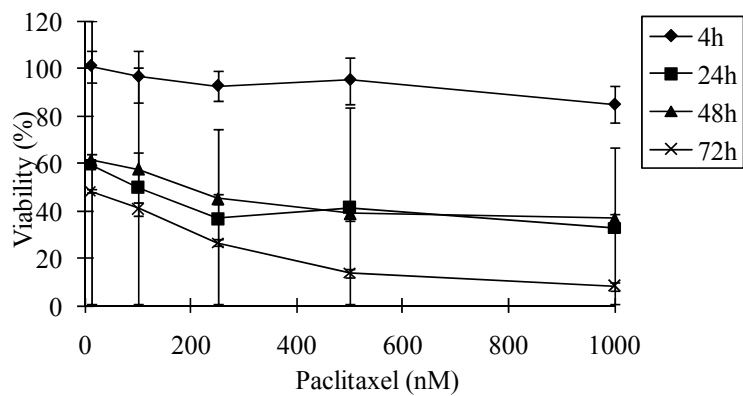
(c)
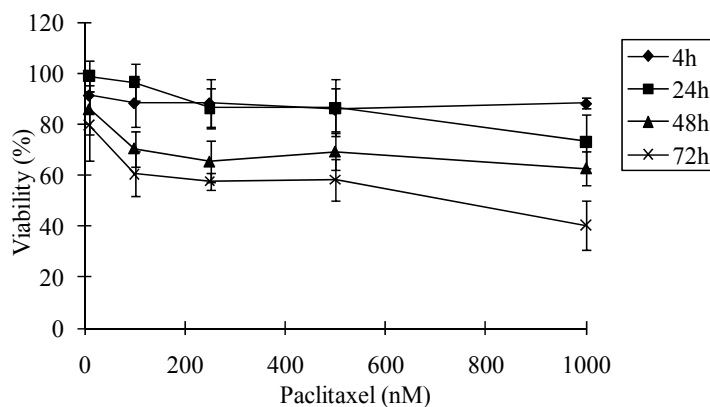
Figure 4.8 *In vitro* cytotoxicity profile of paclitaxel against (a) Caco-2 cells; (b) HT-29 cells; (c) CCD-18Co cells (Mean ± SD, n = 6)

4.4.5 Antiproliferative activity of paclitaxel-loaded PLGA nanoparticles

Figure 4.9 shows the *in vitro* cytotoxicity profiles of P/CreEL, PNP and WNP against the three colon cell lines. Cytotoxicity was evaluated for the paclitaxel concentration range of 0.05 to 50 μg/ml, equivalent to nanoparticle concentration of up to 1 mg/ml, which had previously been shown (section 4.4.2) to be non-cytotoxic to the cells. The nanoparticles were sterilized by gamma-irradiation for 72 h prior to addition to the cells.

The Caco-2, HT-29 and CCD-80Co cells exhibited decreased viability in the presence of increasing concentrations of nanoparticles and upon prolongation of co-incubation time. A comparison of the efficacy of the 3 formulations suggests that WNP was more

effective at lowering the cell viability of Caco-2 and HT-29 cells compared to PNP and P/CreEL. After 72h of co-incubation, Caco-2 cells had less than 40% viability when incubated with 50 µg/ml of WNP (equivalent to a low paclitaxel concentration of 2.5 µg/ml) whereas the P/CreEL formulation produced a viability of 70% in these cells. Of the 3 cell types, HT-29 cells were the most sensitive to the effects of paclitaxel, which was in agreement with the results obtained in section 4.4.4. The WNP formulation was able to reduce the viability of HT-29 cells to below 20% after co-incubation for 72h at concentrations ≥ 50 µg/ml. In contrast, the CCD-80Co cells were least affected by the 3 formulations, although they were still more sensitive to the effects of WNP and PNP, which showed comparable efficacies, than to P/CreEL.

(a)
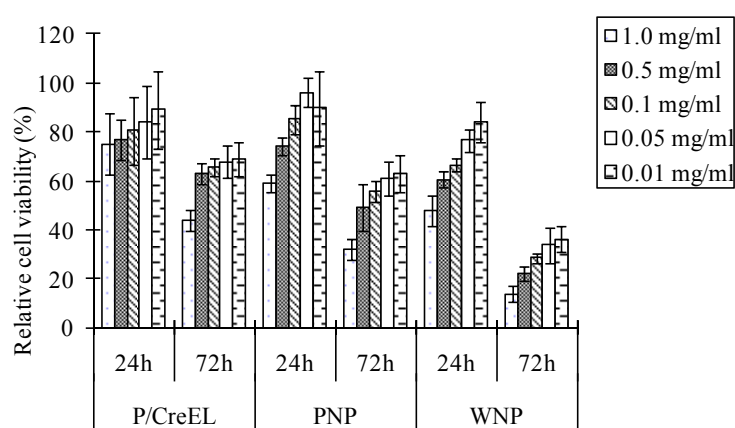
(b)
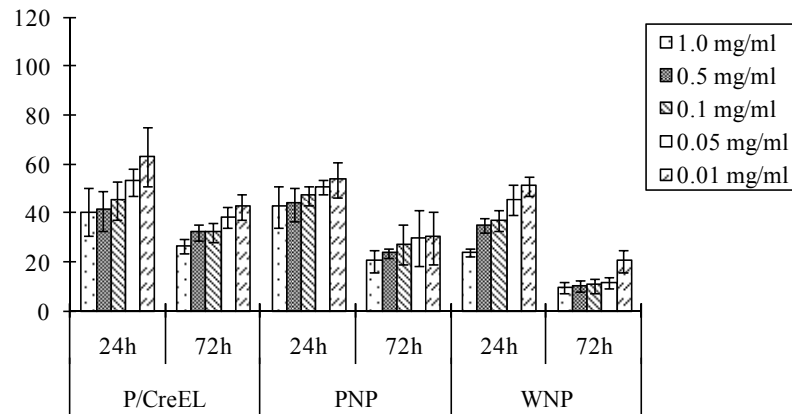
(c)
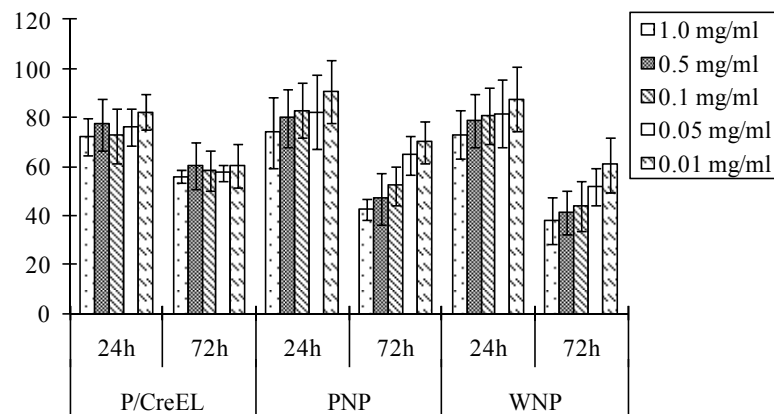
Figure 4.9 *In vitro* cytotoxicity profiles of P/CreEL, , PNP and WNP against (a) Caco-2 cells; (b) HT-29 cells; (c) CCD-18Co cells as a function of incubation time and formulation concentration (Mean ± SD, n = 6)

Sample	Incubation time	Cell type		
		Caco-2	HT-29	CCD-18Co
WNP	24h	1.019±0.233	0.061±0.021*	1.007±0.121*
	72h	0.087±0.020*^	0.028±0.008*^	0.137±0.027*
PNP	24h	1.141±0.341	0.092±0.030*	1.188±0.170
	72h	0.228±0.031*^	0.062±0.015^	0.147±0.035*
P/CreEL	24h	1.387±0.158	0.310±0.019	1.665±0.251
	72h	0.355±0.015	0.069±0.013	0.230±0.021

Table 4.2 IC_{50} values of paclitaxel formulated as WNP, PNP and P/CreEL. IC_{50} values were evaluated after 24 and 72 h exposure and the results represent Mean ± SD values (μg/ml) of three independent experiments, each performed in triplicate. '*' indicates statistical significance compared to P/CreEL ($p < 0.05$), '^' indicates statistical significance between the WNP and PNP formulations ($p < 0.05$).

When the cytotoxicity data were translated into IC_{50} values, calculated on the basis of paclitaxel content (Table 4.2), the WNP and PNP formulations yielded comparable IC_{50} values with the P/CreEL formulation against Caco-2 cells after 24h co-incubation. Enhanced cell-killing effects were observed for WNP, however, upon prolongation of the incubation time to 72h, whereupon the IC50 value was significantly reduced to 0.087 ± 0.020 μg/ml. This value was significantly lower than the IC50 values for PNP and P/CreEL. Similar results were observed for the HT-29 cells.

However, as the HT-29 cells were more sensitive to paclitaxel, the IC50 values for all

3 formulations were lower for this cell model than for the Caco-2 cells. In addition,

the WNP and PNP formulations exhibited greater efficacy than the P/CreEL

formulation at the shorter incubation time of 24h, and there were statistical

differences between the IC50 values for WNP and PNP (Table 4.2) at both 24 and 72h

of incubation. WNP and PNP also showed lower IC50 values in the CCD-18Co cells

compared to the P/CreEL formulation at 24 and 72 h of co-incubation, but there were

no significant differences in performance between the two nanoparticle formulations

of paclitaxel in this cell model.

4.4.6 Cellular accumulation and efflux of paclitaxel

Figure 4.10 shows the data obtained for the cellular accumulation and efflux of

paclitaxel in the Caco-2, HT-29 and CCD-18 Co cells exposed to the P/CreEL, PNP

and WNP formulations. After 2h of incubation, the cellular uptake of WNP was about

1.5 and 2 folds greater than that of PNP in the Caco-2 and HT-29 cells, respectively.

WNP also demonstrated increased intracellular retention (30% of uptake) in the

Caco-2 cells, following post-uptake incubation with fresh medium, compared to the

unconjugated PNP nanoparticles (18%) and the P/CreEL (7%). Similar phenomena

were observed in the HT-29 cells, which retained more than 40% of the internalized

WNP and 27 % of PNP.   The CCD-18Co cells, on the other hand, showed similar

uptake and post-uptake retention profiles of paclitaxel when exposed to the WNP and

PNP formulations.

(a)
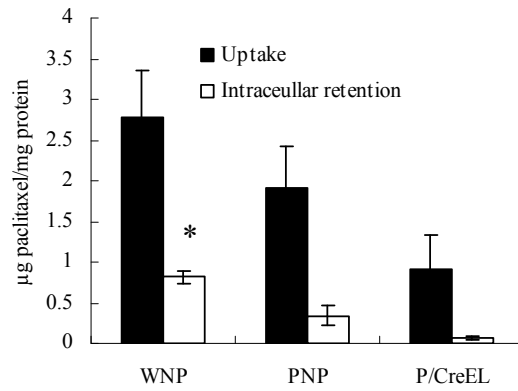
(b)
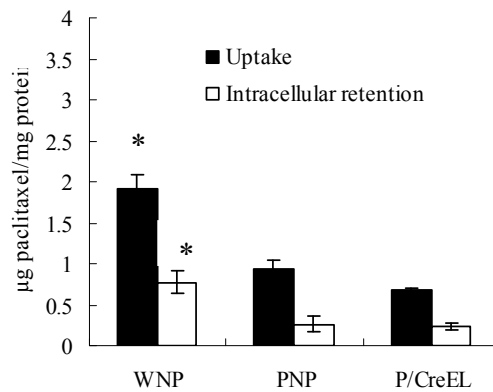
(c)
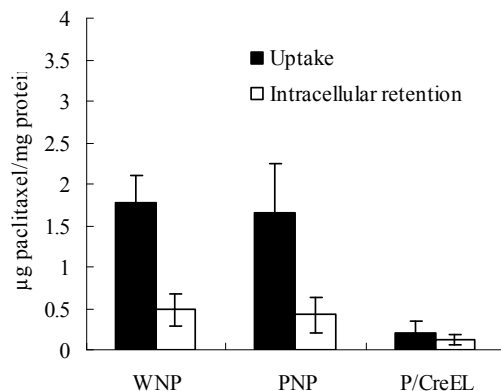
Figure 4.10 Cellular uptake of paclitaxel after 2h exposure to the WNP, PNP and

P/CreEL formulations and intracellular retention of paclitaxel following post-uptake

incubation of the cells with fresh medium (a) Caco-2; (b) HT-29; (c) CCD-18Co cells.

Data represent mean ± SD, n = 3. '*' indicates statistical significance compared to

PNP and P/CreEL ($p < 0.05$)

4.4.7 Visualization of cell-associated nanoparticles

To differentiate between extracellular and internalized WNP, we repeated the uptake

experiments on Caco-2 and HT-29 cells using a WNP formulation prepared with

fWGA. The cells were incubated post-uptake with trypan blue so that any

fluorescence attributed to extracellular WNP might be quenched. Figure 4.11 shows

the confocal microscopic images of the Caco-2 and HT-29 cells before and after

post-uptake TB incubation. In the 1-h uptake experiment with the fluorescent WNP,

there were no significant changes in the cell-associated fluorescence after the cells

were incubated with TB. Fluorescence of the cell lysate before and after TB treatment

was also measured. About 96.3% of the WNP retained after TB treatment, indicating

that the fluorescence seen is caused by the nanoparticles localized inside the cell and

not on the surface.

Before TB treatment   after TB treatment

(a)

(b)
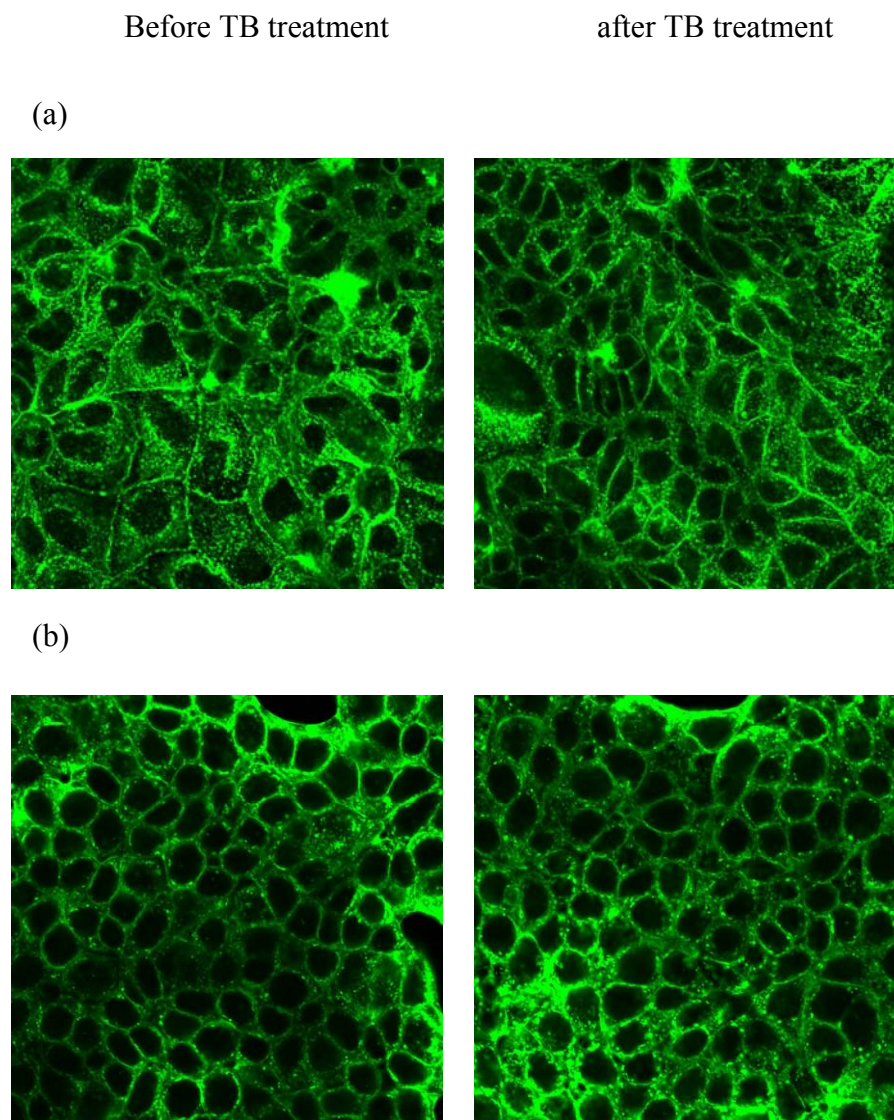
Figure 4.11 Confocal images of (a) Caco-2; (b) HT-29 cells incubated with 1.0 mg/ml

of fluorescent WNP for 1hbefore and after TB treatment.

4.4.8 Cell morphology

Control

4h   24h

WNP
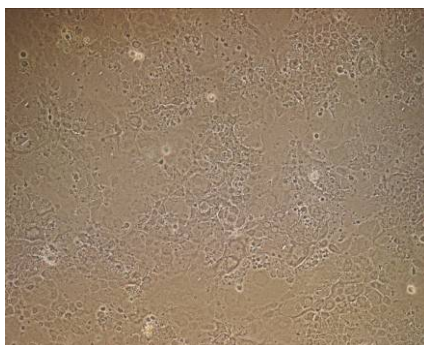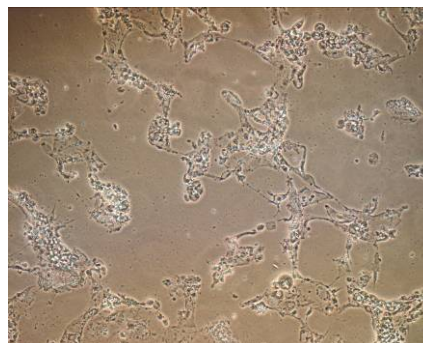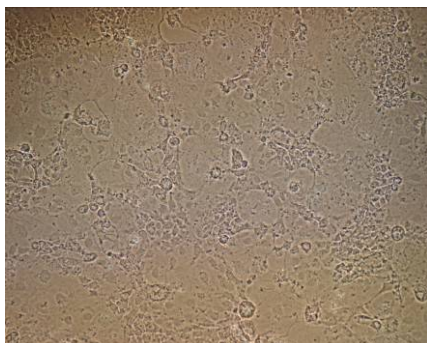
PNP
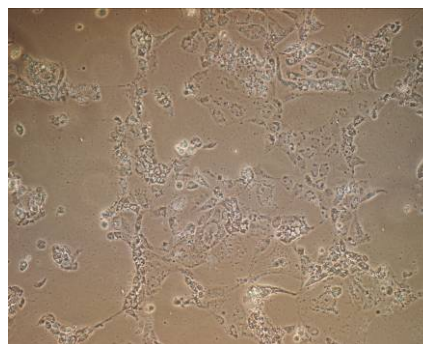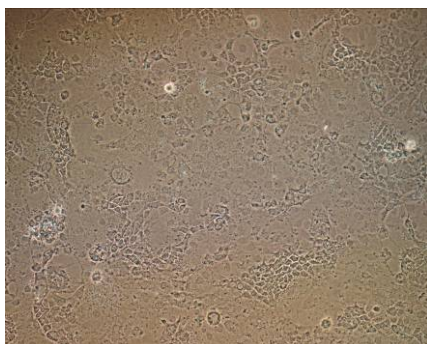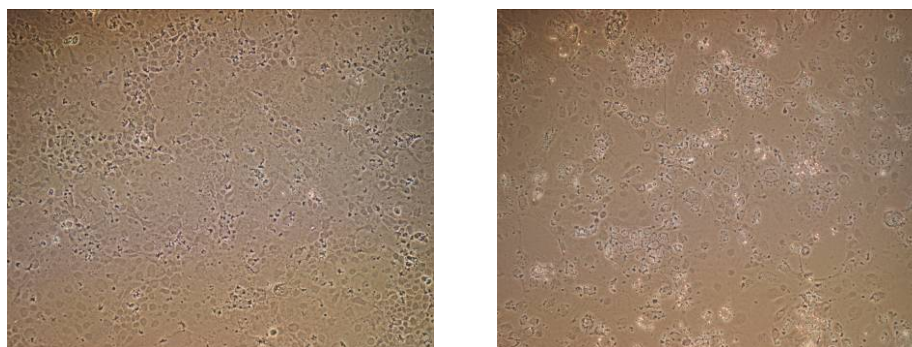
P/CreEL

Figure 4.12 Cell morphology of Caco-2 cells after incubation with WNP, PNP and P/CreEL formulations for 4 and 24h at equivalent paclitaxel concentration of 40 μg/ml.

The microscopic images of Caco-2 cells after treatment with WNP, PNP and P/CreEL for 4 and 24 h are shown in Figure 4.12. The Caco-2 cell monolayers was intact after 4h of co-incubation with all 3 formulations, but the majority of the cells were detached and lost through washing following a prolongation of the incubation time to 24h in the presence of WNP and PNP. By comparison, the Caco-2 cell monolayer remained relatively intact even after 24h treatment with the P/CreEL formulation.

To detect whether there were any nuclei fragmentation indicative of apoptosis, the cell nuclei were stained with Hoechst 33342 and the cells examined under the microscope. The nuclei of control Caco-2 cells showed homogeneous fluorescence with no evidence of segregation and fragmentation (Figure 4.13), and this was also observed of cells exposed for 4h to the WNP, PNP and P/CreEL formulations. In contrast, the cell nuclei became severely fragmented after 24h of incubation with

WNP and PNP, yielding segments of dense fluorescence, suggesting a major breakdown in the chromatin. By comparison, cells treated with P/CreEL for 24h showed a lower level of DNA condensation in the nucleus.

Control

4h   24h

WNP
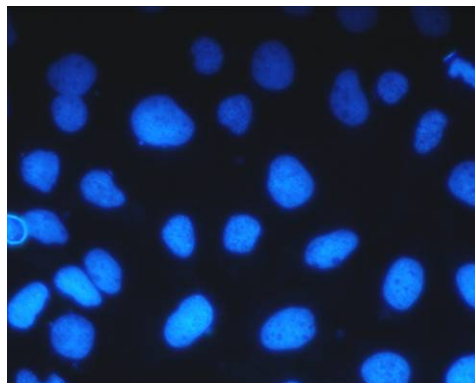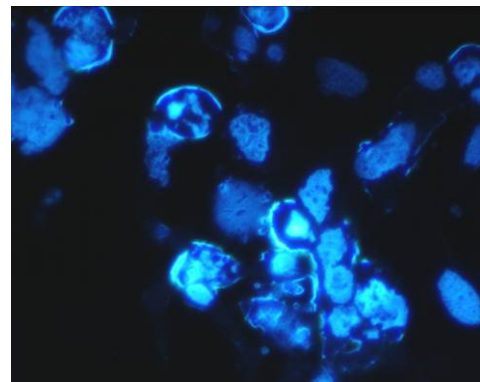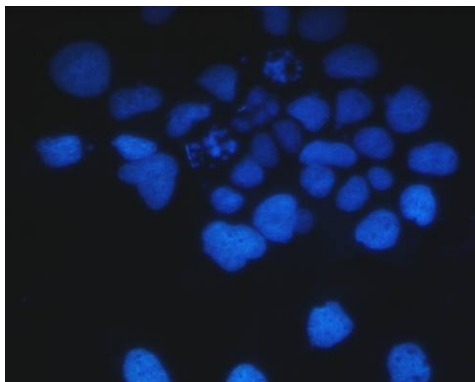
PNP
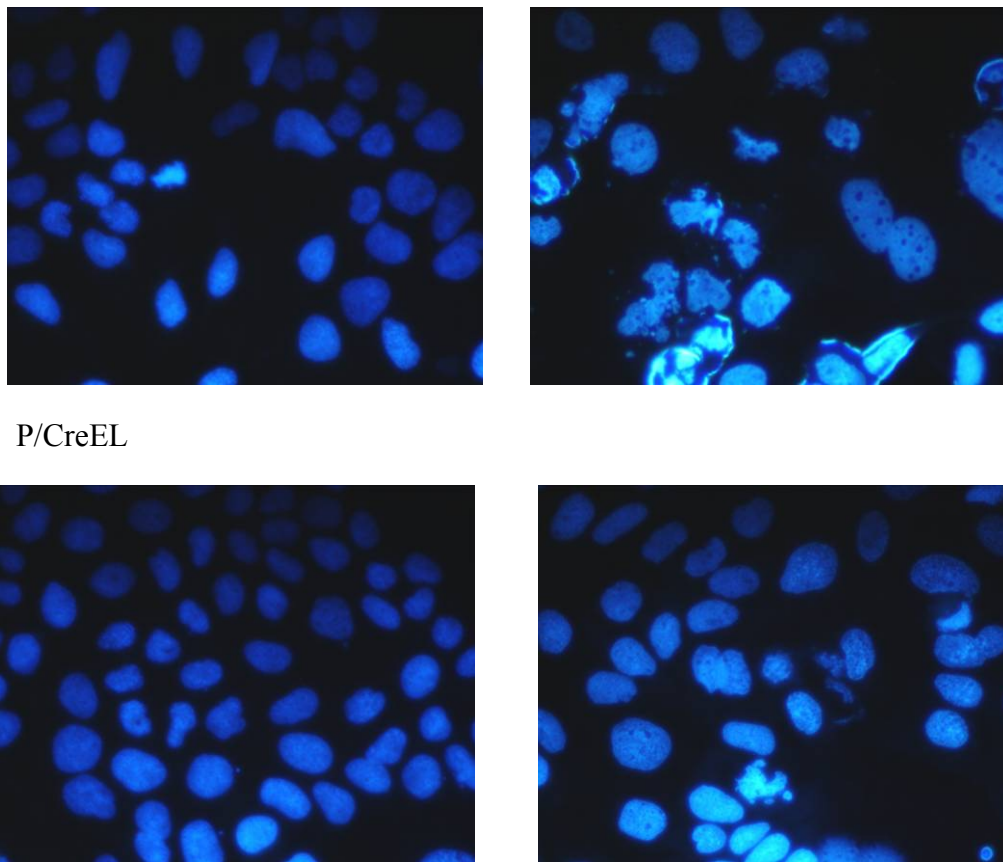
P/CreEL

Figure 4.13 Typical microscopic images of Caco-2 cells following 4 and 24h incubation with WNP, PNP and P/CreEL formulations. Cell nuclei were stained with Hoechst 33342.

4.4.9 Cell cycle analysis

(a)   (b)

(c)   (d)
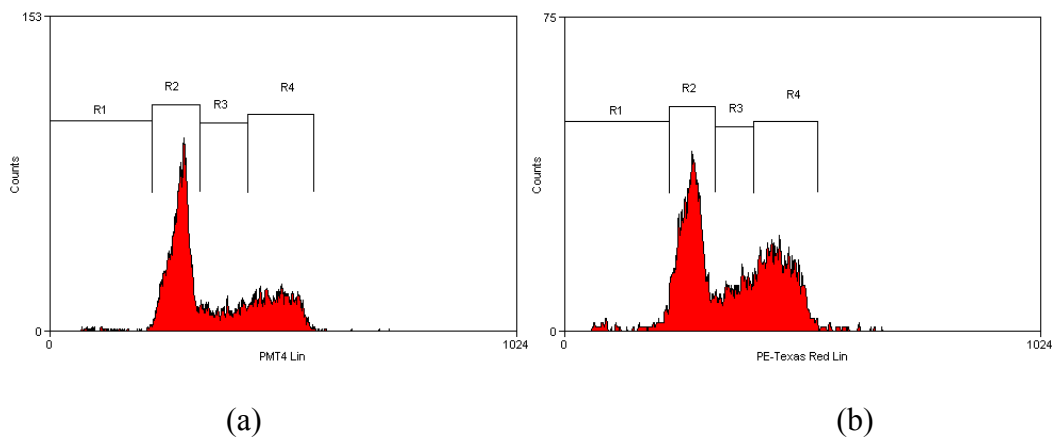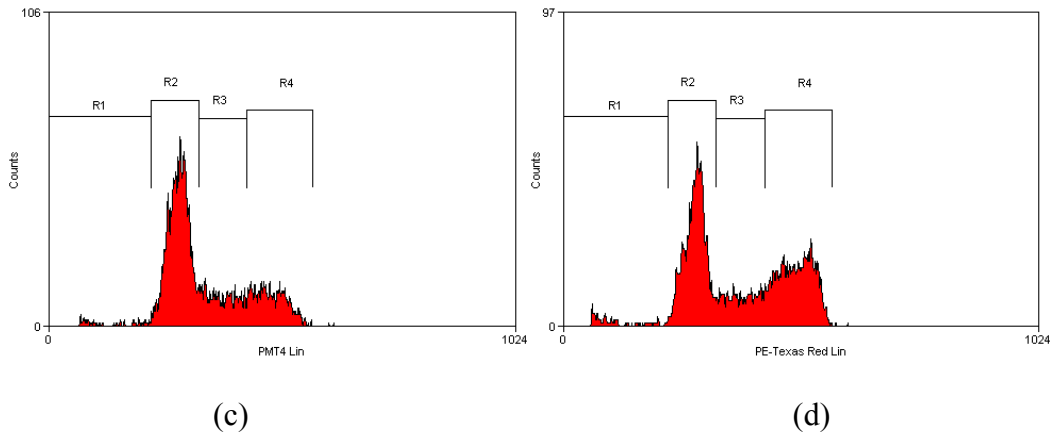
*: R1: sub-G1 phase, dead cell; R2: G1 phase; R3 S phase; R4: G2/M phase

Figure 4.14 Histograms showing the cell cycle distribution of Caco-2 cells after 4h exposure to the paclitaxel formulations. (a) Control; (b) WNP; (c) PNP; (d) P/CreEL.

(a)   (b)

(c)   (d)
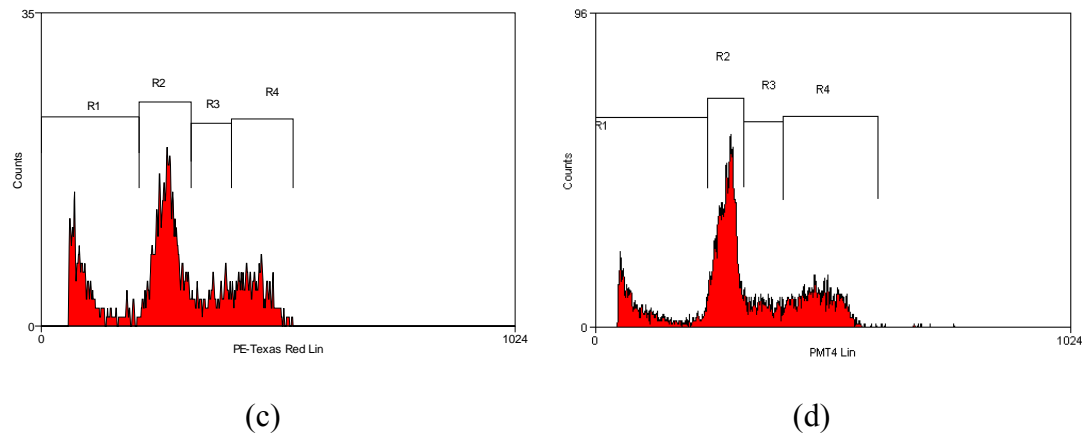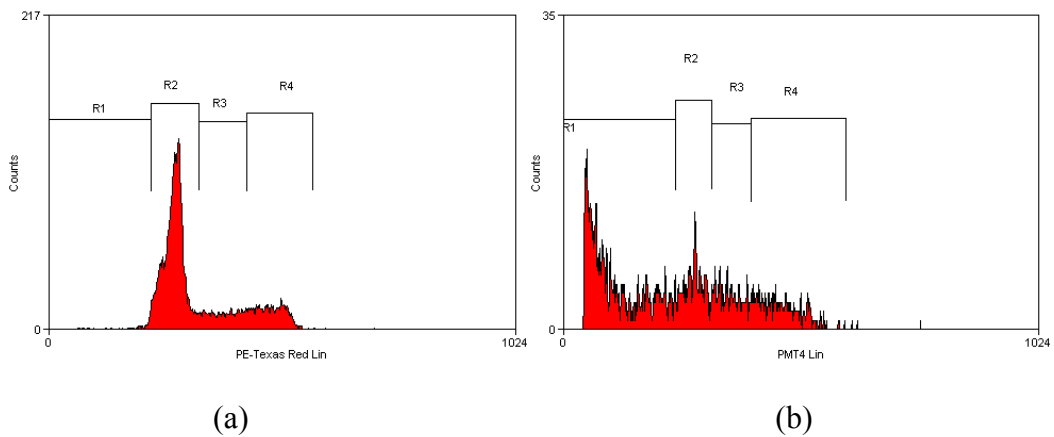
*: R1: sub-G1 phase, dead cell; R2: G1 phase; R3: S phase; R4: G2/M phase

Figure 4.15 Histograms showing the cell cycle distribution of Caco-2 cells after 24h exposure to the paclitaxel formulations. (a) Control; (b) WNP; (c) PNP; (d) P/CreEL

(a)
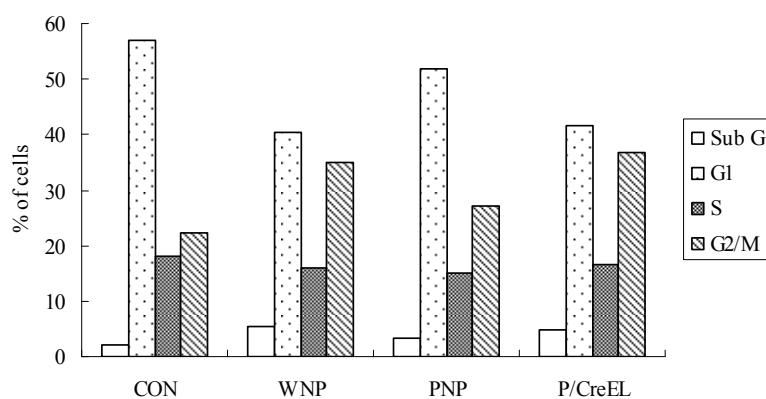
(b)
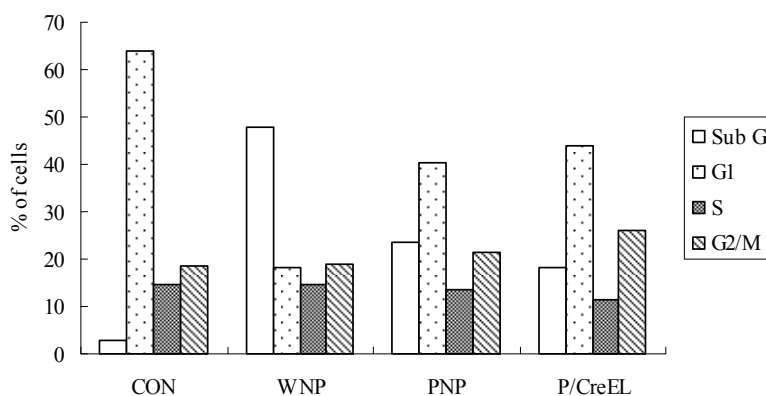
Figure 4.16 Quantitative analysis of the cell cycle distribution of Caco-2 cells co-cultured with paclitaxel formulations for (a) 4h and (b) 24h. CON (Control cells)

Classification of the Caco-2 cells into the various phases of the cell cycle after their incubation with the different paclitaxel formulations is shown in Figures 4.14 and 4.15. Co-incubation with all 3 paclitaxel formulations for 4h did not change the cell cycle distribution patterns of the Caco-2 cells greatly. The WNP and P/CreEL formulations caused a slight accumulation of cells in the G2/M phase after 4h of exposure, as reflected by the increase in percentage of cells from 28.45% (control) to 34.88% (WNP) and 36.72% (P/CreEL) in this phase, respectively. Prolonging the incubation to 24h with the WNP resulted in substantial cell death (47.93%), suggesting that the capacity of WNP to kill the Caco-2 cells was time-dependent. The death rates for cells exposed to the PNP and P/CreEL formulations for 24h were 23.5% and 18.22%, respectively, and these cells also showed a slight increase in the G2/M population. The collective data suggest that the three formulations were effective in inducing the arrest of cell growth, with WNP being the most effective formulation.

4.4.10 Cellular trafficking of WGA-conjugated PLGA nanoparticles

Green channel	Red Channel	Merge of Green and Red

0.5h

1.0h

2.0h

3.0h
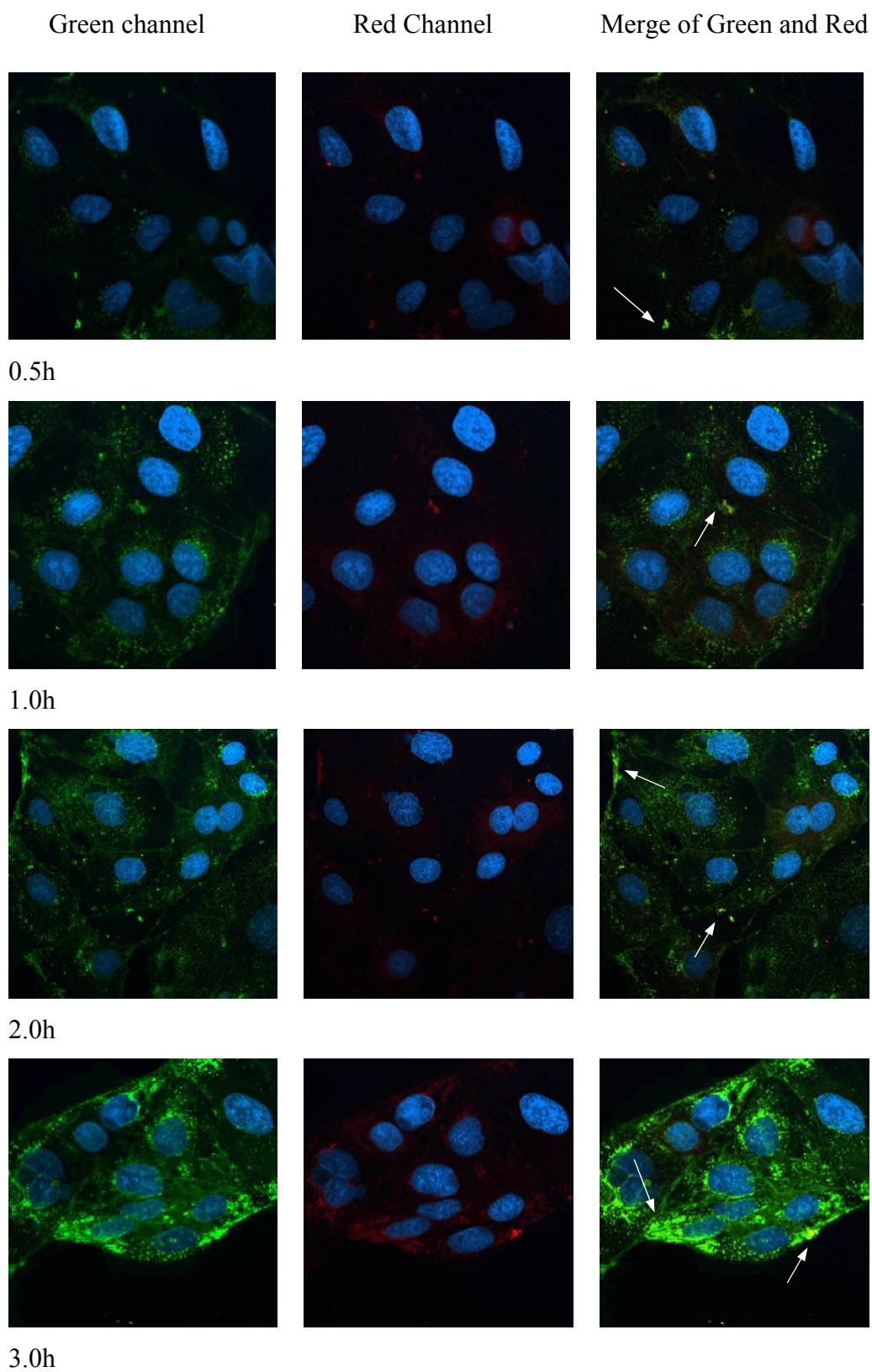
Figure 4.17 Typical images of Caco-2 cells showing the intracellular trafficking of WNP following incubation of the cells with the formulation for various time periods. WNP nanoparticle has green fluorescence, cell nuclear is blue, and the overlap of nanoparticle and lysotracker® fluorescence (red) is shown as yellow.

Confocal analysis of Caco-2 cells incubated with fWNP demonstrated the uptake of the nanoparticles into the intracellular space (Figure 4.17). We stained the acidic compartments (endo-lysosomes) and nucleus of the cell with Lysosensor DND-99 (red) and Hoechst 33258 (blue), respectively, so that the co-localization of endo-lysosomes (red) and WNP (green) may be represented by yellow clusters. However, the yellow clusters were visible only if the red and green intensities are close to each other, thus limiting interpretation from visual inspection alone. To provide a quantitative estimate of the degree of co-localization of WNP and endo-lysosomes, the confocal images were processed with the program ImageJ (National Institutes of Health Bethesda, Maryland, USA). Data represent mean values calculated from the Z-series images of cells sequentially obtained by confocal laser scanning microscopy. This method was preferred to the use of a single confocal image, which represented only a thin slice of the whole cells, and might not be representative of the true distribution of endo-lysosomal compartment and nanoparticles in the whole cell.

Time (h)	Colocalisation (yellow) (%)	Green in red (%)	Red in green (%)
0.5	11.29	32.75	33.56
1	12.75	32.02	29.15
2	13.96	43.80	34.52
3	25.42	53.99	44.90

Table 4.3 Colocalisation of FITC-WNP (green) and endosome/lysosome (red) in Caco-2 cells. Colocalisation percentage is the percentage of voxels which have both red and green intensities above threshold, expressed as a percentage of the total mumber of pixels in the image.

The data show that fWNP was internalized rapidly and could be detected inside the cells after 30 min incubation, both in the endo-lysosomes (yellow) and the cytoplasm (green). The intensity of green fluorescence in the cytoplasm increased with incubation time, which correlates with the increasing amount of internalized WNP with time (section 4.4.3). The containment of the internalized WNP in the late endo-lysosomal compartments also increased with incubation time, with 33% of the internalized fWNP estimated to be colocalized with the acidic compartments at 1h, and almost 54% in 3h. Nevertheless, the green fluorescence in the cytoplasm suggests that endocytosed fWNP was successfully released from the endo-lysosome into the cytoplasm. This release and the subsequent dissociation of paclitaxel from the WNP nanoparticles would be imperative for the drug to exert its pharmacological action through binding with the cellular tubulin.
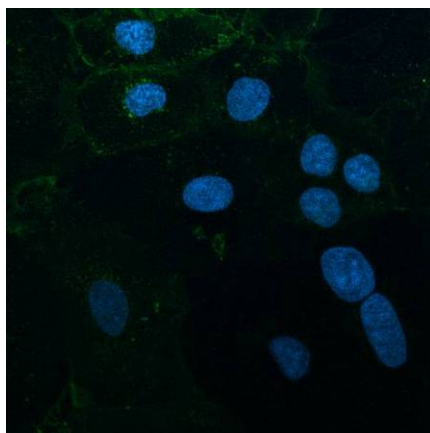
Figure 4.18 Typical confocal image of Caco-2 cells pre-treated with unlabelled WGA and then incubated with fWNP for 3h.

When the Caco-2 cells were pre-treated with unlabelled WGA prior to exposure to fWNP, the uptake of fWNP was greatly reduced. Figure 4.18 show a typical confocal image of the cells taken after 3h incubation with fWNP. The significant absence of green fluorescence in these cells indicated a poor uptake of fWNP. The inhibition of fWNP uptake by pre-incubation with unlabelled WGA suggests the fWNP uptake involved the specific interaction of WGA with its binding receptor in the Caco-2 cells.

4.5 Discussion

In many cases, chemotherapeutic treatment of tumors is limited by the inefficient intracellular delivery of the anticancer agents in current use. The drugs are not specific in their action, with the result that they accumulate not only in the tumor cells but also in healthy tissues. This provides the impetus for new approaches that can deliver anticancer drugs more specifically to the target organs in order to reduce their toxicity (Massing & Fuxius, 2000). Systems capable of intracellular delivery of drugs have been extensively studied for genes and anticancer agents (Devalapally et al., 2008; Lavigne et al., 2008). For some drugs, whose targets are in the cytoplasmic or other intracellular compartments, such as the nucleus or mitochondria, it is necessary for the drug or delivery system to be delivered to these specific locations in order for the drug to exert its pharmacological effect. Such is the case for paclitaxel, whose anticancer activity is realized by its effective binding to the intracellular microtubules (Andreopoulou & Muggia, 2008). In addition to a targeted drug disposition, the duration of drug retention at the target site could be another critical factor to achieve the desired therapeutic outcome in cancer treatment. Cancer is a disease condition that requires prolonged drug exposure to ensure complete regression of the tumor and avoidance of a relapse (Jang et al., 2003). Some studies have shown that anticancer drugs bound to polymeric nanoparticles have prolonged retention in tumors, and are consequently more effective in reducing tumor growth and increasing

animal survival rates than the corresponding free drugs (Akhtar & Lewis, 1997; Park et al., 2006). In particular, nanoparticles formulated with the PLGA polymer offer a nontoxic and efficient carrier system for the sustained intracellular delivery of various therapeutic agents (Panyam & Labhasetwar, 2004; Prabha & Labhasetwar, 2004; Sahoo & Labhasetwar, 2005).

This study evaluated the anticancer activity of different paclitaxel formulations (WNP, PNP and P/CreEL) on the colon cancer cells, Caco-2 and HT-29, and on the colon fibroblast cells, CCD-18Co. The CCD-18Co cell line served as a control in our study, and its use permitted an evaluation of the specificity of the paclitaxel formulations towards cancer cells.

Our hypothesis was that the WGA-conjugated PLGA nanoparticle platform was a promising strategy to improve the bioavailability and intracellular retention time of paclitaxel. *In vitro* anti-proliferation studies of the three colon cell types suggested that the incorporation of WGA enhanced the cytotoxicity of the paclitaxel-loaded PLGA nanoparticles on the cancer cells. Between the 2 colon cancer cell types, the HT-29 cells were more sensitive than the Caco-2 cells to the effects of WNP, which correlated to its greater sensitivity to the anti-cytoproliferation effects of free paclitaxel. WNP was also significantly more cytotoxic towards the Caco-2 cells than

the CCD-18Co cells at 72h, which was in keeping with the uptake data. This indicated that the boosted cytotoxicity observed for WNP was a result of enhanced intracellular paclitaxel concentration. The WNP and PNP formulations showed comparable IC_{50} values with the P/CreEL formulation against Caco-2 cells after 24h co-incubation. The IC50 of paclitaxel when delivered as WNP against the Caco-2 and HT-29 cells were, respectively, 1.6- and 4.9-folds lower than those of P/CreEL after 72h incubation. In the case of the PNP formulation, it was more cytotoxic against the colon cancer cells than against the CCD-18Co cells at 24h incubation, but the differential cytotoxicities were no longer apparent when the incubation time was prolonged to 72h. The conventional formulation, P/CreEL did not exhibit clear differential cytotoxicity profiles towards the cancerous and normal colon cells at 24h and 72h. On this basis, the WNP could be considered a superior paclitaxel formulation compared to PNP and P/CreEL.

The WNP showed time-dependent paclitaxel IC50 values for all three colon cell types, indicating a prolonged incubation time was required to raise the intracellular drug concentration to therapeutic level. This time lag could be required for the drug to be released from the nanoparticles in the cell cytoplasm. Nevertheless, the paclitaxel IC50 values attained with the WNP formulation were consistently lower than those obtained with the P/CreEL and PNP formulations tested under similar conditions. The

greater efficacy of WNP correlated well with the higher cellular uptake and sustained intracellular retention of paclitaxel associated with the formulation. The cellular uptake and retention efficiency for WNP might be attributed to the over-expression of N-acetyl-D-glucosamine-containing glycoprotein on the colon cell surface (section 2.4.2). In particular, binding of the conjugated WGA to glycoproteins expressed on the cytoplasmic side of the cell membrane could be potentially useful for facilitating the intracellular retention of WNP. In addition, WGA conjugation has been observed to decrease the negative surface charge of PLGA nanoparticles, and this in itself could enhance interaction of the nanoparticles with the cell membrane. In contrast, the higher negative surface charge of the PNP formulation could pose a challenge to nanoparticle entry into the cells.

Paclitaxel has an intracellular pharmacological target. Any nanoparticle formulation of paclitaxel must therefore ensure drug access intracellularly. For most such formulations, the nanoparticles would have to first gain access into the cells before the drug could be released to exert its effect. Paclitaxel uptake from the WNP formulation at 2h incubation was the highest in the Caco-2 cells compared to the other two cell lines. On the other hand, the CCD-18Co cells showed comparable uptake of paclitaxel from the WNP and PNP formulations, which could be indicative of the fibroblast cells having a higher non-specific rate of endocytosis than cancerous cells Caco-2 and

HT-29. The two colon cancer cell lines, Caco-2 and HT-29 cells, showed preferential uptake of WNP compared to PNP, suggesting that WGA conjugation to the PLGA nanoparticles was advantageous in facilitating the nanoparticle uptake by the cultured colon cancer cells. To differentiate between the WNP bound to the cell membrane and the WNP taken up into the cell, TB was used to quench the membrane bound fluorescence so that any fluorescence detected could be attributed to the internalized WNP. Our results confirmed that most of the cell-associated fluorescence was located intracellularly. The implication is that WNP was successfully taken up into the cells. The uptake mechanism was further confirmed to be mediated by WGA, as it was readily inhibited by the presence of unlabelled WGA.

We predict that WGA-conjugated nanoparticles would increase the residence time of drugs in the colon due to their interaction with mucins and intestinal epithelium for extended periods, promoting penetration of active drug through and between cells due to the concentration gradient between nanoparticles and intestinal membrane. In this study, we proposed that the uptake of WGA-conjugated nanoparticles via WGA-mediated endocytosis could have an intracellular disposition pathway different from that of unconjugated nanoparticles. This would result in different levels of intracellular retention of nanoparticles and hence therapeutic efficacy of the encapsulated paclitaxel. Although the phenomenon of greater cellular uptake of drug

and drug delivery systems following WGA conjugation has been known (Gabor et al., 2004; Mo & Lim, 2005), the effect of such conjugation on drug retention inside the cells has not been investigated. Our results showed that WGA conjugation on the surface of PLGA nanoparticles could indeed increase the retention of paclitaxel inside the colon cancer cells. It should be pointed out that the advantages of WNP versus P/CreEL would be much more significant if the enhanced cellular uptake, as well as intracellular drug retention and sustainable drug release features were included.

The endocytic and intracellular trafficking pathways are complex and highly regulated processes. Following endocytic uptake, nanoparticles may be transferred into early sorting endosomes and recycling endosomes or transferred from early endosomes to late endosomes -lysosomes (Richardson et al., 2008). The late endosomes and lysosomes have a relatively low pH (5.0 ~ 6.0) and they contain digestive hydrolases such as nucleases, glycosidase, lipases and phosphotases (Alberts et al., 2002). Endosomal escape has been reported for PLGA nanoparticles in gene delivery (Ng et al., 2009). Our study showed about 30% of the endocytosed WNP to be present in the late endo-lysosomes.   Fluorescence attributed to WNP in the cytosolic compartment was observed to increase with incubation time, suggesting successful escape of the WNP from the endo-lysosome compartment into the cytosol. The escape mechanism might be provided by a reversal (from anionic to cationic) of the negative charge on

the PLGA nanoparticle surface when confronted with the acidic pH in the endo-lysosomes compartment (Panyam et al., 2002). The progression of events from cell entry to eventual drug release from the nanoparticles would account for why cell damage/death occurred only after prolonged incubation when WNP was internalized at a rapid rate into the cells. The induction of cell apoptosis, together with an arrest of the cell cycle at the subG1 and G2/M phases, was observed after 24h exposure to WNP, as demonstrated by changes in cell detachment, nuclear morphology and cell cycle distribution. By comparison, P/CreEL and PNP at equivalent paclitaxel doses produced a lower level of l apoptosis under the same test conditions.

4.6 Conclusion

WNP had superior *in vitro* anti-proliferation activity against the colon cancer cell lines, Caco-2 and HT-29, compared with the PNP and P/CreEL formulations and it was less toxic against the normal CCD-18Co cells than against the cancer cells. The enhanced cytotoxicity of WNP in the colon cancer cells could be attributed to a more efficient cellular internalization of paclitaxel via WGA-mediated endocytosis, and a more efficient retention of the drug within the cells. The anti-cytoproliferation activity of WNP was dependent on incubation time and loading concentration, with a time delay noted between WNP internalization by the cells and significant cell death by

apoptosis. Co-localization studies indicated that WNP could escape from the endo-lysosomal compartment into the cytosol.

Chapter 5

Effect of mucin on the uptake of nanoparticles

5.1 Introduction

The gastrointestinal epithelium, cancer tissue and other mucosa are usually covered by mucus. Mucus is present as either a gel layer adherent to the mucosal surface or as a soluble or suspended form in the lumen (Smart 2005). It is a mixture of large glycoproteins, lipids, enzymes, water, electrolytes, sloughed epithelial cells, bacteria and bacterial products (Allen et al. 1990; Rathbone and Hadgraft 1991). The two major components are water, which accounts for more than 95% by weight (Smart 2005), and mucins, which gives the highly hydrated mucus a characteristic gel-like consistency with cohesive and adhesive properties. Mucins are glycoproteins and the chief determinants of the functional and physical properties of mucus (Wirth et al. 2002). They have been identified in two major forms, soluble secretory mucin, which is oligomeric and thought to be responsible for the rheological properties of mucus, and membrane bound mucin, which is monomeric (Filipe 1979; Strous and Dekker 1992; Thornton and Sheehan 2004). There are at least eight different human genes for mucins, each mucin gene is highly polymorphic, several different mucin genes are expressed at each type of mucosal surface, and some epithelial cells expressed more than one mucin gene (Gendler and Spicer 1995).

The colonic mucosa, like other exposed epithelial surfaces, is covered by a mucus layer which protects the underlying epithelium against mechanical, biological and

chemical irritants (Aksoy and Akinci 2004). The mucous layer has varied thickness that decreases in the order of rectum, sigmoid colon, transverse colon, ascending colon, and caecum (Matsuo et al. 1997). Depending on the method employed for measurement, the colonic mucous layer has been reported to have thickness of between 50 and 450 μm (Sonju et al. 1974; Kerss et al. 1982; Allen et al. 1990), and an estimated turnover time equivalent to the gut transit time of 24 – 48 h (Duchene et al. 1988). Human colonic mucosa synthesizes and secretes mucins to form the visco-elastic mucous barrier on the luminal side. The secreted mucins do not only constitute a physical barrier against the extracellular environment, but is also selective towards substances for binding and uptake by the epithelia (Matsuo et al. 1997).

Alterations in intestinal mucin constitution, especially in the glycosylation pattern and expression level, are thought to be associated with diseases such as inflammatory bowel disease and carcinoma (Ho et al. 1993; Tytgat et al. 1993). However, mucin apoprotein and glycosylation patterns during colorectal carcinogenesis is not well-defined (Aksoy et al. 2000). Almost all carcinomas of the colon produce mucin, although the most aggressive tumours, classified as mucinous cancers, make up 10 to 20% of all colon cancers (Park et al. 2008). Mucinous cancers are characterized by abundant production of the goblet cell mucin, MUC2 (Naves et al. 1985; Nozoe et al.

2000), but this is also the prominent mucin in normal human colon (Tytgat et al. 1994).

An abundant gel-like mucous layer can impede drug delivery to colon cancer cells, but it also provides an opportunity for sustained or prolonged drug delivery via the development of mucoadhesive delivery systems (Longer et al. 1985; Lejoyeux et al. 1989). Mucoadhesive delivery platforms are designed to attach to mucus or a mucous membrane *in vivo* (Smart 2005) so as to prolong and intensify drug contact with the underlying mucosal tissue (Junginger 1990).

In this regard, the interaction between mucin and particulate drug delivery system is an important consideration in the understanding of transmucosal drug absorption from nanoparticles. The dynamics of particles in solutions and in gel networks are hard to predict theoretically and therefore need to be characterized experimentally. Fluorescence recovery after photobleaching (FRAP) is a noninvasive measurement technique capable of quantifying particle diffusion and immobilization in pharmaceutical matrices as well as in tissues and cells (Kaufman and Jain 1991), and it allows for the study of particle mobility and interactions in small, intact tissue samples (Meyvis et al. 1999). First proposed by Elson and Reidler (Elson and Reidler 1979) and later expanded by Koppel (Koppel 1981) and Thompson et al. (Thompson

et al. 1981), FRAP is based on laser photobleaching of a small region of a specimen labeled with a fluorescent molecule. Following the photobleaching laser pulse, the recovery of fluorescence due to diffusion and/or flow from the surrounding unbleached areas into the bleached area is monitored with the same but much attenuated laser beam and a photomultiplier tube. The rate of recovery is related to the diffusion coefficient or flow velocity of the fluorescent molecule (Tsay and Jacobson 1991). FRAP has been used to detect macromolecules and particles binding or diffusing in cell membranes (Jacobson et al. 1995), cytoplasm (Seksek et al. 1997; Partikian et al. 1998), mucus (Olmsted et al. 2001) and various in vitro preparations (Kaufman and Jain 1991; Olmsted et al. 2001).

The aim of the experiments in this section of the study was to investigate the effects of mucin on the uptake and cytotoxicity of WNP by/against colonic cells. Mucin secretion by the colon cancer cell model, LS174T, was first investigated by histochemical staining and lectin blot before the FRAP technique was applied to evaluate the diffusion of WNP in the secreting mucin layer of LS174T cells. The LS174T cell line is derived from human colon cancer cells with mucous granules that secrete significant amounts of mucin, similar to goblet cells (Kuan et al. 1987; Kuan et al. 1987). The cells have goblet cell-like characteristics, and have been shown to synthesize several mucins of which the secretory MUC2 was most prominently

expressed (VanKlinken et al. 1996). LS174T cells mimic the mucin expression in the colon and provide a good *in vitro* model for mucin-expressing colon cells. Taken together, LS174T cell line could be an appropriate in vitro model for assessing mucoadhesion.

There are many histochemical methods available for the identification of different types of mucins (Culling et al. 1975; Jansen 1995; Bancroft and Gamble 2008). Histochemical techniques for the localization and differentiation of acidic and neutral mucins are based on selective detection of vicinal diols by their reactivity with the periodic acid Schiff (PAS) procedure, and the affinity of the anionic groups towards the cationic dyes (Yashpal et al. 2007). Alcian blue (AB), a group of water-soluble polyvalent basic dyes, is the most commonly used cationic dye for the demonstration of acid mucins. The blue color is due to the presence of copper in the molecule. At pH 2.5, AB stains both sulfated and carboxylated acid mucopolysaccharides and sulfated and carboxylated glycoproteins. It is believed to form salt linkages with the acid groups in these mucopolysaccharides (Bogomoletz 1986). The PAS stain is applied to detect neutral and acidic polysaccharides. It oxidizes the carbon to carbon bond to form aldehydes, which react with fuchsin-sulfurous acid to yield a magenta product (Bogomoletz 1986). Optimum staining of acidic, neutral and mixtures of acidic and neutral mucins in tissue are obtained by combining the AB and PAS techniques

(Bancroft and Gamble 2008). The rationale is to first apply AB to stain all the acidic mucins, including those which are also PAS positive so that these are blocked from further reaction with PAS. Subsequent application of PAS will therefore detect only the neutral mucins, allowing these to be stained in a contrasting manner (magenta/pink) to the acidic mucins (blue). For cells that contain an admixture of mucin types, the resultant stain will be an intermediate color between magenta and blue, depending on the dominant moiety present.

5.2 Materials

Materials listed in Section 3.2 were used in this study. In addition, the LS174T cell line (passage 109) was obtained from the American Type Culture Collection. Eagle MEM, and the Alcian blue (AB) and periodic acid Schiff (PAS) staining systems were products of the Sigma Chemical Co.

5.3 Methods

5.3.1 Cell culture

LS174T cells were cultured in Eagle's MEM supplemented with 100 U/ml of penicillin, 100 μg/ml of streptomycin and 10% (v/v) of FBS. Cell cultures were incubated at 37°C in a humidified atmosphere of 5% CO_2 and 95% air, with medium exchange on alternate days. Cells were subcultured every 3 days after trypsinization.

5.3.2 Alcian blue (AB) and periodic acid Schiff (PAS) staining

LS174T cells were cultured in a Lab-Tek chamber at a seeding density of 1.0×10^4 cells/cm^2. After 3 or 6 days culture, the cells were fixed with an ethanol-acetic acid (3:1) solution, air-dried, and stained with AB (3% solution in acetic acid, pH 2.5) for 10 min. Following rinsing with PBS three times, the cells were stained with PAS according to the manufacturer's instructions (treatment with a 0.5% periodic acid solution for 5 min at room temperature, followed by Schiff reagent for 15 min). The cells were then counter-stained with hematoxylin for 90 s, and washed with PBS before examination under a microscope (Nikon, Nikon Instruments Inc., Kanagawa, Japan).

5.3.3 Lectin blot

LS174T cells were cultured on 25 cm^2 flasks at a seeding density of 1.0×10^4 cells/cm^2 for 3 or 6 days. Confluent cells were washed thrice with ice-cold PBS, then scraped off into PBS with a cell scraper. Cell membrane protein and intracellular protein were extracted using the Mem-PER eukaryotic membrane protein extraction reagent kit (Pierce Biotechnology, Rockford, IL, USA) according to the manufacturer's instructions as described in section 2.3.3. A 7.5% polyacrylamide resolving gel and a 4% stacking gel were prepared as described in section 2.3.5. Samples equivalent to 5 μg of protein were size-fractionated by electrophoresis and

transferred to PVDF membranes as described in section 2.3.5. The glycoprotein was

detected using the west pico chemiluminescence system. Bands were visualized in a

CCD imaging machine.

5.3.4 Cytotoxicity of WGA

To assess the cytotoxicity of WGA against the LS174T cells, the cells were seeded

onto 96-well plates at a density of 8,000-10,000 cells/well. Confluent cells were

washed with 3×200 μl of PBS before incubation with 200 μl of WGA solution (10 to

200μg/ml) for 4 to 72h. The MTT assay was performed according to the protocols

described in section 3.3.2.

5.3.5 Uptake of FITC-WGA

LS174T cells were seeded onto 96-well plates at a density of about 1.0×10^5 cells/ well.

Confluent cells on Day 3 were washed twice with 200 μl of HBSS/HEPES (HBSS

buffered with 10 mM of HEPES to pH 7.4) before uptake experiments were

performed according to the method described in section 3.3.4.

5.3.6 Anti-proliferation activity of paclitaxel-loaded nanoparticles

For anti-proliferation experiments, LS174T cells were plated at 10,000 cells per well

and subjected to treatment with various doses of the investigational formulations as

free drugs or encapsulated in PLGA nanoparticles diluted in supplemented medium. Treatment with serum-supplemented medium was used as a negative control (0% cell death). WNP, control formulations PNP and P/CreEL were prepared as described in section 4.3.1.

5.3.7 Cellular uptake and efflux of paclitaxel

LS174T cells were cultured in 12-mm petri dishes for 3 or 6 days at a seeding density of 1.0×10^4 cells/cm^2. Intracellular uptake experiments were initiated by the addition of 6 ml of HBSS/HEPES containing appropriate concentrations of WNP, PNP or P/CreEL to give 40 μg/ml of paclitaxel in each dish. After 2h incubation at 37 ˚C, the cells were immediately washed thrice with ice-cold PBS, harvested with a rubber scraper and centrifuged at 10,000 x g for 10 min. Cell pellets were lysed in 300 μl of methanol under sonication, and the supernatant was separated by centrifugation. The drug content in the supernatant was measured by high performance liquid chromatography (HPLC), and expressed as the amount of intracellular paclitaxel (μg) per mg of total cell protein.

To estimate the efflux rate of paclitaxel, subconfluent cells in 12-mm petri dishes on day 3 or 6 were incubated with 6 ml of WNP in HBSS/HEPES for 2 h. After washing with PBS, the cells were further incubated with fresh medium devoid of drug for

another 2 h at 37 ˚C. The cells were washed with PBS three times before they were harvested with a rubber scraper. The paclitaxel content of the harvested cells was quantified by HPLC analysis and expressed as the amount of paclitaxel (µg) per mg of total cell protein.

A HPLC method was developed and validated for the quantification of paclitaxel. Chromatographic separation was achieved on an Agilent 1100 system (Agilent Technologies, Palo Alto, CA) using a C_{18} column (200× 4.6 mm, 5 µm) (Waters, Milford, MA) preceded by a guard column (Waters), flow rate of 1 ml/min and UV detection at 229 nm. The mobile phase consisted of acetonitrile and water at a volume ratio of 1:1. A linear standard curve was obtained over the paclitaxel concentration range of 0.1 to 10 µg/ml in methanol ($R^2 > 0.99$). The relative standard deviations (RSD) for day-to-day and within-day precisions for this assay were less than 10%. The HPLC peaks were recorded and integrated using the Agilent data analysis software.

5.3.8 Diffusion measurements (FRAP)

In this study, we aimed to investigate the diffusion property of nanoparticle fWNP in PBS and mucin layer. To investigate the influence of interaction of WGA and its receptor in mucin on the nanoparticle's diffusion, we studied the diffusion of fWNP

and BSA-NP in mucin layer of LS174T cells. LS174T cells were cultured in Lab-Tek chambere at a seeding density of 1.0×10^4 cells/cm^2. After 6 days, the cells were rinsed twice with prewarmed HBSS/HEPES and preincubated for 30 min at 37°C with 0.2 ml of HBSS/HEPES before they were separately incubated for 1 h at 37 °C with 0.2 ml of the fWGA, fWNP, and fBSA-NP (FITC-BSA conjugated PLGA nanoparticles) samples (HBSS/HEPES as vehicle). In order to tell the diffusion difference between the small molecule fWGA and fWGA-conjugated nanoparticles, the diffusion of fWNP and fWGA was also investigated in PBS. The cells were analyzed as follows: an attenuated laser beam focused onto an area of the mucus layer on the cell surface was gradually increased in intensity to approximately 10^3 to 10^4 fold, causing a rapid bleaching of the fluorescent molecules in the area. Residual fluorescence in the same area was monitored by an attenuated laser beam, which showed the fluorescent signal returned to a new steady-state value as unbleached probes from the surrounding areas diffused into the partially bleached area. The rate of recovery of fluorescence was calculated as a measure of the rate of diffusion of the fluorescent particles in the sample, the fractional recovery of fluorescent signal corresponding to the fraction of mobile fluorescent particles.

5.3.9 Visualization of fWNP uptake by LS174T cells

LS174T cells were grown on Lab-Tek chamber at a density of 1.0×10^4 cells/cm^2, and incubated at 37°C in 95% air/5% CO_2 environment overnight. On the 3rd or 6th day post-seeding, the cell monolayers were rinsed twice with prewarmed HBSS/HEPES and preincubated for 30 min at 37°C with 0.2 ml of HBSS/HEPES before they were incubated for 1 h at 37 °C with the fWNP sample (1 mg/ml in HBSS/HEPES). TB was used to extinguish the outside fluorescence of the cells as described in section 3.3.5. Uptake was terminated by washing the cells thrice with ice-cold PBS. The cells were fixed by incubation for 10 min in 0.5 ml of acetone/methanol (1:1) at 0 °C, and observed under a confocal laser scanning microscope.

5.3.10 Statistical analysis

Data are presented as mean ± standard deviation. Differences between mean values were analyzed for significance by one-way ANOVA using the SPSS 10.0 software. P values ≤ 0.05 were considered significantly different.

5.4 Results

5.4.1 Alcian blue (AB) and periodic acid Schiff (PAS) staining

AB and PAS staining study of the LS174T cells showed a marked increase in neutral and acidic mucopolysaccarides on the cell surface following prolonged culture

(Figure 5.1). The profusion of magenta and blue spots in Figure 5.1a suggests extensive mucin coverage of the cells after 6 days of culture, although a significant amount of mucin glycoprotein was also produced after 3 days of culture (Figure 5.1 b). These images confirmed an intact mucin secretory function for the LS174T cell line used in the study.
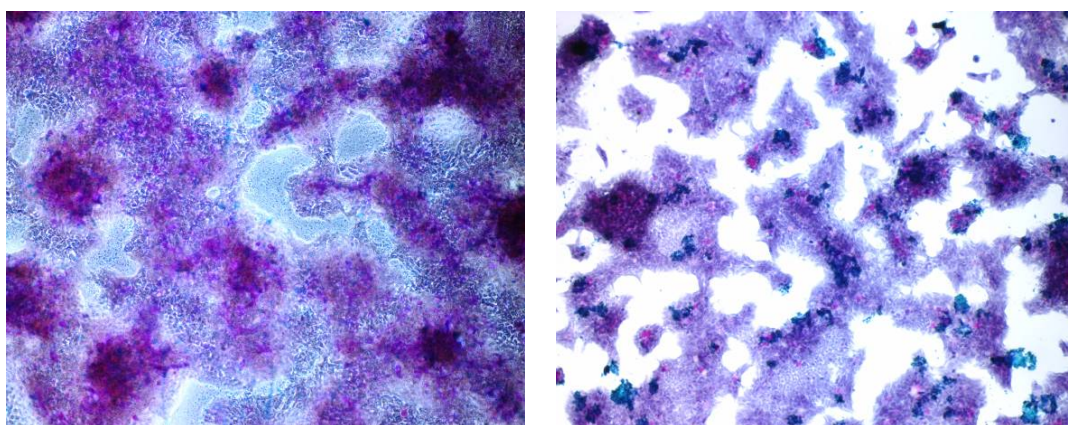
Figure 5.1 Alcian blue and PAS staining of mucin in LS174T cells following (a) 6 days culture and (b) 3 days culture. Cells were observed at magnification of 10×.

5.4.2 Lectin blot analysis

SDS-PAGE analyses detected WGA-reactive glycoproteins in the cell membrane and cytoplasm of the LS174T cells. Multiple proteins with molecular size ≥ 75 kDa were detected (Figure 5.2), the number of proteins increasing after 6 days of culture compared with 3 days of culture.

(a)   (b)
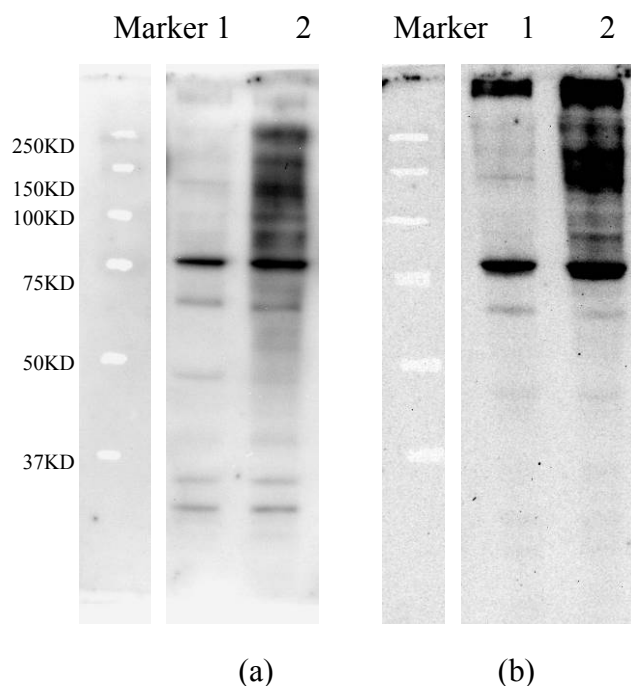
Figure 5.2 Lectin blot analysis for WGA-recognizable proteins among the (a) cell membrane proteins, and (b) intracellular proteins in the LS174T cells. Lane 1 - 3 days of culture; lane 2 - 6 days of culture.

5.4.3 *In vitro* cytotoxicity profile of WGA against LS174T

The viability of LS174T cells was not significantly affected by up to 72h incubation with WGA. Even when exposed to high WGA concentrations of 100 and 200 µg/ml, the viability of the LS174T cells did not fall below 80% at any of the incubation time points studied (Figure 5.3). There were no significant differences in cell viability either at different WGA concentrations or upon prolonged incubation, suggesting that the LS174T cells were relatively insensitive to WGA.
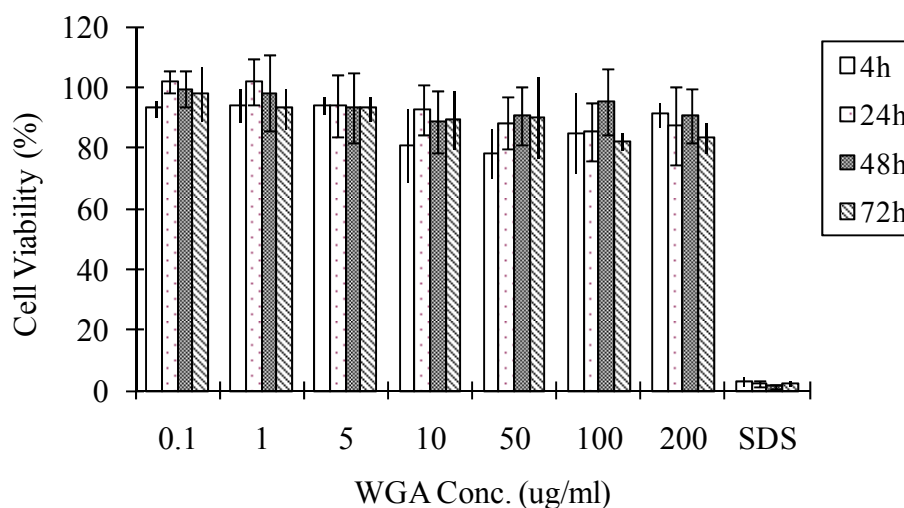
Figure 5.3 *In vitro* cytotoxicity profiles of WGA against the LS174T cells as a function of exposure time. WGA was applied at loading concentrations of 0.1, 1, 5, 10, 50, 100 and 200 μg/ml. Cell viability determined by the MTT assay was expressed as a percent of that obtained for cells exposed to culture medium. Data represent mean ± SD, n=6.

5.4.4 Uptake of FITC-WGA

Uptake of fWGA by the LS174T cells was studied at fWGA loading concentrations of 5, 10, 20 and 50 μg/ml, and the data were normalized against the cellular protein content. At all fWGA loading concentrations, cellular fWGA uptake by the LS174T cells increased with prolongation of incubation time from 0.5 to 5h. Cellular uptake was rapid. The amount of fWGA associated with LS174T cells at 30 min were

5.3±0.2, 7.7±0.4, 10.2±0.3 and 13.6±0.2 μg WGA/mg cell protein at the loading

concentration 5, 10, 20 and 50μg/ml, respectively. These correspond to 15%, 11%,

11.5% and 7.3% of the initial fWGA load.
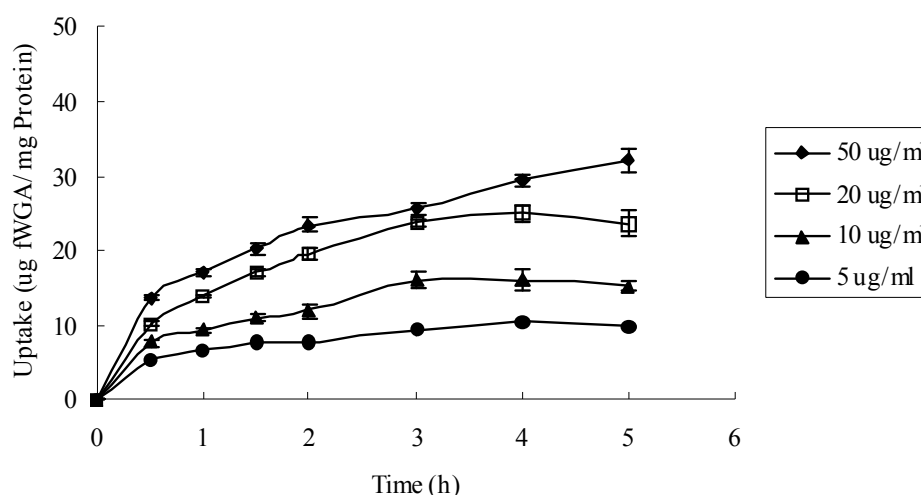
Figure 5.4 Uptake of fWGA by LS174T cells as a function of incubation time (Data

represent mean ± SD, n=4)

5.4.5 Antiproliferation activity of paclitaxel-loaded nanoparticles

Figure 5.5 showed cytotoxicity of WNP, PNP and P/CreEL against LS174T cells. The

cell viability decreased as we increased the concentration of nanoparticles and

incubation time. The result showed there was no significant difference of the

cytotoxicity at 24h. However, when the incubation time was prolonged to 72h, WNP

showed advantages in achieving lower cell viability compared to PNP and P/CreEL (p

< 0.05).
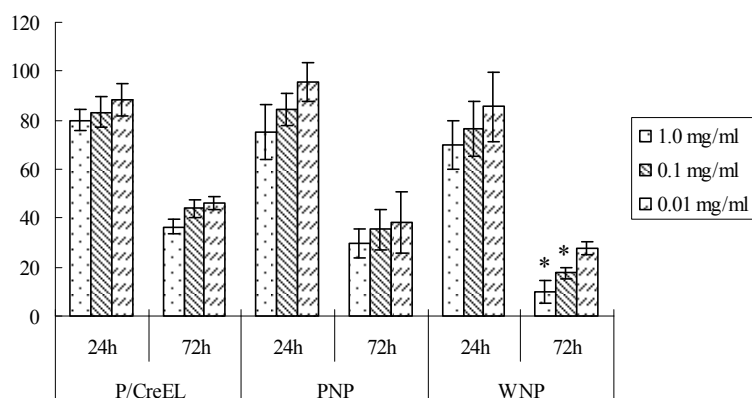
Figure 5.5 *In vitro* cytotoxicity of P/CreEL, PNP and WNP against LS174T cells (n = 6). '*' indicates statistical significance compared to PNP ($p < 0.05$).

5.4.6 Cellular uptake and efflux of paclitaxel

Figure 5.6 showed the data for cellular paclitaxel uptake from the WNP, PNP and P/CreEL samples by the LS174T cells at 3 and 6 days of culture. Cells at 3 days of culture had been shown to produce less mucin than those cultured over 6 days. The difference in mucin production did not, however, caused the cells to show significant differences in paclitaxel uptake from the WNP, PNP and P/CreEL samples, although an upward trend in cellular uptake was noted in the 6-day old cells. On the other hand, the LS174T cells, regardless of the days in culture, showed much higher cellular uptake of paclitaxel from the nanoparticle formulations, WNP and PNP, than from the P/CreEL formulation. These results were consistent with Caco-2 and HT-29 cells, which were not known to be mucin-producing colonic cells. Therefore, it may be

concluded that the presence of mucin on the LS174T cell surface did not impede

paclitaxel uptake from the nanoparticulate formulations.

(a)
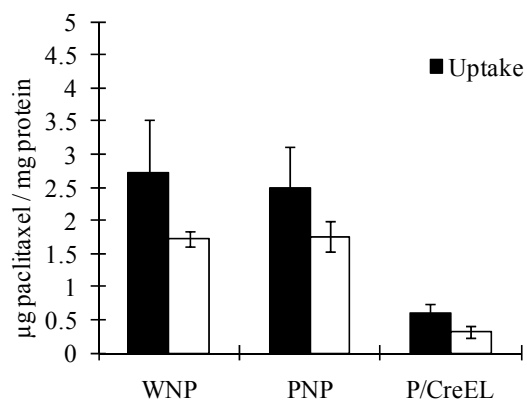
(b)
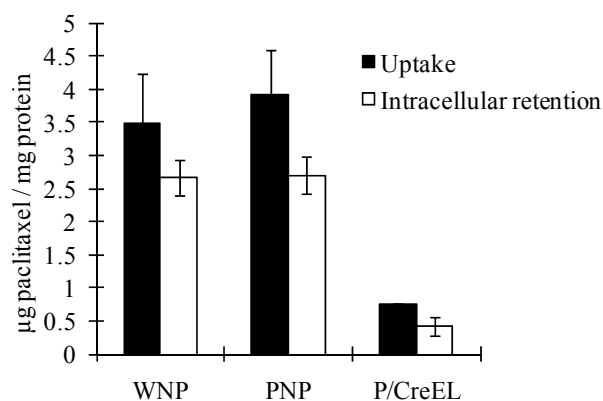
Figure 5.6 Cellular uptake and intracellular retention of paclitaxel from the WNP,

PNP and P/CreEL formulations by the LS174T cells following (a) 3 days of culture;

and (b) 6 days of culture. Data represent Mean ± SD, n = 3.

5.4.7 Diffusion measurements (FRAP)

FRAP plots showing fluorescence recovery as a function of time was fitted to a single exponential function (Figures 5.7 and 5.8) and the corresponding parameters compiled in Table 5.1. The "mobile fraction" refers to the fraction of fluorescent molecules that were free to move within the bleached region while "half-time for recovery" was the time taken to reach 50% of the steady state fluorescence. The FRAP plots suggest that significant portions of the fWGA molecules and fWNP nanoparticles in the PBS vehicle were mobile, the observed recovery rates reaching 93 and 76%, respectively. Although fWGA had significantly higher steady state fluorescence (plateau value of the recovery curve) implicating a greater mobile fraction, the two species had comparable recovery half-times. By comparison, fWNP had an almost 8-fold slower recovery half-time in the mucus layer of the LS174T cell sample (Table 5.1). The mucus layer did not only slow down the diffusion of fWNP, but also impeded the overall mobility of the nanoparticles, reducing the mobile fraction to only 49%. These results were comparable to those obtained for fBSA-NP. In addition, a higher variability in mobility of the fWNP nanoparticles was noted in the cell sample than in the PBS vehicle, again testifying to the thicker mucus posing a greater barrier to particle mobility.
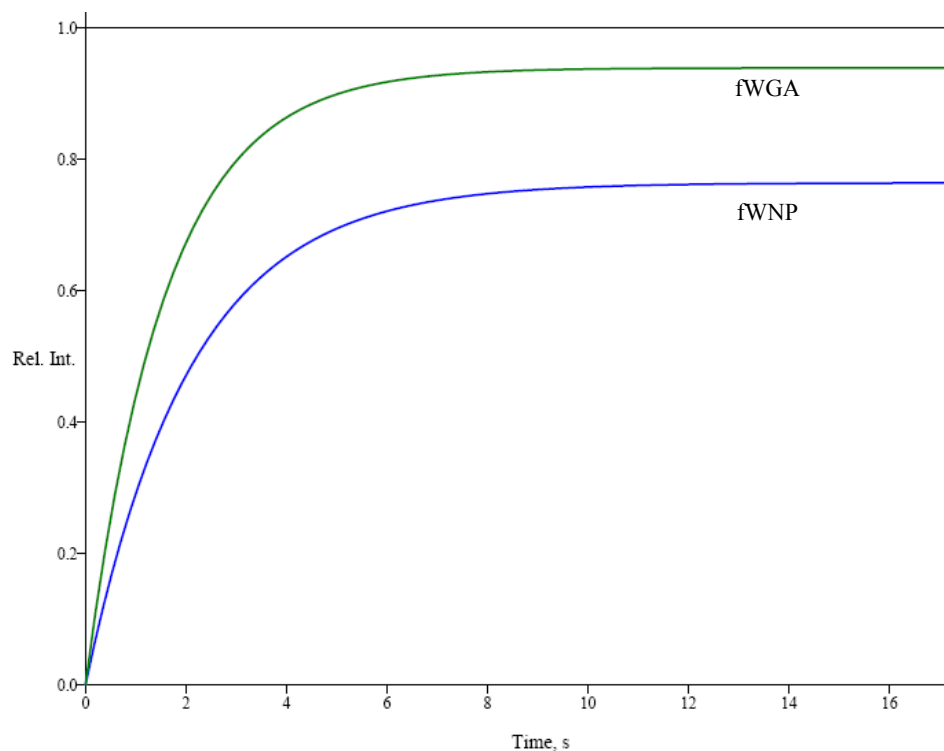
Figure 5.7 Fluorescence recovery curves of fWNP and fWGA in PBS solution
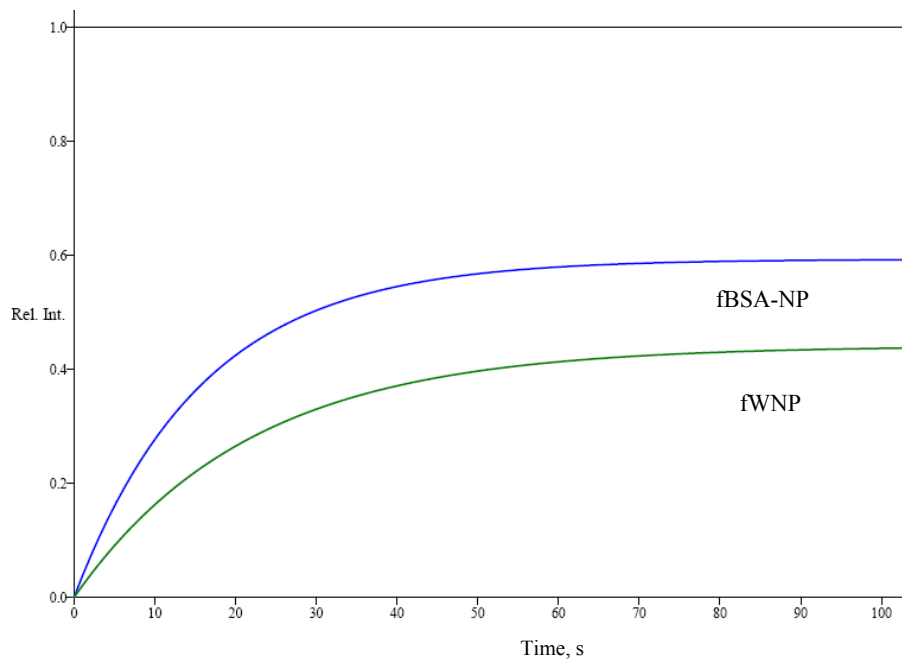
Figure 5.8 Fluorescence recovery curves of fWNP and fBSA-NP in the surface mucin

layer of LS174T cells

Table 5.1 Mobile fraction and half-time to steady state fluorescence obtained from the

FRAP plots for fWGA, fWNP and fBSA-NP particles in PBS and the mucin layer of

LS174T samples (Mean ± SD, n=4)

Sample		Mobile fraction	Half-time (s)
fWGA	PBS	0.93±0.06	1.3±0.34
fWNP	PBS	0.76±0.05	1.5±0.14
	Mucin layer	0.49±0.07	11.5±5.7
fBSA-NP	Mucin layer	0.59±0.16	7.5±4.9

5.4.8 Visualization of fWNP uptake by LS174T cells

Confocal laser scanning microscopic examination before and after trypan blue

staining indicated that fWNP were not only bound to, but also internalized by the

LS174T cells (Figure 5.9). Figure 5.9 (b) shows that the fluorescence in the cell

sample attributed to fWNP was lower following incubation of the cells with trypan

blue, which would bleach any extracellular fluorescence. The incomplete quenching

of the fluorescent signals suggests that a significant amount of the cell-associated

fWNP was internalized by the cells. Figure 5.9 (c) shows the mucin layer on the

surface of LS174T cells after 1h incubation with fWNP. The plenty of green

fluorescence indicated the interaction of fWNP and mucin glycoprotein.

(a)

(b)

(c)
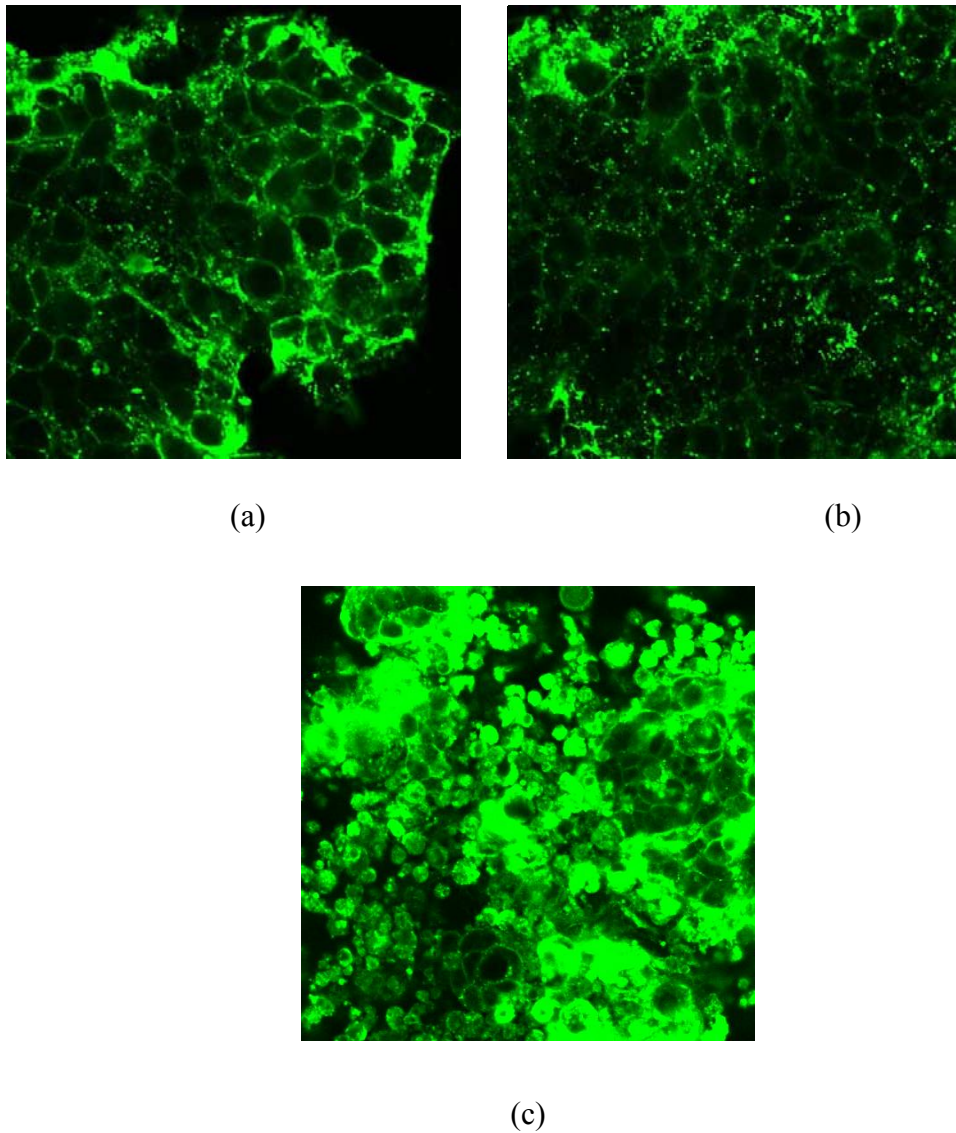
Figure 5.9 Confocal images of LS174T cells incubated with 1.0 mg/ml of fluorescent fWNP for 1h; (a) before trypan blue treatment, (b) after incubation for 3 min with 0.2 mg/ml of trypan blue, and (c) focus on mucin layer

5.5 Discussion

WGA has been shown to react with cell membrane glycoproteins in a wide variety of neoplastic tissues (Bresalier et al. 1990; Mody et al. 1995). Cytotoxicity of LS174T

was not affected remarkably by treatment of WGA even at higher concentration, while the cytotoxicity of Caco-2 and HT-29 were affected by the concentration of WGA and/or the incubation time. In general, the cell viability of Caco-2 and HT-29 was reduced when the WGA concentration was increased and/or when the incubation time was prolonged. Lectin blot analysis showed LS174T cells under 3 days culture expressed less WGA-recognized glycoproteins on cell membrane compared to the other colon cancer cell line Caco-2 and HT-29. It was found that WGA must be internalized to exhibit a cytotoxic effect in the study of pancreatic cancer cells (Schwarz et al. 1999). Since there was not much WGA binding sites on the cell surface, it is easy to understand that viability of LS174T cells is not affected remarkably. The uptake of fWGA by LS174T cells was time and concentration dependent. Compared with Caco-2 and HT-29 cells, LS174T cells showed the weakest uptake of fWGA at all time points. On the other hand, like the Caco-2 and HT-29 cells, cellular uptake of WGA by LS174T cells was rapid followed by internalization.

Studies on the mucin production of the LS174T cells has shown the expression of a variety of mucin glycoproteins (Kuan et al. 1987; VanKlinken et al. 1996), including the MUC1 and MUC2, which are implicated in host-pathogen relationships. Alcian blue/PAS staining showed both acidic and neutral mucins were produced by the

LS174T cells after 6 days culturing. Other researchers' study also showed LS174T contained mucinous secretory granules (Kuan et al. 1987). The glycoprotein production of LS174T was also examined by lectin blot in this study. Our results confirmed there was higher level of WGA-binding glycoproteins both in the cell membrane protein fraction and the cytoplasmic protein fraction of 6-day culture compared with that of 3-day culture. Due to the water insoluble property of most of mucin glycoprotein (Bhavanandan 1991; Carlstedt et al. 1993; Axelsson et al. 1998), we could predict most of the mucin glycoprotein was located in cell membrane protein fraction. Thus the increase expression of WGA-binding glycoproteins might attribute to the production of mucin glycoprotein.

Generally, the presence of overlying mucus is a significant barrier to the permeation of lipophilic drugs, and the uptake of hydrophobic nanoparticles by absorptive epithelial cells. However, bioadhesive drug delivery systems may overcome this barrier by prolonging the residence time and intensifying drug contact with the underlying epithelial at the site of drug absorption. Paclitaxel uptake from the WNP formulations by the LS174T cells showed no significant differences between the 3-day culture LS174T (less mucin production) and 6-day culture LS174T (more mucin production). This result indicated that the presence of mucin may not be a barrier for the uptake of WGA conjugated nanoparticles by LS174T cells. The uptake

result also showed there was no significant difference in paclitaxel uptake from the WNP and PNP. The binding of fWNP to cell surface ligands and followed internalization into the cells was confirmed by Confocal study. The trypan blue treated cell layers showed plenty of fluorescence. This means the fluorescence we imaged under confocal microscope is the nanoparticles located intracellularly after 1h uptake. The interaction of fWNP and mucin glycoprotein on the LS174T cell surface was also confirmed by confocal images.

Cytotoxicity study of three paclitaxel formulations showed the three formulations had comparable *in vitro* cytotoxicity against LS174T cells at 24h. However, when the incubation time was prolonged from 24h to 72h, WNP began to exhibit significant difference of cytotoxicity at the loading concentration of 1 and 0.1 mg/ml. This was not consistent with the comparable paclitaxel uptake from WNP and PNP in the uptake study. The discrepancy might due to the different study time of uptake and cytotoxicity study. The uptake study was terminated at 2h, while the cytotoxicity data were obtained at 24 and 72h. Uptake study was not conducted longer due to the consideration of cytotoxicity of formulations at longer incubation. Though the uptake of WNP by LS174T cells occurred quickly after the co-incubation, the significant cell death occurred only at 72h. The reason of the delayed onset probably because the retained WNP onto the cell surface and inside the cells need time to transport inside

the cells or release the drug at the action site. The interaction of WGA and Mucin glycoprotein might be a reason for helping the retention of WNP.

FRAP is a powerful method for measuring the dynamics of biomolecules. It provides qualitative and quantitative data that can be useful for a number of biological studies, such as particle diffuse in different medium. Our FRAP result showed fWGA could diffuse rapidly in PBS. Similar with fWGA, fWNP could also diffuse rapidly in PBS, though the mobile fraction is much lower. This matched what would be expected for small molecules and large particles in PBS. To investigate whether the nanoparticles can diffuse in mucus and whether nanoparticles are retarded by the mesh spacing and/or by high-affinity bonds with mucins, we studied the diffusion of fluorescence labeled nanoparticles (fWNP) in mucin layer on the LS174T cell surface. Slow diffusion of both fWNP and fBSA-NP was detectable with FRAP. fWNP was slowed significantly in mucin layer. This is because mucin layer is viscous and fWNP could stick to mucin fibers or be hindered by the size of the mesh spacing between the mucin fibers.

Our experiments suggested that fWNP and fBSA-NP were capable of diffusing through the mucus layer of LS174T cells slowly, though they are retarded by mucin. These observations are consistant with the observations that small polystyrene

microspheres (415nm) placed in the distal colon of rats were later observed adjacent

to the mucosa after passing through the mucus layer of the colon (Szentkuti 1997).

fBSA-NP was partially mobile in our study which indicated that part of nanoparticles

was trapped by the mesh spacing of mucus layer. fWNP showed a little more

immobile fraction. This indicated that the motion of fWNP was retarded by both the

mesh spacing between fibers of mucin and high-affinity bonds with mucins. The

fWGA on the surface of fWNP sticked to the certain mucin glycoprotein and

therefore the fWNP was trapped by the mucus gel. Except for the retardness of fWNP,

the mobile fraction showed fWNP has a certain ability to move through the mucus.

The partial mobility of fWNP is very important for their uptake by the underlying

cells. If fWNP was completely stuck by mucin fibers, the mucin layer will totally be a

diffusional barrier for the surfaces they cover. If fWNP could diffuse freely in mucin

layer, the mucin layer could not help to retain the particles close to the absorption site.

The partial mobility of fWNP would not only help the particles stay close to the cells,

thus increasing the concentration gradient of the drug, but also enabled the particles to

be transported into the cells. Thus, mucin layer could be serving as a bridge between

the WGA conjugated nanoparticles and the colon cancer cells under the mucin layer

by using the interaction of mucin glycoprotein and WGA. Our cytotoxicity study

showed that the WNP exhibited superior cytotoxicity effect at 72 h compared to the

PNP and P/CreEL formulations. This might be attributed to the retention of WNP by mucin glycoproteins.

5.6 Conclusion

In summary, this study has confirmed that LS174T is a mucin producing cell model. It may have useful application in screening mucoadhesives under physiological conditions. WNP had a certain mobile fraction in mucin layer. This indicated WNP could diffuse through the mucin layer slowly. The binding of WGA and the mucin glycoproteins could serve for mucoadhesive drug delivery to prolong the residence time at the colon site and improve the bioavailability of anticancer drug delivery systems.

Chapter 6

Conclusions

6. Conclusion

WGA was reported to bind to oligosaccharides containing terminal N-acetyl-D-glucosamine and *N*-acetyl-D-neuraminic acid residues on human colonocytes. This project was initiated to prove the hypothesis that the conjugation of WGA to PLGA nanoparticles loaded with paclitaxel (WNP) could improve the delivery of paclitaxel to colonic cancer cells. WGA, as a targeting moiety, was first evaluated for its cytotoxiciy and cellular uptake in colon cancer cell models, represented by the Caco-2 and HT-29 cells. The colon fibroblasts, CCD-18Co cells, served as control normal cells. The ideal targeting moiety should not exert notable toxic effects on normal cells/tissues. It should also be used at concentrations that caused minimal cytotoxicity to the cancer cells so as not to complicate the screening of the drug delivery system. To determine the sub-cytotoxic concentrations of WGA for subsequent experimentation, the MTT assay was applied to evaluate the cytotoxicity of WGA at concentrations ranging from 0.1 to 200 μg/ml against the Caco-2, HT-29 and CCD-18Co cells. WGA showed a concentration- and time-dependent cytotoxicity against the 3 cell lines studied. It was cytotoxic to all three colon cell lines at concentrations ≥ 50 μg/ml, particularly upon prolonged exposure of 72h.

Cancer-cell selectivity of WGA was also evaluated by comparing its uptake, in the

form of fWGA, by the Caco-2, HT-29 and CCD-18Co cells as a function of time. The uptake results showed a higher fWGA uptake by the colon cancer cells compared to the colon normal cells. The uptake profile typically showed a rapid initial uptake rate followed by a slower rate of uptake after 30 min. WGA uptake by the Caco-2 cells at the loading concentration of 20 µg/ml was about 2.5 and 3.0 times higher than those of the HT-29 and CCD-18Co cells, respectively. Although the Caco-2 cells showed a consistent 1.5 fold higher uptake of fWGA compared to HT-29 cells at all time points examined, the HT-29 cells also exhibited a substantial capacity for WGA binding, the cellular WGA uptake reaching about 50% of the initial fWGA load administered to the cells at the loading concentration of 10µg/ml at 2h. The rank order of fWGA uptake was Caco-2 > HT-29 > CCD-18Co cells. Higher cancer-to-normal cellular uptake of WGA was observed. The selectivity of WGA for agglutination with the colon cancer cells relative to the normal fibroblast CCD-18Co cells underscored the potential for formulating a WGA-mediated targeting chemotherapeutic drug delivery system for the treatment of colon cancer.

An ideal way for understanding glycosylation changes during oncogenesis of colon cancer is to map the full-range of glycosylation patterns of various colon cancer cells and normal colon cells. In order to use WGA as a tumor-targeting ligand, there is a need to establish the expression profile of its receptor glycoproteins in target cells. In

this study, lectin blot analysis was used to investigate the surface and intracellular glycoproteins expressed in the model colon cells. Our results confirmed the differential expression levels of N-acetyl-D-glucosamine-containing glycoproteins in the cell membrane and intracellular compartments of Caco-2, HT-29 and CCD-18Co cells. The ranking order of expression of these glycoproteins in the cells was HT-29 > Caco-2 > CCD-18Co, suggesting that normal colon cells may express lower levels of WGA-recognizable glycoproteins than the cancerous colon cells. fWGA cellular uptake data supported the hypothesis that WGA-binding residues were expressed in the glycocalyx of the three cell lines, particularly the Caco-2 and HT-29 cell lines. The existence of N-acetyl-D-glucosamine proteins in the cell membrane could facilitate WGA-membrane receptor recognition and enhance the endocytosis of WGA.

WGA-conjugated, paclitaxel-loaded PLGA nanoparticles were prepared by a modified emulsion solvent evaporation method (MESE). As shown previously by our laboratory, and confirmed in this study, the MESE was a simple and reproducible method for the preparation of WGA-conjugated PLGA nanoparticles. The *in vitro* anticancer activity of WNP was evaluated by determination of the IC50 of the formulation against cancer and normal colon cells. Control formulations included PNP, which comprised paclitaxel-loaded PLGA nanoparticles without WGA

conjugation, and P/CreEL, similar to the conventional clinical formulation of paclitaxel. *In vitro* anti-proliferation studies of WNP against the three colon cell types suggested that the incorporation of WGA enhanced the cytotoxicity of the paclitaxel-loaded PLGA nanoparticles against the cancer cells. WNP was significantly more cytotoxic towards the Caco-2 and HT-29 cells than the CCD-18Co cells at 72h, which was in keeping with the cellular uptake data. This indicated that the boosted cytotoxicity observed for WNP was a result of enhanced intracellular paclitaxel concentration. The IC50 of paclitaxel when delivered as WNP against the Caco-2 and HT-29 cells were, respectively, 1.6- and 4.9-folds lower than those of P/CreEL after 72h incubation. PNP was more cytotoxic against the colon cancer cells than against the CCD-18Co cells at 24h incubation, but the differential cytotoxicities were no longer apparent when the incubation time was prolonged to 72h. The conventional formulation, P/CreEL did not exhibit clear differential cytotoxicity profiles towards the cancerous and normal colon cells at 24h and 72h.

The greater efficacy of WNP correlated well with the higher cellular uptake and sustained intracellular retention of paclitaxel associated with the formulation. The cellular uptake and retention efficiency for WNP might be attributed to the over-expression of N-acetyl-D-glucosamine-containing glycoprotein on the colon cell surface. Caco-2 and HT-29 cells showed preferential uptake of WNP compared to

PNP, suggesting that WGA conjugation to the PLGA nanoparticles was advantageous in facilitating the nanoparticle uptake by the cultured colon cancer cells. Paclitaxel uptake from the WNP formulation at 2h incubation was the highest in the Caco-2 cells compared to the other two cell lines. Confocal study confirmed that most of the cell-associated fluorescence was located intracellularly. The implication is that WNP was successfully taken up into the cells. In the presence of free WGA, the uptake of the WNP was inhibited. This indicated that the cellular uptake was mediated by WGA.

Internalization of WNP by Caco-2 cells, with co-localization with endo-lysosomes in 30 min incubation, was demonstrated. The intensity of green fluorescence in the cytoplasm increased with incubation time, which correlates with the increasing amount of internalized WNP with time. Using Lysotracker Red and FITC-WGA as markers, we were able to show that the internalized WNP was delivered to the endo-lysosomes. Escape of WNP from the endo-lysosomal compartment was implicated, together with the release of paclitaxel from the nanoparticles into the cytoplasm. Endo-lysosomal escape of WNP might be attributed to the selective reversal of the surface charge of nanoparticles. However, this needs to be confirmed by further experiments. The induction of apoptosis, together with an arrest of the cell cycle at the subG1 and G2/M phases, was observed after 24h exposure to WNP. By

comparison, P/CreEL and PNP at equivalent paclitaxel doses produced a lower level of apoptosis under the same test conditions.

In order to evaluate the effect of mucin on the intracellular delivery of WNP, a mucin-secreting colon cancer cell line, LS174T, was used in this study. Alcian blue/PAS staining showed both acidic and neutral mucins were produced by the LS174T cells after 6 days of culture. Lectin blot results confirmed the presence of higher levels of WGA-binding glycoproteins both in the cell membrane protein fraction and the cytoplasmic protein fraction of the 6-day culture compared with that of the 3-day culture. However, the 2 cell cultures showed no significant differences in the cellular uptake of paclitaxel from the WNP formulation, indicating that the mucin may not be a barrier for the uptake of WGA-conjugated nanoparticles by the LS174T cells. The MTT assay showed the three paclitaxel formulations, WNP, PNP and P/CreEL, to have comparable *in vitro* cytotoxicity against the LS174T cells after 24h incubation. However, differential cytotoxicites against the LS174T cells were observed when the incubation time was prolonged to 72h, with WNP exhibiting greater cytotoxicity compared to PNP and P/CreEL. The enhanced cell-killing effects might due to the retention of WNP through the interaction of WGA and the mucin glycoproteins. FRAP experiments suggested that fWNP was capable of diffusing through the mucus layer of LS174T cells slowly. The mobility of fWNP in the mucin

layer would not only help the particles stay close to the cells, thus increasing the concentration gradient of the drug, but also enabled the particles to be transported into the cells.

To summarize, WNP had superior *in vitro* anti-proliferation activity against the representative colon cancer cells. The enhanced cytotoxicity of WNP in the colon cancer cells could be attributed to a more efficient cellular internalization of paclitaxel via WGA-mediated endocytosis, and a more efficient retention of the drug within the cells. The *in vitro* studies indicate that WNP may serve as a promising carrier for the targeted delivery of paclitaxel to colon cancer cells, and that WGA could be a useful tool for the realization of colon-cancer targeting of chemotherapeutic agents. The present study has also provided some information on the glycosylation patterns of colon cells, interaction of WGA and its receptor glycoproteins, and the cellular trafficking of WNP in Caco-2 cells. These data may further advance the development of WGA-based targeting platforms for the delivery of anticancer agents.

Chapter 7

Limitation of the Study and Future Directions

7. Limitation of the study and Future Directions

Results from this project have shown that the conjugation of WGA onto PLGA nanoparticles could improve the cytoadhesive and cytoinvasive properties of the nanoparticles and enhance the intracellular retention of paclitaxel by the colon cancer cells. Our results confirmed WNP had superior *in vitro* anti-proliferation activity against the colon cancer cell lines, Caco-2 and HT-29, compared with the PNP and P/CreEL formulations, and it was less toxic against the normal CCD-18Co cells than against the cancer cells. The enhanced cytotoxicity of the WNP in the colon cancer cells could be attributed to a more efficient cellular internalization of paclitaxel via WGA-mediated endocytosis, and a more efficient retention of the drug within the cells. However, the final goal would be testing the efficacy of the WNP *in vivo*. For translating the present work from preclinical to clinical study, much work remains to be done. Studies may have to be done to confirm its targeting capability and efficacy *in vivo*. Biodistribution and pharmacokinetic/pharmacodynamic studies should also be conducted on the WNP in a suitable animal tumor model. In particular, it will be interesting to evaluate if the WNP is capable of trafficking across absorptive epithelia *in vivo*. In addition, safety is a major concern in clinical application. Cytotoxicity studies in our project were only conducted for 4 to 72 h exposure in a limited number of colon cancer and fibroblast cell models. Thus, the results may not truly reflect the effect of WNP *in vivo*. Long-term toxicity studies, particularly pertaining to the accumulation of the slowly-degrading PLGA and WGA, were also imperative to provide further toxicology data for the safety evaluation of WNP.

In order to understand the influence of the interaction between mucin and particulate drug delivery system, a mucin-secreting colon cancer cell model LS174T was used in this project. The cytotoxicity, uptake and diffusion of WNP were investigated in this cell model. However, the mucus layer of the LS174T cell model may not be representative of the mucus lining in the human gastrointestinal tract. Moreover, the *in vitro* cell culture model is inadequate to produce a stable and reproducible mucus gel layer for measuring nanoparticle adherence and diffusion. Further studies will have to be performed in appropriate animal model(s) to confirm our findings, and to provide a greater understanding of the interaction between mucin glycoproteins and WNP in the more complex *in vivo* environments.

The intracellular trafficking study indicated that about 30% of the endocytosed WNP was present in the late endo-lysosomes, and that WNP could escape from the endo-lysosomal compartment into the cytosol. However, the escape mechanism, as well as the intracellular fate of the WNP, remains to be ascertained. It may be worthwhile to further explore the intracellular trafficking of WGA-conjugated nanoparticle systems to gain a deeper insight into the mechanism of the endocytosis process with a view to improve the uptake efficiency of WGA-conjugated nanoparticles *in vitro* and *in vivo*. More experiments are necessary to further elucidate the mechanisms of adhesion, internalization and intracellular distribution of WGA-conjugated nanoparticles.

In this project, the glycosylation patterns of two colon cancer cells and a colon fibroblast cell line was investigated at the membrane protein level. Mucin production of LS174T cells was also studied by lectin blot. Further studies may be carried out to

investigate the glycoprotein and mucin expression at mRNA level in the cultured cells. To date, nine mucin genes have been identified, named MUC1 to MUC9 (Thornton et al., 2000). Mucin expression is tissue- as well as cell-type specific, and it varies according to cell proliferation and differentiation. For instance MUC2 is confined to goblet cells while MUC3 is largely confined to enterocytes (VanKlinken et al., 1996). The characterization of mucin expression at the mRNA level may provide a better understanding of cancer-associated aberrant glycosylation patterns. More colon cell models or human colon tissues could be used to expand the range of glycosylation patterns studied so as to enable a fuller understanding of the glycosylation changes in colon cancer cells. This will aid in the prediction of the effectiveness of WNP in the treatment of colon cancer.

Chapter 8

References

Chapter 8 References

Abbas, A. O., Donovan, M. D., et al. (2008). "Formulating poly(lactide-co-glycolide) particles for plasmid DNA delivery." Journal of Pharmaceutical Sciences **97**(7): 2448-2461.

Abraham, J., Gulley, J. L., et al. (2005). Bethesda handbook of clinical oncology Philadelphia, Lippincott Williams & Wilkins.

Abu-Dahab, R., Schafer, U. F., et al. (2001). "Lectin-functionalized liposomes for pulmonary drug delivery: effect of nebulization on stability and bioadhesion." European Journal of Pharmaceutical Sciences **14**(1): 37-46.

Akay, C., Thomas, C., 3rd, et al. (2004). "Arsenic trioxide and paclitaxel induce apoptosis by different mechanisms." Cell Cycle **3**(3): 324-334.

Akhtar, S. and Lewis, K. J. (1997). "Antisense oligonucleotide delivery to cultured macrophages is improved by incorporation into sustained-release biodegradable polymer microspheres." International Journal of Pharmaceutics **151**(1): 57-67.

Aksoy, N. and Akinci, O. F. (2004). "Mucin macromolecules in normal, adenomatous, and carcinomatous colon: evidence for the neotransformation." Macromolecular Bioscience **4**(5): 483-496.

Aksoy, N., Corfield, A. P., et al. (2000). "Preliminary study pointing out a significant alteration in the biochemical composition of MUC2 in colorectal mucinous carcinoma." Clinical Biochemistry **33**(3): 167-173.

Alberts, B., Johnson, A., et al., Eds. (2002). Molecular biology of the cell, Garland science.

Alexiou, C., Schmid, R. J., et al. (2006). "Targeting cancer cells: magnetic nanoparticles as drug carriers." European Biophysics Journal with Biophysics Letters **35**(5): 446-450.

Allen, A., Cunliffe, W. J., et al. (1990). "The adherent gastric mucus gel barrier in man and changes in peptic ulceration." Journal of Internal Medicine Supplement **732**: 83-90.

Allen, T. M. (2002). "Ligand-targeted therapeutics in anticancer therapy." Nature Reviews Cancer **2**(10): 750-763.

Ameller, T., Marsaud, V., et al. (2003). "In vitro and in vivo biologic evaluation of long-circulating biodegradable drug carriers loaded with the pure antiestrogen RU

58668." International Journal of Cancer **106**(3): 446-454.

Amoresano, A., Amedeo, S., et al. (2000). "N-Linked glycans of proteins from mitral valves of normal pigs and pigs affected by endocardiosis." European Journal of Biochemistry **267**(5): 1299-1306.

Anderson, J. M. and Shive, M. S. (1997). "Biodegradation and biocompatibility of PLA and PLGA microspheres." Advanced Drug Delivery Reviews **28**(1): 5-24.

Andreopoulou, E. and Muggia, F. (2008). "Pharmacodynamics of tubulin and tubulin-binding agents: Extending their potential beyond taxanes." Clinical Breast Cancer **8**: S54-S60.

Astete, C. E. and Sabliov, C. M. (2006). "Synthesis and characterization of PLGA nanoparticles." Journal of Biomaterials Science-Polymer Edition **17**(3): 247-289.

Aub, J. C., Tieslau, C., et al. (1963). "Reactions of Normal and Tumor Cell Surfaces to Enzymes. I. Wheat-Germ Lipase and Associated Mucopolysaccharides." Proceedings of National Academy of Sciences of the United States of America **50**: 613-619.

Avgoustakis, K. (2004). "Pegylated poly(lactide) and poly(lactide-co-glycolide) nanoparticles: preparation, properties and possible applications in drug delivery." Current Drug Delivery **1**(4): 321-333.

Axelsson, M. A. B., Asker, N., et al. (1998). "O-glycosylated MUC2 monomer and dimer from LS 174T cells are water-soluble, whereas larger MUC2 species formed early during biosynthesis are insoluble and contain nonreducible intermolecular bonds." Journal of Biological Chemistry **273**(30): 18864-18870.

Bancroft, J. D. and Gamble, M., Eds. (2008). Theory and practice of histological techniques. Carbohydrates. Churchill Livingstone, Edinburgh.

Behrens, M., Bufe, B., et al. (2004). "Molecular cloning and characterisation of DESC4, a new transmembrane serine protease." Cellular and Molecular Life Sciences **61**(22): 2866-2877.

Berthiervergnes, O., Reano, A., et al. (1986). "Lectin Binding Glycoproteins in Human-Melanoma Cell-Lines with High or Low Tumorigenicity." International Journal of Cancer **37**(5): 747-751.

Betancourt, T., Brown, B., et al. (2007). "Doxorubicin-loaded PLGA nanoparticles by nanoprecipitation: preparation, characterization and in vitro evaluation." Nanomedicine **2**(2): 219-232.

Bhavanandan, V. P. (1991). "Cancer-associated mucins and mucin-type glycoproteins." Glycobiology **1**(5): 493-503.

Bogomoletz, W. V. (1986). "MUCIN HISTOCHEMISTRY IN COLORECTAL DISEASE - PRINCIPLES AND POTENTIAL CLINICAL-APPLICATIONS." International Journal of Colorectal Disease **1**(4): 259-264.

Boland, C. R., Montgomery, C. K., et al. (1982). "Alterations in human colonic mucin occurring with cellular differentiation and malignant transformation." Proceedings of the National Academy of Sciences of the United States of America **79**(6): 2051-2055.

Brandhonneur, N., Chevanne, F., et al. (2009). "Specific and non-specific phagocytosis of ligand-grafted PLGA microspheres by macrophages." European Journal of Pharmaceutical Sciences **36**(4-5): 474-485.

Brannon-Peppas, L. and Blanchette, J. O. (2004). "Nanoparticle and targeted systems for cancer therapy." Advanced Drug Delivery Reviews **56**(11): 1649-1659.

Brehier, A. and Thomasset, M. (1988). "Human colon cell line HT-29: characterisation of 1,25-dihydroxyvitamin D3 receptor and induction of differentiation by the hormone." Journal of Steroid Biochemistry **29**(2): 265-270.

Bresalier, R. S., Rockwell, R. W., et al. (1990). "CELL-SURFACE SIALOPROTEIN ALTERATIONS IN METASTATIC MURINE COLON CANCER CELL-LINES SELECTED IN AN ANIMAL-MODEL FOR COLON CANCER METASTASIS." Cancer Research **50**(4): 1299-1307.

Brigger, I., Dubernet, C., et al. (2002). "Nanoparticles in cancer therapy and diagnosis." Advanced Drug Delivery Reviews **54**(5): 631-651.

Burger, M. M. and Goldberg, A. R. (1967). "Identification of a Tumor-Specific Determinant on Neoplastic Cell Surfaces." Proceedings of the National Academy of Sciences of the United States of America **57**(2): 359-366.

Caldero, J., Campo, E., et al. (1989). "Regional Distribution of Glycoconjugates in Normal, Transitional and Neoplastic Human Colonic Mucosa - a Histochemical-Study Using Lectins." Virchows Archiv a-Pathological Anatomy and Histopathology **415**(4): 347-356.

Campo, E., Condom, E., et al. (1988). "Lectin Binding Patterns in Normal and Neoplastic Colonic Mucosa - a Study of Dolichos-Biflorus Agglutinin, Peanut Agglutinin, and Wheat-Germ Agglutinin." Diseases of the Colon & Rectum **31**(11):

892-899.

Carlstedt, I., Herrmann, A., et al. (1993). "Characterization of two different glycosylated domains from the insoluble mucin complex of rat small intestine." Journal of Biological Chemistry **268**(25): 18771-18781.

Casadei, M. A., Pitarresi, G., et al. (2008). "Biodegradable and pH-sensitive hydrogels for potential colon-specific drug delivery: Characterization and in vitro release studies." Biomacromolecules **9**(1): 43-49.

Cavalli, F., Hansen, H. H., et al. (2000). Textbook of medical oncology London, Martin Dunitz ; Malden, MA : Distributed in the U.S. by Blackwell Science.

Chan, V., Mao, H. Q., et al. (2001). "Effect of chitosan molecular weight in gene delivery process." Abstracts of Papers of the American Chemical Society **221**: U347-U347.

Chang, H. C., Huang, Y. C., et al. (2003). "Antiproliferative and chemopreventive effects of adlay seed on lung cancer in vitro and in vivo." Journal of Agricultural and Food Chemistry **51**(12): 3656-3660.

Chavanpatil, M. D., Khdair, A., et al. (2006). "Nanoparticles for cellular drug delivery: Mechanisms and factors influencing delivery." Journal of Nanoscience and Nanotechnology **6**(9-10): 2651-2663.

Chen, H. W., Gao, J., et al. (2008). "Preparation and characterization of PE38KDEL-loaded anti-HER2 nanoparticles for targeted cancer therapy." Journal of Controlled Release **128**(3): 209-216.

Cheng, J., Teply, B. A., et al. (2007). "Formulation of functionalized PLGA-PEG nanoparticles for in vivo targeted drug delivery." Biomaterials **28**(5): 869-876.

Chourasia, M. K. and Jain, S. K. (2003). "Pharmaceutical approaches to colon targeted drug delivery systems." Journal of Pharmacy and Pharmaceutical Sciences **6**(1): 33-66.

Chu, T. C., Marks, J. W., et al. (2006). "Aptamer : toxin conjugates that specifically target prostate tumor cells." Cancer Research **66**(12): 5989-5992.

Clark, M. A., Hirst, B. H., et al. (2000). "Lectin-mediated mucosal delivery of drugs and microparticles." Advanced Drug Delivery Review **43**(2-3): 207-223.

Cohen, S., Regev, A., et al. (1997). "Small polydispersed circular DNA (spcDNA) in human cells: association with genomic instability." Oncogene **14**(8): 977-985.

Conner, S. D. and Schmid, S. L. (2003). "Regulated portals of entry into the cell." Nature **422**(6927): 37-44.

Conradt, H. S. (1991). Protein glycosylation : cellular, biotechnological, and analytical aspects. New York, VCH

Couvreur, P., Kante, B., et al. (1980). "Tissue distribution of antitumor drugs associated with polyalkylcyanoacrylate nanoparticles." Journal of Pharmaceutical Sciences **69**(2): 199-202.

Cullander, C. (1998). "Light microscopy of living tissue: the state and future of the art." The Journal of Investigative Dermatology. Symposium Proceedings **3**(2): 166-171.

Culling, C. F., Reid, P. E., et al. (1975). "A histochemical method of differentiating lower gastrointestinal tract mucin from other mucins in primary or metastatic tumours." Journal of Clinical Pathology **28**(8): 656-658.

Dalla Pellegrina, C., Rizzi, C., et al. (2005). "Plant lectins as carriers for oral drugs: Is wheat germ agglutinin a suitable candidate?" Toxicology and Applied Pharmacology **207**(2): 170-178.

Damge, C., Reis, C. P., et al. (2008). "Nanoparticle strategies for the oral delivery of insulin." Expert Opinion on Drug Delivery **5**(1): 45-68.

Das, M., Mishra, D., et al. (2008). "Bio-functionalization of magnetite nanoparticles using an aminophosphonic acid coupling agent: new, ultradispersed, iron-oxide folate nanoconjugates for cancer-specific targeting." Nanotechnology **19**(41).

Day, R. M., Maquet, V., et al. (2005). "In vitro and in vivo analysis of macroporous biodegradable poly(D,L-lactide-co-glycolide) scaffolds containing bioactive glass." Journal of Biomedical Materials Research Part A **75A**(4): 778-787.

de Salamanca, A. E., Diebold, Y., et al. (2006). "Chitosan nanoparticles as a potential drug delivery system for the ocular surface: Toxicity, uptake mechanism and in vivo tolerance." Investigative Ophthalmology & Visual Science **47**(4): 1416-1425.

Desai, M. P., Labhasetwar, V., et al. (1996). "Gastrointestinal uptake of biodegradable microparticles: Effect of particle size." Pharmaceutical Research **13**(12): 1838-1845.

Desai, M. P., Labhasetwar, V., et al. (1997). "The mechanism of uptake of biodegradable microparticles in Caco-2 cells is size dependent." Pharmaceutical Research **14**(11): 1568-1573.

Devalapally, H., Duan, Z. F., et al. (2008). "Modulation of drug resistance in ovarian adenocarcinoma by enhancing intracellular ceramide using tamoxifen-loaded biodegradable polymeric nanoparticles." Clinical Cancer Research **14**(10): 3193-3203.

Dodov, M. G., S. Calis, et al. (2009). "Wheat germ agglutinin-conjugated chitosan-Ca-alginate microparticles for local colon delivery of 5-FU: Development and in vitro characterization." International Journal of Pharmaceutics **381**(2): 166-175.

Duchene, D., Touchard, F., et al. (1988). "Pharmaceutical and medical aspects of bioadhesive systems for drug administration." Drug Development and Industrial Pharmacy **14**(2-3): 283-318.

East, J. A., Langdon, S. P., et al. (1992). "The influence of type-1 collagen on the growth and differentiation of the human colonic adenocarcinoma cell line HT-29 *in vitro*." Differentiation **50**(3): 179-188.

Elson, E. L. and Reidler, J. A. (1979). "Analysis of cell-surface interactions by measurements of lateral mobility." Journal of Supramolecular Structure **12**(4): 481-489.

Ertl, B., Heigl, F., et al. (2000). "Lectin-mediated bioadhesion: Preparation, stability and Caco-2 binding of wheat germ agglutinin-functionalized poly(D,L-lactic-co-glycolic acid)-microspheres." Journal of Drug Targeting **8**(3): 173-+.

Farokhzad, O. C., Jon, S. Y., et al. (2004). "Nanopartide-aptamer bioconjugates: A new approach for targeting prostate cancer cells." Cancer Research **64**(21): 7668-7672.

Filipe, M. I. (1979). "Mucins in the human gastrointestinal epithelium: a review." Investigative & Cell Pathology **2**(3): 195-216.

Fireman, Z., Paz, D., et al. (2005). "Capsule endoscopy: improving transit time and image view." World Journal of Gastroenterology **11**(37): 5863-5866.

Florence, A. T. (2004). "Issues in oral nanoparticle drug carrier uptake and targeting." Journal of Drug Targeting **12**(2): 65-70.

Florence, A. T., Hillery, A. M., et al. (1995). "Nanoparticles as Carriers for Oral Peptide Absorption - Studies on Particle Uptake and Fate." Journal of Controlled Release **36**(1-2): 39-46.

Fonseca, C., Simoes, S., et al. (2002). "Paclitaxel-loaded PLGA nanoparticles: preparation, physicochemical characterization and in vitro anti-tumoral activity." Journal of Controlled Release **83**(2): 273-286.

Fukumori, Y. and Ichikawa, H. (2006). "Nanoparticles for cancer therapy and diagnosis." Advanced Powder Technology **17**(1): 1-28.

Gabor, F., Bogner, E., et al. (2004). "The lectin-cell interaction and its implications to intestinal lectin-mediated drug delivery." Advanced Drug Delivery Reviews **56**(4): 459-480.

Gabor, F., Schwarzbauer, A., et al. (2002). "Lectin-mediated drug delivery: binding and uptake of BSA-WGA conjugates using the Caco-2 model." International Journal of Pharmaceutics **237**(1-2): 227-239.

Gabor, F., Stangl, M., et al. (1998). "Lectin-mediated bioadhesion: binding characteristics of plant lectins on the enterocyte-like cell lines Caco-2, HT-29 and HCT-8." Journal of Controlled Release **55**(2-3): 131-142.

Gabor, F., Wirth, M., et al. (1997). "Lectin-mediated bioadhesion: Proteolytic stability and binding-characteristics of wheat germ agglutinin and Solanum tuberosum lectin on Caco-2, HT-29 and human colonocytes." Journal of Controlled Release **49**(1): 27-37.

Garber, K. (2004). "Improved paclitaxel formulation hints at new chemotherapy approach." Journal of the National Cancer Institute **96**(2): 90-91.

Gautier, F., Lassort, D., et al. (1999). "Production and characterisation of a monoclonal antibody specific for apoptotic bodies derived from several tumour cell lines." Journal of Immunology Methods **228**(1-2): 49-58.

Gendler, S. J. and Spicer, A. P. (1995). "Epithelial mucin genes." Annual Review of Physiology **57**: 607-634.

Geyer, H. and Geyer, R. (2006). "Strategies for analysis of glycoprotein glycosylation." Biochimica et Biophysica Acta **1764**(12): 1853-1869.

Giannasca, P. J., Giannasca, K. T., et al. (1994). "Regional differences in glycoconjugates of intestinal M cells in mice: potential targets for mucosal vaccines." American Journal of Physiology **267**(6 Pt 1): G1108-1121.

Gilman, A. and Philips, F. S. (1946). "The Biological Actions and Therapeutic Applications of the B-Chloroethyl Amines and Sulfides." Science **103**(2675): 409-436.

Gordon, B. B. and Pena, S. D. J. (1982). "The Surface Glycoproteins of Human-Skin Fibroblasts Detected after Electrophoresis by the Binding of Peanut (Arachis-Hypogaea) Agglutinin and Ricinus-Communis (Castor-Bean) Agglutinin-I." Biochemical Journal **208**(2): 351-358.

Gradishar, W. J., Tjulandin, S., et al. (2005). "Phase III trial of nanoparticle albumin-bound paclitaxel compared with polyethylated castor oil-based paclitaxel in women with breast cancer." Journal of Clinical Oncology **23**(31): 7794-7803.

Green, N. M. (1975). "Avidin." Advances in Protein Chemistry **29**: 85-133.

Gref, R., Minamitake, Y., et al. (1994). "Biodegradable Long-Circulating Polymeric Nanospheres." Science **263**(5153): 1600-1603.

Gryparis, E. C., Hatziapostolou, M., et al. (2007). "Anticancer activity of cisplatin-loaded PLGA-mPEG nanoparticles on LNCaP prostate cancer cells." European Journal of Pharmaceutics and Biopharmaceutics **67**(1): 1-8.

Guerrero, S., Muniz, E., et al. (2007). "Ketotifen-loaded microspheres prepared by spray-drying poly(D,L-lactide) and poly(D,L-lactide-co-glycolide) polymers: Characterization and in vivo evaluation." Journal of Pharmeutical Sciences.

Haley, B. and Frenkel, E. (2008). "Nanoparticles for drug delivery in cancer treatment." Urologic Oncology-Seminars and Original Investigations **26**(1): 57-64.

Hariharan, S., Bhardwaj, V., et al. (2006). "Design of estradiol loaded PLGA nanoparticulate formulations: A potential oral delivery system for hormone therapy." Pharmaceutical Research **23**(1): 184-195.

Heinrich, E. L., Welty, L. A. Y., et al. (2005). "Direct targeting of cancer cells: A multiparameter approach." Acta Histochemica **107**(5): 335-344.

Hennenfent, K. L. and Govindan, R. (2006). "Novel formulations of taxanes: a review. Old wine in a new bottle?" Annals of Oncology **17**(5): 735-749.

Hidalgo, I. J., Raub, T. J., et al. (1989). "CHARACTERIZATION OF THE HUMAN-COLON CARCINOMA CELL-LINE (CACO-2) AS A MODEL SYSTEM FOR INTESTINAL EPITHELIAL PERMEABILITY." Gastroenterology **96**(3): 736-749.

Ho, S. B., Niehans, G. A., et al. (1993). "Heterogeneity of Mucin Gene-Expression in Normal and Neoplastic Tissues." Cancer Research **53**(3): 641-651.

Hoffman, A. S., Stayton, P. S., et al. (2001). Design of "smart" polymers that can

direct intracellular drug delivery. 6th International Symposium on Polymers for Advanced Technologies, Elat, Israel.

Horwitz, S. B. (1994). "Taxol (paclitaxel): mechanisms of action." Annual Oncology **5 Suppl 6**: S3-6.

Howell, S., Kenny, A. J., et al. (1992). "A survey of membrane peptidases in two human colonic cell lines, Caco-2 and HT-29." Biochemistry Journal **284 (Pt 2)**: 595-601.

Hughes, R. C. and Pena, S. D. J. (1981). Carbohydrate Metabolism and Its Disorders. New York, Academic Press.

Hui, S. W., Langner, M., et al. (1996). "The role of helper lipids in cationic liposome-mediated gene transfer." Biophysical Journal **71**(2): 590-599.

Hussain, N., Jani, P. U., et al. (1997). "Enhanced oral uptake of tomato lectin-conjugated nanoparticles in the rat." Pharmaceutical Research **14**(5): 613-618.

Ibrahim, N. K., Desai, N., et al. (2002). "Phase I and pharmacokinetic study of ABI-007, a Cremophor-free, protein-stabilized, nanoparticle formulation of paclitaxel." Clinical Cancer Research **8**(5): 1038-1044.

Ignatius, A. A. and Claes, L. E. (1996). "In vitro biocompatibility of bioresorbable polymers: Poly(L,DL-lactide) and poly(L-lactide-co-glycolide)." Biomaterials **17**(8): 831-839.

Imam, A. and Taylor, C. R. (1989). "Biochemical and immunological characterizations of antigens recognised by human monoclonal antibodies." British Journal of Cancer **59**(6): 922-928.

Irache, J. M., Durrer, C., et al. (1994). "Preparation and characterization of lectin-latex conjugates for specific bioadhesion." Biomaterials **15**(11): 899-904.

Ishiguro, M., Nakashima, H., et al. (1992). "Interaction of toxic lectin ricin with epithelial cells of rat small intestine in vitro." Chemical & Pharmaceutical Bulletin (Tokyo) **40**(2): 441-445.

Jacobson, K., Sheets, E. D., et al. (1995). "REVISITING THE FLUID MOSAIC MODEL OF MEMBRANES." Science **268**(5216): 1441-1442.

Jalil, R. and Nixon, J. R. (1990). "Biodegradable Poly(Lactic Acid) and Poly(Lactide-Co-Glycolide) Microcapsules - Problems Associated with Preparative Techniques and Release Properties." Journal of Microencapsulation **7**(3): 297-325.

Jang, S. H., Wientjes, M. G., et al. (2003). "Drug delivery and transport to solid tumors." Pharmaceutical Research **20**(9): 1337-1350.

Jansen, R. P. S. (1995). "ULTRASTRUCTURE AND HISTOCHEMISTRY OF ACID MUCUS GLYCOPROTEINS IN THE ESTROUS MAMMAL OVIDUCT." Microscopy Research and Technique **32**(1): 29-49.

Jiang, W. L., Gupta, R. K., et al. (2005). "Biodegradable poly(lactic-co-glycolic acid) microparticles for injectable delivery of vaccine antigens." Advanced Drug Delivery Reviews **57**(3): 391-410.

Jones, R. A., Cheung, C. Y., et al. (2003). "Poly(2-alkylacrylic acid) polymers deliver molecules to the cytosol by pH-sensitive disruption of endosomal vesicles." Biochemical Journal **372**: 65-75.

Jordan, M. A. and Kamath, K. (2007). "How do microtubule-targeted drugs work? An overview." Current Cancer Drug Targets **7**(8): 730-742.

Jumarie, C. and Malo, C. (1991). "Caco-2 Cells Cultured in Serum-Free Medium as a Model for the Study of Enterocytic Differentiation Invitro." Journal of Cellular Physiology **149**(1): 24-33.

Junginger, H. E. (1990). "Bioadhesive Polymer Systems for Peptide Delivery." Acta Pharmaceutica Technologica-International Journal of Drug Forumlation and Biopharmaceutics **36**(3): 110-126.

Kang, S. U., Fuchs, K., et al. (2008). "Proteomic study of hydrophobic (membrane) proteins and hydrophobic protein complexes." Ekc2008: Proceedings of the Eu-Korea Conference on Science and Technology **124**: 429-436.

Kanzawa, F., Akiyama, Y., et al. (2003). "In vitro effects of combinations of cis-amminedichloro (2-methylpyridine) platinum (II) (ZD0473) with other novel anticancer drugs on the growth of SBC-3, a human small cell lung cancer cell line." Lung Cancer **40**(3): 325-332.

Kashino, Y. (2003). "Separation methods in the analysis of protein membrane complexes." Journal of Chromatography B-Analytical Technologies in the Biomedical and Life Sciences **797**(1-2): 191-216.

Kaufman, E. N. and Jain, R. K. (1991). "Measurement of mass-transport and reaction parameters in bulk solution using photobleaching-reaction limited binding regime." Biophysical Journal **60**(3): 596-610.

Keegan, M. E., Royce, S. M., et al. (2006). "In vitro evaluation of biodegradable

microspheres with surface-bound ligands." Journal of Controlled Release **110**(3): 574-580.

Keen, J. (2008). "A step towards a new targeted nanotherapy for pancreatic cancer." Cancer & Biology Therapy **7**(10): 1591-1592.

Kennedy, J. F., Palva, P. M. G., et al. (1995). "Lectins, Versatile Proteins of Recognition - a Review." Carbohydrate Polymers **26**(3): 219-230.

Kerss, S., Allen, A., et al. (1982). "A simple method for measuring thickness of the mucus gel layer adherent to rat, frog and human gastric mucosa: influence of feeding, prostaglandin, N-acetylcysteine and other agents." Clinical Science (Lond) **63**(2): 187-195.

Khanvilkar, K., Donovan, M. D., et al. (2001). "Drug transfer through mucus." Advanced Drug Delivery Reviews **48**(2-3): 173-193.

Kim, G. and Nie, S. (2005). "Targeted cancer nanotherapy." Materials Today **8**: 28-33.

Kim, M., Rao, M. V., et al. (1993). "Lectin-induced apoptosis of tumor cells." Glycobiology **3**(5): 447-453.

Kim, S. H., Jeong, J. H., et al. (2005). "Target-specific cellular uptake of PLGA nanoparticles coated with poly(L-lysine)-poly(ethylene glycol)-folate conjugate." Langmuir **21**(19): 8852-8857.

Kim, S. Y., Lee, Y. M., et al. (2005). "Indomethacin-loaded methoxy poly(ethylene glycol)/poly(D,L-lactide) amphiphilic diblock copolymeric nanospheres: Pharmacokinetic and toxicity studies in rodents." Journal of Biomedical Materials Research Part A **74A**(4): 581-590.

Kim, T. Y., Kim, D. W., et al. (2004). "Phase I and pharmacokinetic study of Genexol-PM, a cremophor-free, polymeric micelle-formulated paclitaxel, in patients with advanced malignancies." Clinical Cancer Research **10**(11): 3708-3716.

Kimura, A., Orn, A., et al. (1979). "Unique lectin-binding characteristics of cytotoxic T lymphocytes allowing their distinction from natural killer cells and "K" cells." European Journal of Immunology **9**(7): 575-578.

Kitao, T., Hattori, K., et al. (1978). "Agglutination of leukemic cells and daunomycin entrapped erythrocytes with lectin in vitro and in vivo." Experientia **34**(1): 94-95.

Kocbek, P., Obermajer, N., et al. (2007). "Targeting cancer cells using PLGA

nanoparticles surface modified with monoclonal antibody." <u>Journal of Controlled Release</u> **120**(1-2): 18-26.

Komath, S. S., Kavitha, M., et al. (2006). "Beyond carbohydrate binding: new directions in plant lectin research." <u>Organic & Biomolecular Chemistry</u> **4**(6): 973-988.

Koppel, D. E. (1981). "Association dynamics and lateral transport in biological-membranes." <u>Journal of Supramolecular Structure and Cellular Biochemistry</u> **17**(1): 61-67.

Kreusel, K. M., Fromm, M., et al. (1991). "Cl- secretion in epithelial monolayers of mucus-forming human colon cells (HT-29/B6)." <u>American Journal of Physiology</u> **261**(4 Pt 1): C574-582.

Kreuter, J., Ramge, P., et al. (2003). "Direct evidence that polysorbate-80-coated poly(butylcyanoacrylate) nanoparticles deliver drugs to the CNS via specific mechanisms requiring prior binding of drug to the nanoparticles." <u>Pharmaceutical Research</u> **20**(3): 409-416.

Kuan, S. F., Byrd, J. C., et al. (1987). "Characterization of quantitative mucin variants from a human colon cancer cell line." <u>Cancer Research</u> **47**(21): 5715-5724.

Kuebler, J. P., Wieand, H. S., et al. (2007). "Oxaliplatin combined with weekly bolus fluorouracil and leucovorin as surgical adjuvant chemotherapy for stage II and III colon cancer: Results from NSABP C-07." <u>Journal of Clinical Oncology</u> **25**(16): 2198-2204.

Kumar, C. S. S. R. (2007). <u>Nanomaterials for Medical Diagnosis and Therapy</u>, Weinheim: Wiley-VCH.

Laemmli, U. K. (1970). "Cleavage of structural proteins during the assembly of the head of bacteriophage T4." <u>Nature</u> **227**(5259): 680-685.

Large, D. G. and Warren, C. D. (1997). <u>Glycopeptides and related compounds : synthesis, analysis, and applications</u>. New York Marcel Dekker.

Laurent, M., Johannin, G., et al. (1994). "Power and limits of laser scanning confocal microscopy." <u>Biology of the Cell</u> **80**(2-3): 229-240.

Lavelle, E. C., Grant, G., et al. (2000). "Mucosal immunogenicity of plant lectins in mice." <u>Immunology</u> **99**(1): 30-37.

Laverman, P., Carstens, M. G., et al. (2001). "Recognition and clearance of methoxypoly(ethyleneglycol)2000-grafted liposomes by macrophages with enhanced

phagocytic capacity - Implications in experimental and clinical oncology." <u>Biochimica Et Biophysica Acta-General Subjects</u> **1526**(3): 227-229.

Lavigne, M. D., Yates, L., et al. (2008). "Nuclear-targeted chimeric vector enhancing nonviral gene transfer into skeletal muscle of Fabry mice in vivo." <u>Faseb Journal</u> **22**(6): 2097-2107.

Le Bivic, A., Hirn, M., et al. (1988). "HT-29 cells are an in vitro model for the generation of cell polarity in epithelia during embryonic differentiation." <u>Proceedings of the National Academy of Sciences of the United States of America</u> **85**(1): 136-140.

Lecaroz, M. C., Blanco-Prieto, M. J., et al. (2007). "Poly(D,L-lactide-coglycolide) particles containing gentamicin: Pharmacokinetics and pharmacodynamics in Brucella melitensis-infected mice." <u>Antimicrobial Agents and Chemotherapy</u> **51**(4): 1185-1190.

Lechardeur, D. and Lukacs, G. L. (2006). "Nucleocytoplasmic transport of plasmid DNA: A perilous journey from the cytoplasm to the nucleus." <u>Human Gene Therapy</u> **17**(9): 882-889.

Lehr, C. M. (1994). <u>Drug Absorption Enhancement-Concepts, Possibilities, Limitations and Trends</u>. Chur, Switzerland Harwood academic, Chur, Switzerland.

Lehr, C. M. (1999). <u>Lectin-mediated drug delivery: The second generation of bioadhesives</u>. 9th International Symposium on Recent Advances in Drug Delivery Systems, Salt Lake City, Utah.

Lehr, C. M. (2000). "Lectin-mediated drug delivery: The second generation of bioadhesives." <u>Journal of Controlled Release</u> **65**(1-2): 19-29.

Lejoyeux, F., Ponchel, G., et al. (1989). "Bioadhesive tablets influence of the testing medium composition on bioadhesion." <u>Drug Development and Industrial Pharmacy</u> **15**(12): 2037-2048.

Lesuffleur, T., Kornowski, A., et al. (1991). "Adaptation to 5-fluorouracil of the heterogeneous human colon-tumor cell line HT-29 results in the selection of cells committed to differentiation." <u>International Journal of Cancer</u> **49**(5): 721-730.

Lesuffleur, T., Porchet, N., et al. (1993). "Differential expression of the human mucin genes muc1 to muc5 in relation to growth and differentiation of different mucus-secreting HT-29 cell subpopulations." <u>Journal of Cell Science</u> **106**: 771-783.

Li, X. M., Xu, Y. L., et al. (2008). "PLGA nanoparticles for the oral delivery of

5-fluorouracil using high pressure homogenization-emulsification as the preparation method and in vitro/in vivo studies." Drug Development and Industrial Pharmacy **34**(1): 107-115.

Lin, S. Y., Chen, K. S., et al. (2000). "In vitro degradation and dissolution behaviours of microspheres prepared by three low molecular weight polyesters." Journal of Microencapsulation **17**(5): 577-586.

Lochner, N., Pittner, F., et al. (2003). "Wheat germ agglutinin binds to the epidermal growth factor receptor of artificial Caco-2 membranes as detected by silver nanoparticle enhanced fluorescence." Pharmaceutical Research **20**(5): 833-839.

Longer, M. A., Chng, H. S., et al. (1985). "Bioadhesive polymers as platforms for oral controlled drug delivery 3. oral delivery of chlorothiazide using a bioadhesive polymer." Journal of Pharmaceutical Sciences **74**(4): 406-411.

Ma, P., Dong, X. W., et al. (2009). "Development of Idarubicin and Doxorubicin Solid Lipid Nanoparticles to Overcome Pgp-Mediated Multiple Drug Resistance in Leukemia." Journal of Biomedical Nanotechnology **5**(2): 151-161.

Macfarlane, S., Woodmansey, E. J., et al. (2005). "Colonization of mucin by human intestinal bacteria and establishment of biofilm communities in a two-stage continuous culture system." Applied and Environmental Microbiology **71**(11): 7483-7492.

Mamot, C., Ritschard, R., et al. (2006). "EGFR-targeted immunoliposomes derived from the monoclonal antibody EMD72000 mediate specific and efficient drug delivery to a variety of colorectal cancer cells." Journal of Drug Targeting **14**(4): 215-223.

Massing, U. and Fuxius, S. (2000). "Liposomal formulations of anticancer drugs: selectivity and effectiveness." Drug Resistance Updates **3**(3): 171-177.

Mathot, F., van Beijsterveldt, L., et al. (2006). "Intestinal uptake and biodistribution of novel polymeric micelles after oral administration." Journal of Controlled Release **111**(1-2): 47-55.

Matsuda, K., Masaki, T., et al. (2000). "Clinical significance of MUC1 and MUC2 mucin and p53 protein expression in colorectal carcinoma." Japanese Journal of Clinical Oncology **30**(2): 89-94.

Matsumoto, B. (1993). Cell biology applications of confocal microscopy. San Diego, California, Academic Press.

Matsuo, K., Ota, H., et al. (1997). "Histochemistry of the surface mucous gel layer of the human colon." Gut **40**(6): 782-789.

McCarron, P. A., Marouf, W. M., et al. (2008). "Antibody targeting of camptothecin-loaded PLGA nanoparticles to tumor cells." Bioconjugate Chemistry **19**(8): 1561-1569.

McGuire, W. P. and Rowinsky, E. K. (1995). Paclitaxel in cancer treatment New York, M. Dekker

Merisko-Liversidge, E., Liversidge, G. G., et al. (2003). "Nanosizing: a formulation approach for poorly-water-soluble compounds." European Journal of Pharmaceutical Sciences **18**(2): 113-120.

Meyvis, T. K. L., De Smedt, S. C., et al. (1999). "Fluorescence recovery after photobleaching: A versatile tool for mobility and interaction measurements in pharmaceutical research." Pharmaceutical Research **16**(8): 1153-1162.

Miller, R. C. and Bowles, D. J. (1982). "A comparative study of the localization of wheat-germ agglutinin and its potential receptors in wheat grains." The Biochemical Journal **206**(3): 571-576.

Mo, Y. and Lim, L. Y. (2004). "Mechanistic study of the uptake of wheat germ agglutinin-conjugated PLGA nanoparticles by A549 cells." Journal of Pharmaceutical Sciences **93**(1): 20-28.

Mo, Y. and Lim, L. Y. (2005). "Paclitaxel-loaded PLGA nanoparticles: Potentiation of anticancer activity by surface conjugation with wheat germ agglutinin." Journal of Controlled Release **108**(2-3): 244-262.

Mo, Y. and Lim, L. Y. (2005). "Preparation and in vitro anticancer activity of wheat germ agglutinin (WGA)-conjugated PLGA nanoparticles loaded with paclitaxel and isopropyl myristate." Journal of Controlled Release **107**(1): 30-42.

Mody, R., Joshi, S., et al. (1995). "Use of lectins as diagnostic and therapeutic tools for cancer." Journal of Pharmacological and Toxicological Methods **33**(1): 1-10.

Moghimi, S. M., Hunter, A. C., et al. (2001). "Long-circulating and target-specific nanoparticles: Theory to practice." Pharmacological Reviews **53**(2): 283-318.

Mohamed, F. and van der Walle, C. F. (2008). "Engineering biodegradable polyester particles with specific drug targeting and drug release properties." Journal of Pharmaceutical Sciences **97**(1): 71-87.

Monsigny, M., Roche, A. C., et al. (1980). "Sugar-Lectin Interactions - How Does Wheat-Germ-Agglutinin Bind Sialoglycoconjugates." European Journal of Biochemistry **104**(1): 147-153.

Monsigny, M., Sene, C., et al. (1979). "Properties of succinylated wheat-germ agglutinin." European Journal of Biochemistry **98**(1): 39-45.

Moore, A., McGuirk, P., et al. (1995). "Immunization with a soluble recombinant HIV protein entrapped in biodegradable microparticles induces HIV-specific CD8(+) cytotoxic T lymphocytes and CD4(+) Th1 cells." Vaccine **13**(18): 1741-1749.

Mu, L. and Feng, S. S. (2003). "A novel controlled release formulation for the anticancer drug paclitaxel (Taxol): PLGA nanoparticles containing vitamin E TPGS." Journal of Controlled Release **86**(1): 33-48.

Munshi, N., De, T. K., et al. (1997). "Size modulation of polymeric nanoparticles under controlled dynamics of microemulsion droplets." Journal of Colloid and Interface Science **190**(2): 387-391.

Murakami, H., Kobayashi, M., et al. (1999). "Preparation of poly(DL-lactide-co-glycolide) nanoparticles by modified spontaneous emulsification solvent diffusion method." International Journal of Pharmaceutics **187**(2): 143-152.

Musumeci, T., Vicari, L., et al. (2006). "Lyoprotected nanosphere formulations for paclitaxel controlled delivery." Journal of Nanoscience and Nanotechnology **6**(9-10): 3118-3125.

Nakamori, S., Ota, D. M., et al. (1994). "Muc1 Mucin Expression as a Marker of Progression and Metastasis of Human Colorectal-Carcinoma." Gastroenterology **106**(2): 353-361.

Natarajan, A., Xiong, C. Y., et al. (2008). "Development of multivalent radioimmunonanoparticles for cancer imaging and therapy." Cancer Biotherapy and Radiopharmaceuticals **23**(1): 82-91.

Naves, A. E., Mortera, M., et al. (1985). "Mucinous carcinoma of the colon and rectum and its relation with adenomas." Medicina-Buenos Aires **45**(3): 252-256.

Nellans, H. N. (1991). "Mechanisms of Peptide and Protein-Absorption .1. Paracellular Intestinal Transport - Modulation of Absorption." Advanced Drug Delivery Reviews **7**(3): 339-364.

Ng, C. P., Goodman, T. T., et al. (2009). "Bio-mimetic surface engineering of plasmid-loaded nanoparticles for active intracellular trafficking by actin comet-tail

motility." <u>Biomaterials</u> **30**(5): 951-958.

Nie, S., Xing, Y., et al. (2007). "Nanotechnology applications in cancer." <u>Annual Review of Biomedical Engineering</u> **9**: 257-288.

Nizheradze, K. A. (2000). "Binding of wheat germ agglutinin to extracellular network produced by cultured human fibroblasts." <u>Folia Histochemica et Cytobiologica</u> **38**(4): 167-173.

Nobs, L., Buchegger, F., et al. (2004). "Current methods for attaching targeting ligands to liposomes and nanoparticles." <u>Journal of Pharmaceutical Sciences</u> **93**(8): 1980-1992.

Nozoe, T., Anai, H., et al. (2000). "Clinicopathological characteristics of mucinous carcinoma of the colon and rectum." <u>Journal of Surgical Oncology</u> **75**(2): 103-107.

Oehler, C. and Ciernik, I. F. (2006). "Radiation therapy and combined modality treatment of gastrointestinal carcinomas." <u>Cancer Treatment Reviews</u> **32**(2): 119-138.

Okada, H., Doken, Y., et al. (1994). "Preparation of 3-Month Depot Injectable Microspheres of Leuprorelin Acetate Using Biodegradable Polymers." <u>Pharmaceutical Research</u> **11**(8): 1143-1147.

Olmsted, S. S., Padgett, J. L., et al. (2001). "Diffusion of macromolecules and virus-like particles in human cervical mucus." <u>Biophysical Journal</u> **81**(4): 1930-1937.

Ono, K., Nishitani, C., et al. (2006). "Mannose-binding lectin augments the uptake of lipid A, Staphylococcus aureus, and Escherichia coli by Kupffer cells through increased cell surface expression of scavenger receptor A." <u>Journal of Immunology</u> **177**(8): 5517-5523.

Owens, D. E., 3rd and Peppas, N. A. (2006). "Opsonization, biodistribution, and pharmacokinetics of polymeric nanoparticles." <u>International Journal of Pharmaceutics</u> **307**(1): 93-102.

Pan, L. J., Li, Z. F., et al. (2005). "Characterization of gp41 gene of Spodoptera litura multicapsid nucleopolyhedrovirus." <u>Virus Research</u> **110**(1-2): 73-79.

Panagi, Z., Beletsi, A., et al. (2001). "Effect of dose on the biodistribution and pharmacokinetics of PLGA and PLGA-mPEG nanoparticles." <u>International Journal of Pharmaceutics</u> **221**(1-2): 143-152.

Pancino, G., Osinaga, E., et al. (1991). "Purification and characterisation of a breast-cancer-associated glycoprotein not expressed in normal breast and identified by

monoclonal antibody 83D4." British Journal of Cancer **63**(3): 390-398.

Panyam, J. and Labhasetwar, V. (2003). "Biodegradable nanoparticles for drug and gene delivery to cells and tissue." Advanced Drug Delivery Reviews **55**(3): 329-347.

Panyam, J. and Labhasetwar, V. (2003). "Dynamics of endocytosis and exocytosis of poly(D,L-lactide-co-glycolide) nanoparticles in vascular smooth muscle cells." Pharmaceutical Research **20**(2): 212-220.

Panyam, J. and Labhasetwar, V. (2004). "Sustained cytoplasmic delivery of drugs with intracellular receptors using biodegradable nanoparticles." Molecular Pharmaceutics **1**(1): 77-84.

Panyam, J., Zhou, W. Z., et al. (2002). "Rapid endo-lysosomal escape of poly(DL-lactide-co-glycolide) nanoparticles: implications for drug and gene delivery." Faseb Journal **16**(10).

Park, E. T., Gum, J. R., et al. (2008). "Aberrant expression of SOX2 upregulates MUC5AC gastric foveolar mucin in mucinous cancers of the colorectum and related lesions." International Journal of Cancer **122**(6): 1253-1260.

Park, J. H., Kwon, S., et al. (2006). "Self-assembled nanoparticles based on glycol chitosan bearing hydrophobic moieties as carriers for doxorubicin: In vivo biodistribution and anti-tumor activity." Biomaterials **27**(1): 119-126.

Park, J. S., Han, T. H., et al. (2006). "N-acetyl histidine-conjugated glycol chitosan self-assembled nanoparticles for intracytoplasmic delivery of drugs: Endocytosis, exocytosis and drug release." Journal of Controlled Release **115**(1): 37-45.

Partikian, A., Olveczky, B., et al. (1998). "Rapid diffusion of green fluorescent protein in the mitochondrial matrix." Journal of Cell Biology **140**(4): 821-829.

Patel, M., Shah, T., et al. (2007). "Therapeutic opportunities in colon-specific drug-delivery systems." Critical Reviews in Therapeutic Drug Carrier Systems **24**(2): 147-202.

Pfeifer, R. W., Hale, K. N., et al. (1993). "Precipitation of paclitaxel during infusion by pump." American Journal of Hospital Pharmacy **50**(12): 2518- 2521.

Prabha, S. and Labhasetwar, V. (2004). "Nanoparticle-mediated wild-type p53 gene delivery results in sustained antiproliferative activity in breast cancer cells." Molecular Pharmaceutics **1**(3): 211-219.

Pratt, W. B., Ruddon, R. W., et al. (1994). The anticancer drugs. New York, Oxford

University Press.

Pusztai, A., Ewen, S. W. B., et al. (1993). "Antinutritive Effects of Wheat-Germ-Agglutinin and Other N-Acetylglucosamine-Specific Lectins." British Journal of Nutrition **70**(1): 313-321.

Qaddoumi, M. and Lee, V. H. L. (2004). "Lectins as endocytic ligands: An assessment of lectin binding and uptake to rabbit conjunctival epithelial cells." Pharmaceutical Research **21**(7): 1160-1166.

Quintanar-Guerrero, D., Allemann, E., et al. (1998). "Preparation techniques and mechanisms of formation of biodegradable nanoparticles from preformed polymers." Drug Development and Industrial Pharmacy **24**(12): 1113-1128.

Raghuvanshi, R. S., Katare, Y. K., et al. (2002). "Improved immune response from biodegradable polymer particles entrapping tetanus toxoid by use of different immunization protocol and adjuvants." International Journal of Pharmaceutics **245**(1-2): 109-121.

Rapin, A. M. and Burger, M. M. (1974). "Tumor cell surfaces: general alterations detected by agglutinins." Advanced Cancer Research **20**: 1-91.

Rathbone, M. J. and Hadgraft, J. (1991). "ABSORPTION OF DRUGS FROM THE HUMAN ORAL CAVITY." International Journal of Pharmaceutics **74**(1): 9-24.

Raub, T. J., Denny, J. B., et al. (1986). "Cell surface glycoproteins of CHO cells. I. Internalization and rapid recycling." Experimental Cell Research **165**(1): 73-91.

Reano, A., Vergnes, O. B., et al. (1986). "Lectin Binding Glycoproteins in Human-Melanoma Cell-Lines with High or Low Tumorigenicity." Journal of Investigative Dermatology **87**(1): 163-163.

Rhodes, J. M. and Milton, J. D. (1998). Lectin methods and protocols Humanna Press.

Robinson, J. P. (2001). "Principles of confocal microscopy." Methods Cell Biology **63**: 89-106.

Rodrigues, J. S., Santos-Magalhaes, N. S., et al. (2003). "Novel core (polyester)-shell(polysaccharide) nanoparticles: protein loading and surface modification with lectins." Journal of Controlled Release **92**(1-2): 103-112.

Rodrigues, J. S., Santos-Magalhaes, N. S., et al. (2003). "Novel core(polyester)-shell(polysaccharide) nanoparticles: protein loading and surface modification with lectins." Journal of Controlled Release **92**(1-2): 103-112.

Rohringer, R. and Holden, D. W. (1985). "Protein Blotting - Detection of Proteins with Colloidal Gold, and of Glycoproteins and Lectins with Biotin-Conjugated and Enzyme Probes." Analytical Biochemistry **144**(1): 118-127.

Ross, J. F., Chaudhuri, P. K., et al. (1994). "Differential regulation of folate receptor isoforms in normal and malignant-tissues in vivo and in established cell lines-physiological and clinical implications." Cancer **73**(9): 2432-2443.

Roth, J. (1983). "Application of lectin--gold complexes for electron microscopic localization of glycoconjugates on thin sections." Journal of Histochemistry and Cytochemistry **31**(8): 987-999.

Sahlin, S., Hed, J., et al. (1983). "Differentiation between Attached and Ingested Immune-Complexes by a Fluorescence Quenching Cytofluorometric Assay." Journal of Immunological Methods **60**(1-2): 115-124.

Sahoo, S. K. and Labhasetwar, V. (2003). "Nanotech approaches to delivery and imaging drug." Drug Discovery Today **8**(24): 1112-1120.

Sahoo, S. K. and Labhasetwar, V. (2005). "Enhanced antiproliferative activity of transferrin-conjugated paclitaxel-loaded nanoparticles is mediated via sustained intracellular drug retention." Molecular Pharmaceutics **2**(5): 373-383.

Sahoo, S. K., Ma, W., et al. (2004). "Efficacy of transferrin-conjugated paclitaxel-loaded nanoparticles in a murine model of prostate cancer." International Journal of Cancer **112**(2): 335-340.

Schaeferhenrich, A., Beyer-Sehlmeyer, G., et al. (2003). "Human adenoma cells are highly susceptible to the genotoxic action of 4-hydroxy-2-nonenal." Mutation Research **526**(1-2): 19-32.

Schwarz, R. E., Wojciechowicz, D. C., et al. (1999). "Wheatgerm agglutinin mediated toxicity in pancreatic cancer cells." British Journal of Cancer **80**(11): 1754-1762.

Scudiero, D. A., Shoemaker, R. H., et al. (1988). "Evaluation of a soluble tetrazolium formazan assay for cell growth and drug sensitivity in culture using human and other tumor cell lines." Cancer Research **48**(17): 4827-4833.

Segretain, D., Egloff, M., et al. (1992). "Receptor-mediated and absorptive endocytosis by male germ cells of different mammalian species." Cell Tissue Res **268**(3): 471-478.

Seksek, O., Biwersi, J., et al. (1997). "Translational diffusion of macromolecule-sized solutes in cytoplasm and nucleus." Journal of Cell Biology **138**(1): 131-142.

Serpe, L., Catalano, M. G., et al. (2004). "Cytotoxicity of anticancer drugs incorporated nanoparticles on HT-29 colorectal cancer in solid lipid cell line." European Journal of Pharmaceutics and Biopharmaceutics **58**(3): 673-680.

Shah, K. U. and Rocca, J. G. (2004). "Lectins as next-generation mucoadhesives for specific targeting of the gastrointestinal tract." Drug Delivery Technology **4**(5).

Sharon, N. and Lis, H. (2004). "History of lectins: from hemagglutinins to biological recognition molecules." Glycobiology **14**(11): 53R-62R.

Sherwood, S. W. and Schimke, R. T. (1995). Cell-cycel analysis of apoptosis using flow-cytometry. Methods in Cell Biology, Vol 46. **46:** 77-97.

Singhal, A. and Hakomori, S. (1990). "Molecular-Changes in Carbohydrate Antigens Associated with Cancer." Bioessays **12**(5): 223-230.

Singla, A. K., Garg, A., et al. (2002). "Paclitaxel and its formulations." International Journal of Pharmaceutics **235**(1-2): 179-192.

Smart, J. D. (2005). "The basics and underlying mechanisms of mucoadhesion." Advanced Drug Delivery Reviews **57**(11): 1556-1568.

Soepenberg, O., Sparreboom, A., et al. (2004). "Real-time pharmacokinetics guiding clinical decisions; phase I study of a weekly schedule of liposome encapsulated paclitaxel in patients with solid tumours." European Journal of Cancer **40**(5): 681-688.

Song, C., Labhasetwar, V., et al. (1998). "Arterial uptake of biodegradable nanoparticles for intravascular local drug delivery: results with an acute dog model." Journal of Controlled Release **54**(2): 201-211.

Sonju, T., Christensen, T. B., et al. (1974). "Electron microscopy, carbohydrate analyses and biological activities of the proteins adsorbed in two hours to tooth surfaces in vivo." Caries Research **8**(2): 113-122.

Straubinger, R. M. (1995). Taxol® : science and applications. New York CRC Press

Strous, G. J. and Dekker, J. (1992). "MUCIN-TYPE GLYCOPROTEINS." Critical Reviews in Biochemistry and Molecular Biology **27**(1-2): 57-92.

Strugala, V., Allen, A., et al. (2003). "Colonic mucin: methods of measuring mucus thickness." The Proceedings of the Nutrition Society **62**(1): 237-243.

Studzinski, G., Ed. (1995). Cell growth and apoptosis: A practical approach. New York,

IRL Press at Oxford Univesity Press.

Suffness, M. and Wall, M. E. (1995). Taxol® : science and applications Boca Raton, Fla. : CRC Press

Sugawara, K., Terauchi, A., et al. (2008). "Voltammetric behaviors of wheat-germ agglutinin on a chitin-modified carbon-paste electrode." Analytical Sciences **24**(5): 583-587.

Sun, Y., Wang, J. C., et al. (2008). "Synchronic release of two hormonal contraceptives for about one month from the PLGA microspheres: In vitro and in vivo studies." Journal of Controlled Release **129**(3): 192-199.

Sung, J. (2007). "Colorectal cancer screening: Its time for action in Asia." Cancer Detection and Prevention **31**(1): 1-2.

Surti, N., S. Naik, et al. (2007). "Assessment of in-vitro antiproliferative activity after intracellular drug delivery from wheat germ agglutinin-conjugated budesonide nanoparticles." Journal of Biomedical Nanotechnology **3**(1): 61-67.

Surti, N. and A. Misra (2008). "Wheat germ agglutinin-conjugated nanoparticles for sustained cellular and lung delivery of budesonide." Drug Delivery **15**(2): 81-86.

Surti, N., S. Naik, et al. (2008). "Intracellular delivery of nanoparticles of an antiasthmatic drug." Aaps Pharmscitech **9**(1): 217-223.

Szentkuti, L. (1997). "Light microscopical observations on luminally administered dyes, dextrans, nanospheres and microspheres in the pre-epithelial mucus gel layer of the rat distal colon." Journal of Controlled Release **46**(3): 233-242.

Taluja, A., Youn, Y. S., et al. (2007). "Novel approaches in microparticulate PLGA delivery systems encapsulating proteins." Journal of Materials Chemistry **17**(38): 4002-4014.

Tang, W., Guo, Q., et al. (2005). "Histochemical expression of sialoglycoconjugates in carcinoma of the papilla of Vater." Hepatogastroenterology **52**(61): 67-71.

Terho, P. and Lassila, O. (2006). "Novel method for cell debris removal in the flow cytometric cell cycle analysis using carboxy-fluorescein diacetate succinimidyl ester." Cytometry Part A **69A**(6): 552-554.

Thiele, L., Rothen-Rutishauser, B., et al. (2001). "Evaluation of particle uptake in human blood monocyte-derived cells in vitro. Does phagocytosis activity of dendritic

cells measure up with macrophages?" Journal of Controlled Release **76**(1-2): 59-71.

Thompson, N. L., Burghardt, T. P., et al. (1981). "Measuring surface dynamics of biomolecules by total internal-reflection fluorescence with photobleaching recovery of correlation spectroscopy." Biophysical Journal **33**(3): 435-454.

Thornton, D. J., T. Gray, et al. (2000). "Characterization of mucins from cultured normal human tracheobronchial epithelial cells." American Journal of Physiology - Lung Cellular and Molecular Physiology **278**(6): L1118-28.

Thornton, D. J. and Sheehan, J. K. (2004). "From mucins to mucus: toward a more coherent understanding of this essential barrier." Proceedings of the American Thoracic Society **1**(1): 54-61.

Trissel, L. A. (1996). Pharmaceutical properties of paclitaxel and their effects on preparation and administration. University-of-Maryland-Cancer-Center Conference on Antineoplastics, San Francisco, Ca.

Trissel, L. A., Xu, Q. Y., et al. (1994). "Compatibility of paclitaxel injection vehicle with intravenous administration and extension sets." American Journal of Hospital Pharmacy **51**(22): 2804-2810.

Tsay, T. T. and Jacobson, K. A. (1991). "Spatial fourier-analysis of video photobleaching measurements- principles and optimization." Biophysical Journal **60**(2): 360-368.

Tytgat, K., Buller, H. A., et al. (1994). "Biosynthesis of human colonic mucin- muc2 is the prominent secretory mucin." Gastroenterology **107**(5): 1352-1363.

Tytgat, K. M., Dekker, J., et al. (1993). "Mucins in Inflammatory Bowel-Disease." European Journal of Gastroenterology & Hepatology **5**(3): 119-127.

Valentich, J. D., Popov, V., et al. (1997). "Phenotypic characterization of an intestinal subepithelial myofibroblast cell line." American Journal of Physiology-Cell Physiology **41**(5): C1513-C1524.

van Vlerken, L. E., Duan, Z. F., et al. (2007). "Modulation of intracellular ceramide using polymeric nanoparticles to overcome multidrug resistance in cancer." Cancer Research **67**(10): 4843-4850.

VanKlinken, B. J. W., Oussoren, E., et al. (1996). "The human intestinal cell lines Caco-2 and LS174T as models to study cell-type specific mucin expression." Glycoconjugate Journal **13**(5): 757-768.

Vasir, J. K. and Labhasetwar, V. (2007). "Biodegradable nanoparticles for cytosolic delivery of therapeutics." Advanced Drug Delivery Reviews **59**(8): 718-728.

Vicari, L., Musumeci, T., et al. (2008). "Paclitaxel loading in PLGA nanospheres affected the in vitro drug cell accumulation and antiproliferative activity." Bmc Cancer **8**: 212-222

Villegas, J. C. and Broadwell, R. D. (1993). "Transcytosis of protein through the mammalian cerebral epithelium and endothelium 2. adsorptive transcytosis of WGA-HRP and the blood-brain and brain blood barriers." Journal of Neurocytology **22**(2): 67-80.

Vinogradov, S. V., Bronich, T. K., et al. (2002). "Nanosized cationic hydrogels for drug delivery: preparation, properties and interactions with cells." Advanced Drug Delivery Reviews **54**(1): 135-147.

Wang, H. X., Ng, T. B., et al. (2000). "Effects of lectins with different carbohydrate-binding specificities on hepatoma, choriocarcinoma, melanoma and osteosarcoma cell lines." International Journal of Biochemistry & Cell Biology **32**(3): 365-372.

Wang, J., Ng, C. W., et al. (2003). "Release of paclitaxel from polylactide-co-glycolide (PLGA) microparticles and discs under irradiation." Journal of Microencapsulation **20**(3): 317-327.

Wang, T. H., Wang, H. S., et al. (2000). "Paclitaxel-induced cell death - Where the cell cycle and apoptosis come together." Cancer **88**(11): 2619-2628.

Wang, X., Yang, L. L., et al. (2008). "Application of nanotechnology in cancer therapy and imaging." Ca-a Cancer Journal for Clinicians **58**(2): 97-110.

Wang, X. Q., Dai, J. D., et al. (2004). "Bioavailability and pharmacokinetics of cyclosporine A-loaded pH-sensitive nanoparticles for oral administration." Journal of Controlled Release **97**(3): 421-429.

Wang, Y., Ao, X., et al. (2008). "Membrane glycoproteins associated with breast tumor cell progression identified by a lectin affinity approach." Journal of Proteome Research **7**(10): 4313-4325.

Wang, Y. F., O'Brate, A., et al. (2005). "Resistance to microtubule-stabilizing drugs involves two events - beta-tubulin mutation in one allele followed by loss of the second allele." Cell Cycle **4**(12): 1847-1853.

Watzl, B., Neudecker, C., et al. (2001). "Dietary wheat germ agglutinin modulates

ovalbumin-induced immune responses in Brown Norway rats." <u>British Journal of Nutrition</u> **85**(4): 483-490.

Weissenbock, A., Wirth, M., et al. (2004). "WGA-grafted PLGA-nano spheres: preparation and association with Caco-2 single cells." <u>Journal of Controlled Release</u> **99**(3): 383-392.

Werther, K., Normark, M., et al. (2000). "The use of the CELLection kit in the isolation of carcinoma cells from mononuclear cell suspensions." <u>Journal of Immunological Methods</u> **238**(1-2): 133-141.

Westedt, U., Kalinowski, M., et al. (2007). "Poly(vinyl alcohol)-graft-poly(lactide-co-glycolide) nanoparticles for local delivery of paclitaxel for restenosis treatment." <u>Journal of Controlled Release</u> **119**(1): 41-51.

Wirth, M., Fuchs, A., et al. (1998). "Lectin-mediated drug targeting: Preparation, binding characteristics, and antiproliferative activity of wheat germ agglutinin conjugated doxorubicin on Caco-2 cells." <u>Pharmaceutical Research</u> **15**(7): 1031-1037.

Wirth, M., Gerhardt, K., et al. (2002). "Lectin-mediated drug delivery: influence of mucin on cytoadhesion of plant lectins in vitro." <u>Journal of Controlled Release</u> **79**(1-3): 183-191.

Wirth, M., Kneuer, C., et al. (2002). "Lectin-mediated drug delivery: Discrimination between cytoadhesion and cytoinvasion and evidence for lysosomal accumulation of wheat germ agglutinin in the Caco-2 model." <u>Journal of Drug Targeting</u> **10**(6): 439-448.

Wong, H. L., Rauth, A. M., et al. (2006). "A new polymer-lipid hybrid nanoparticle system increases cytotoxicity of doxorubicin against multidrug-resistant human breast cancer cells." <u>Pharmaceutical Research</u> **23**(7): 1574-1585.

Wong, S. Y., Pelet, J. M., et al. (2007). "Polymer systems for gene delivery-past, present, and future." <u>Progress in Polymer Science</u> **32**(8-9): 799-837.

Wright, C. S. (1987). "Refinement of the crystal-structure of wheat-germ-agglutinin isolectin 2 at 1.8 a resolution." <u>Journal of Molecular Biology</u> **194**(3): 501-529.

Xie, M., Hu, J., et al. (2009). "Lectin-modified trifunctional nanobiosensors for mapping cell surface glycoconjugates." <u>Biosensors & Bioelectronics</u> **24** (5): 1311-1317

Yang, J., Lee, C. H., et al. (2007). "Antibody conjugated magnetic PLGA nanoparticles for diagnosis and treatment of breast cancer." <u>Journal of Materials</u>

Chemistry **17**(26): 2695-2705.

Yang, L. (2008). "Biorelevant dissolution testing of colon-specific delivery systems activated by colonic microflora." Journal of Controlled Release **125**(2): 77-86.

Yashpal, M., Kumari, U., et al. (2007). "Histochemical characterization of glycoproteins in the buccal epithelium of the catfish, Rita rita." Acta Histochemica **109**(4): 285-303.

Yaszemski, M. J. and Wise, D. L. (2004). Tissue Engineering and Novel Delivery Systems, CRC Press.

Yezhelyev, M. V., Gao, X., et al. (2006). "Emerging use of nanoparticles in diagnosis and treatment of breast cancer." Lancet Oncology **7**(8): 657-667.

Yi, S. M., Harson, R. E., et al. (2001). "Lectin binding and endocytosis at the apical surface of human airway epithelia." Gene Therapy **8**(24): 1826-1832.

Yih, T. C. and Al-Fandi, M. (2006). "Engineered nanoparticles as precise drug delivery systems." Journal of Cellular Biochemistry **97**(6): 1184-1190.

Zhang, N., Ping, Q. N., et al. (2006). "Lectin-modified solid lipid nanoparticles as carriers for oral administration of insulin." International Journal of Pharmaceutics **327**(1-2): 153-159.